



UNIVERSIDADE ESTADUAL DE CAMPINAS

INSTITUTO DE BIOLOGIA

RAFAEL GARCIA TAVARES

DELLA, THE GENE OF THE GREEN REVOLUTION.
CHARACTERIZATION AND ANALYSIS OF ITS FUNCTION IN THE
SUCROSE ACCUMULATION AND SOURCE-SINK REGULATION IN
SUGARCANE.

DELLA, O GENE DA REVOLUÇÃO VERDE. CARACTERIZAÇÃO E
ANÁLISE DE SUA FUNÇÃO NO ACÚMULO DE SACAROSE E NA
REGULAÇÃO FONTE-DRENO EM CANA-DE-AÇÚCAR

CAMPINAS
2017

RAFAEL GARCIA TAVARES

**DELLA, THE GENE OF THE GREEN REVOLUTION. CHARACTERIZATION AND
ANALYSIS OF ITS FUNCTION IN THE SUCROSE ACCUMULATION AND
SOURCE-SINK REGULATION IN SUGARCANE.**

**DELLA, O GENE DA REVOLUÇÃO VERDE. CARACTERIZAÇÃO E ANÁLISE DE
SUA FUNÇÃO NO ACÚMULO DE SACAROSE E NA REGULAÇÃO FONTE-
DRENO EM CANA-DE-AÇÚCAR**

Thesis presented to the Institute of Biology of the University of Campinas in partial fulfillment of the requirements for the degree of Doctor in Genetics and Molecular Biology (Plant Genetics and Breeding).

Tese apresentada ao Instituto de Biologia da Universidade Estadual de Campinas como parte dos requisitos exigidos para a obtenção do Título de Doutor em Genética e Biologia Molecular, na área de Genética Vegetal e Melhoramento.

ESTE ARQUIVO DIGITAL CORRESPONDE À VERSÃO FINAL DA TESE DEFENDIDA PELO ALUNO RAFAEL GARCIA TAVARES E ORIENTADA PELO PROF. DR. MARCELO MENOSSI TEIXEIRA.

Orientador: Prof. Dr. Marcelo Menossi Teixeira

**CAMPINAS
2017**

Agência(s) de fomento e nº(s) de processo(s): FAPESP, 2012/06877-9

Ficha catalográfica
Universidade Estadual de Campinas
Biblioteca do Instituto de Biologia
Mara Janaina de Oliveira - CRB 8/6972

T197d Tavares, Rafael Garcia, 1981-
DELLA, the gene of the green revolution. Characterization and analysis of its function in the sucrose accumulation and source-sink regulation in sugarcane / Rafael Garcia Tavares. – Campinas, SP : [s.n.], 2017.

Orientador: Marcelo Menossi Teixeira.
Tese (doutorado) – Universidade Estadual de Campinas, Instituto de Biologia.

1. Cana-de-açúcar. 2. Giberelina. 3. Plantas – Proteínas. 4. Plantas - Reguladores. 5. Crescimento (Plantas). I. Menossi, Marcelo, 1968-. II. Universidade Estadual de Campinas. Instituto de Biologia. III. Título.

Informações para Biblioteca Digital

Título em outro idioma: DELLA, o gene da revolução verde. Caracterização e análise de sua função no acúmulo de sacarose e na regulação fonte-dreno em cana-de-açúcar

Palavras-chave em inglês:

Sugarcane

Gibberellins

Plant proteins

Plant regulators

Growth (Plants)

Área de concentração: Genética Vegetal e Melhoramento

Titulação: Doutor em Genética e Biologia Molecular

Banca examinadora:

Marcelo Menossi Teixeira [Orientador]

Rafael Vasconcelos Ribeiro

Luciano Freschi

Luiz Gonzaga Esteves Vieira

Paulo Cezar de Lucca

Data de defesa: 18-04-2017

Programa de Pós-Graduação: Genética e Biologia Molecular

Campinas, 18 de abril de 2017

COMISSÃO EXAMINADORA

Prof. Dr. Marcelo Menossi Teixeira

Prof. Dr. Rafael Vasconcelos Ribeiro

Prof. Dr. Luciano Freschi

Prof. Dr. Luiz Gonzaga Esteves Vieira

Dr. Paulo Cezar de Lucca

Os membros da Comissão Examinadora acima assinaram a Ata de defesa, que se encontra no processo de vida acadêmica do aluno.

Acknowledgements

My sincere gratitude to:

My advisor Prof. Dr. Marcelo Menossi for the opportunity, the continuous support and guidance of my Ph.D study. Thanks for your motivation, engagement, passion and deeper knowledge. Thank you for the countless hours guiding me to overcome some difficulties during this work.

Prof. Dr. Edgar Peiter, who provided me an opportunity to join his laboratory in the Martin-Luther University Halle-Wittenberg. Thank you for accepting me as your student and the fruitful discussion about the experiments.

Dr. Prakash Lakshmanan, who also provided me an opportunity to join his group in Sugar Research Australia –SRA. Thank you for the trust you had in our project research.

My sincere thanks also goes to Dr. Renato Vicentini, Dr. Camila Caldana, Dr. José Sérgio Soares and Dr. Anthony O’Connell for their contributions during this research.

I would like to thank my thesis committee for their insightful comments and discussions.

I thank my fellow labmates, those who I had the opportunity to meet during this long journey in the lab. Thanks for the stimulating discussions and all the fun we have had over the years.

I thank FAPESP (São Paulo Research Foundation) for the financial support in the grants 2012/06877-9 and BEPE 2014/15458-5.

Last but not the least, I would like to thank my family. I DEDICATE this thesis for my parents and my wife. A special thanks to my lovely mother Elizabeth who gave to me all the support to achieve this goal. Another special thanks to my lovely wife Camila for standing by my side and supporting me in all situations. Finally, I OFFER this thesis to my lovely grandma Tereza who set the example for me.

Resumo

DELLA, o gene da revolução verde. Caracterização e análise de sua função no acúmulo de sacarose e na regulação fonte-dreno em cana-de-açúcar

A regulação fonte-dreno para o balanço energético é vital para as plantas. Os mecanismos moleculares que atuam nessa regulação desenvolvimental devem estar conectados com os estímulos causados por estresses abióticos e bióticos ao longo do ciclo de vida das plantas, permitindo uma homeostase da produção de energia. Os hormônios vegetais desempenham um papel chave entre o desenvolvimento e os estresses ambientais. Por exemplo, a síntese do hormônio do crescimento giberelina é bloqueada sob estresse abióticos, permitindo as plantas regularem seu desenvolvimento até que retornem as condições ideais. Em cana-de-açúcar, o crescimento está estritamente relacionado com o acúmulo de açúcar nos entrenós e o aumento de biomassa para a produção de bioenergia. Todavia, a parada do crescimento é uma das primeiras respostas sob estresses abióticos em cana, afetando dessa forma sua produtividade. A proteína DELLA, por ser um mediador da ação hormonal na repressão do crescimento, é um interessante candidato no estudo da regulação do desenvolvimento e fonte-dreno em cana. Nesta tese, nós caracterizamos molecularmente o gene *ScGAI* que codifica a proteína DELLA de cana. *ScGAI* apresenta diferentes níveis de expressão nos tecidos foliar e ao longo dos entrenós. Em folha, a proteína ScGAI é conjugada com SUMO, um processo pós-traducional conhecido como SUMOlização, em uma maneira espaço-temporal no controle da alongação foliar. Plantas transgênicas de cana superexpressando o gene *ScGAI* (*ScGAI*OE) apresentaram um crescimento retardado, grande número de perfilhos e um déficit de energia. Por outro lado, plantas silenciadas para o gene *ScGAI* (*HpScGAI*) são mais altas com diâmetro preservado, apresentam maiores números de entrenós e precoce alongação, sem comprometimento no acúmulo de sacarose em comparação com as plantas do tipo selvagem. Assim como demonstrado para as proteínas DELLA em *Arabidopsis*, a proteína ScGAI também interagiu com as proteínas ScPIF3/ScPIF4 e os fatores de transcrição ScEIN3/ScEIL1 no controle do crescimento em cana-de-açúcar. Nossos dados demonstram que a proteína ScGAI atua como um elo entre o crescimento e a regulação de energia em cana-de-açúcar.

Abstract

DELLA, the gene of the green revolution. Characterization and analysis of its function in the sucrose accumulation and source-sink regulation in sugarcane

The source-sink regulation for the energy balance is vital for all plants. The molecular mechanisms that act in this developmental regulation must be connected to the abiotic and biotic stresses-related stimuli throughout the life cycle of plants, providing energy homeostasis. Plant hormones play a key role in the interaction between development and environmental stresses. For instance, the biosynthesis of the growth hormone gibberellin is blocked under abiotic stresses, allowing the plants adjust their development until optimum conditions. In sugarcane, the growth is strictly related to the sucrose accumulation in the internodes and the increase of biomass for bioenergy production. Besides, growth arrest is one of the first responses under abiotic stress, affecting cane and sugar yields. The *DELLA* gene, that mediates the hormonal arrest of development, is an interesting candidate in the study of the developmental process and source-sink in cane. In this thesis, we characterized the *ScGAI* gene that encodes a DELLA protein from sugarcane. *ScGAI* presents different expression levels in leaf tissue and along the stem. In leaf, ScGAI protein is conjugated to SUMO, a post-translational process known as SUMOylation, in a spatio-temporal manner to control leaf elongation. Transgenic sugarcane plants overexpressing the *ScGAI* gene (ScGAI^{OE}) showed a retarded growth, a large number of tillers and an energy deficit. On the other hand, silenced plants for the *ScGAI* gene (HpScGAI) are higher with preserved diameter, increased number of internodes, earlier onset of the elongated internodes without compromised sucrose levels in comparison with wild-type plants. As demonstrated for DELLA proteins from *Arabidopsis*, the ScGAI protein also interacted with the ScPIF3/ScPIF4 proteins and the transcription factors ScEIN3/ScEIL1 for the controlling of growth in sugarcane. Our data demonstrated that ScGAI protein acts as a hub between growth and energy status in sugarcane.

Contents

| | |
|---|----|
| Resumo | iv |
| Abstract | v |
| 1 Introduction | 9 |
| 2 Chapter 1 - Literature review | 10 |
| 2.1 The source-sink communication in sugarcane..... | 10 |
| 2.2 DELLA, the central repressor of gibberellin (GA) signaling..... | 10 |
| 2.3 Gibberellin hormone signaling pathway..... | 11 |
| 3 Chapter 2 - DELLA coordinates Growth and Energy Status in Sugarcane Plants | 15 |
| 3.1 Abstract..... | 16 |
| 3.2 Introduction..... | 17 |
| 3.3 Methods..... | 18 |
| 3.4 Results..... | 24 |
| 3.4.1 <i>ScGAI</i> encodes a DELLA protein..... | 24 |
| 3.4.2 <i>ScGAI</i> was most expressed in the shoot apex whereas GA ₃ content was highest in the mature part of the culm..... | 28 |
| 3.4.3 <i>ScGAI</i> is a regulatory component of spatio-temporal leaf growth in sugarcane, and its action is modulated by SUMOylation..... | 31 |
| 3.4.4 <i>ScGAI</i> -misexpression alters sugarcane morphology..... | 32 |
| 3.4.5 <i>ScGAI</i> -misexpressing lines are hypersensitive to GA and paclobutrazol (PAC) treatments..... | 36 |
| 3.4.6 <i>ScGAI</i> misexpression alters gene expression profiles..... | 36 |
| 3.4.7 Metabolite profiling..... | 37 |
| 3.4.8 <i>ScGAI</i> interacts with ScPIF3/PIF4 and ScEIN3/ScEIL1 proteins..... | 39 |
| 3.5 Discussion..... | 42 |
| 3.5.1 The GA signaling in sugarcane..... | 42 |
| 4 Concluding remarks | 47 |
| 5 Supplementary Materials | 47 |
| 6 References | 75 |
| 7 Anexos | 84 |

1 Introduction

The worldwide interest in renewable energy has increased the focus on biomass production of “energy canes” rather than sucrose yield alone. The physiological source and sink communication is important for both biomass production and sucrose accumulation in sugarcane. Environmental factors are the major drivers for sugarcane productivity, once they alter this source-sink relationship. As internal signals, hormones have been known for a long time to mediate plant responses upon environmental stress. In sugarcane, there has been a relatively slow progress in the understanding at the functional and molecular levels of the source-sink communication. Thereby, the aim of our study was to understand the role played by ScGAI, a growth repressor of the gibberellin signaling, in the sugarcane development and consequently in the source-sink regulation.

The thesis is organized in two chapters. Firstly, we present a literature review and then we present a chapter with a manuscript that will be submitted to a peer reviewed Journal. In this manuscript we describe the molecular characterization of the *ScGAI* gene and its physiological importance in the sugarcane development and physiology through its misexpression in transgenic plants.

2 Chapter 1 - Literature review

2.1 The source-sink communication in sugarcane

Sugarcane (*Saccharum* spp. hybrids) is one of the most efficient crop in the conversion of solar energy into carbohydrates ¹. As any C4 plant, photosynthesis and carbon assimilation occur in the leaf mesophyll chloroplasts and bundle sheath cells. Once the carbon is fixed and converted into sugar or sugar derivatives in these source cells, the main soluble disaccharide form, sucrose, is then distributed to sink cells through the phloem. In the stem, sucrose may take two different fates: consumption or storage. The sugarcane developmental stage and environmental stimulus will determine how carbon will be partitioned in the stem^{2,3}.

During the first stages in the sugarcane life cycle, environmental stimulus such as high temperature, water availability and nutrient-rich soil promote stem growth and elongation ⁴. At the whole-plant level, this rapid metabolism of sugar in the sink tissues (sink strength) demands a optimum sucrose supply from the source, helping to minimize sugar repression of photosynthesis in the leaves ⁵. In the last decades, a few studies on source-sink communication in sugarcane revealed this dominant influence of sink activity on source photosynthesis ^{6,7}. On the other hand, any unfavorable environmental condition such as low temperature and mild water stress will restrain sugarcane growth. Recently, new insights were reported in the leaf growth regulation under drought stress. The abscisic acid (ABA) level increased while gibberellin decreased in the leaf upon severe water stress ⁸. In the last sugarcane developmental stage, such abiotic stresses induce a switch from growth phase to ripening ⁹, blocking the growth of the upper internodes and directing the sucrose accumulation toward the whole plant ². However, the molecular mechanisms underpinning the ripening process in sugarcane remain completely unknown.

2.2 DELLA, the central repressor of gibberellin (GA) signaling

DELLA proteins are nuclear transcriptional regulators involved in the GA signaling in plants ¹⁰. Like all GRAS [named after its first three members: GA INSENSITIVE (GAI), REPRESSOR of *gal-3* (RGA), and SCARECROW (SCR)] proteins, DELLAs share a conserved C-terminal GRAS domain composed by two leucine heptad repeats (LHRI and LHRII) and three conserved motifs, VHIID, PFYRE and SAW. Nevertheless, DELLAs contain a unique N-terminal DELLA domain (which give them their name) with two highly conserved motifs (DELLA and VHYNP), which distinguish them from the rest of the GRAS family members ¹¹. This

DELLA/VHYNP motifs directly participate in the interaction with the GA receptor GID1 (for GA-INSENSITIVE DWARF1)^{12,13} (the mechanism of GA action will be described below). Mutations in these regions result in a GA-insensitive phenotype due to the inability of DELLAs to interact with GID1 even in the presence of GA¹⁴. Additionally, DELLA/VHYNP possesses transactivation activity¹⁵. DELLAs act as a transcriptional coactivator through interaction with other transcription factors, whereas DELLAs do not contain a DNA-binding domain (DBD). Recently, DELLAs have been shown to interact to IDD (INDETERMINATE DOMAIN) and BOI (BOTRYTIS SUSCEPTIBLE1 INTERACTOR) proteins to regulate the expression of other genes in GA signaling^{16,17}. Besides, DELLAs also interact with SWI3C and PICKLE proteins both involved in the chromatin remodeling in plants^{18,19}.

Thereby, the major mechanism of DELLA-regulated gene expression is through their ability to interact with several regulatory proteins. The conserved LHR motif within the GRAS domain has been described to mediate the protein-protein interactions. For example, DELLA regulate the stem growth by interacting with PHYTOCHROME INTERACTING FACTORS (PIFs)^{20,21} and BRASSINAZOLE RESISTANT1 (BZR1)²², the floral transition and fruit patterning by respectively interacting with SQUAMOSA PROMOTER BINDING-LIKE (SPL)²³ and ACATRAZ (ALC)²⁴, photoperiod by interacting to CONSTANS (CO)²⁵ and also contribute to plant defense by interacting with JASMONATE ZIM-DOMAIN (JAZ) proteins. Through these interactions, DELLAs may regulate the activation or repression of the downstream genes, sequestering and impairing of the DNA-binding capacity of transcription factors. In addition, post-translational modifications have also been demonstrated to stabilize or to change the conformation structure of DELLA proteins, regulating these protein-protein interactions.

2.3 Gibberellin hormone signaling pathway

GAs are plant hormone essential for a diversity of the developmental processes in plants, including seed germination, stem and leaf elongation, sex determination, flowering, and senescence²⁶. In total, more than 136 natural GAs have been identified in plants, fungi and bacteria so far; most of them either act as precursors for the bioactive GAs (GA₁, GA₃, GA₄ and GA₇) or are inactive catabolites²⁷. The GA biosynthesis pathway, therefore, presents many steps controlled by enzymes belonging to multigenic families. The members of two gene families encoding the GA20 oxidases and GA3 oxidases, which are involved in the last step in the synthesis of bioactive GAs, are control points in the pathway²⁸. Besides, the members of GA2 oxidase family are also tightly regulated to

modulate the deactivation of bioactive GAs, ensuring the GA homeostasis. The GA signal is perceived by the GA receptor GID1, which is a soluble protein, resembling to hormone-sensitive lipases, localized to both cytoplasm and nucleus²⁹. GA-binding GID1 enhances the interaction between GID1 and DELLA³⁰. The GID1-GA-DELLA protein complex formation triggers the polyubiquitination, predominantly ubiquitin chain with Lys-29 linkages, of DELLAs through the binding of the F-box sub-units SLY1 (for SLEEPY1 in *Arabidopsis*) and GID2 (for GA-INSENSITIVE DWARF2 in rice) of the E3 ligase complex, targeting DELLA for destruction by the 26S proteasome³¹.

Three alternative mechanisms for this DELLA destruction model have been recently described. Firstly, GA signal may be transduced without DELLA degradation. GA treatment in the *sly1* and *gid2* mutants resulted in some increase in stem elongation, indicating that they are not completely GA-insensitive³². In addition, overexpression of GID1 receptor rescued these partial GA-insensitive phenotypes of *sly1* and *gid2* mutants, without DELLA degradation. Thereby, GA and GID1 receptors can overcome DELLA repression in F-box mutants impaired to destroy DELLA proteins via 26S proteasome³². Secondly, DELLA proteins may be regulated in a GA-independent manner³³. Different from rice that contains a single *OsGID1* GA receptor gene³⁴, *Arabidopsis* contains three *GID1a*, *GID1b*, *GID1c* GA receptor genes²⁹. Interestingly, the GID1b receptor has the ability to interact with DELLA proteins even in the absence of GA. Despite the rice OsGID1 protein shows higher identity to *Arabidopsis* GID1ac-type receptors, i.e. GA-dependent interaction with DELLA, a P99S single amino acid substitution close to the N-terminal lid domain, allowed OsGID1^{P99S} to bind DELLA in the absence of GA, mimicking the *Arabidopsis* GID1b phenotype³⁵. This proline (Pro) amino acid in the “hinge” region likely pull the lid closed, preventing DELLA-binding when GA is not present. In the *Arabidopsis* GID1b receptor, the Pro amino acid is replaced by His-91, while in GID1a the Pro-92 and GID1c the Pro-91 are conserved³⁶. GID1b homologues in *Brassica* and soybean also demonstrated GA-independent DELLA binding activity³⁶. Thirdly, DELLA proteins are regulated by post-translational modification (PTM) affecting their activity, such as: phosphorylation³⁷, O-GlcNAcylation³⁸, SUMOylation³⁹ and O-fucosylation⁴⁰.

Various proteins are ubiquitinated and targeted for destruction in response to phosphorylation⁴¹. However, this is not the case for DELLA proteins. Rice SLR1 (rice DELLA) is phosphorylated in a GA-independent manner, and both phosphorylated and unphosphorylated forms of the SLR1 interacted to the F-box GID2³⁷. On the other hand, protein phosphatase inhibitors demonstrated to inhibit degradation of barley DELLA SLN1 and *Arabidopsis* AtRGA and AtRGL2

proteins^{42,43}. Recent studies on casein kinase I EIL1 (for EARLY FLOWERING1) in rice and TOPP4 (for TYPE ONE PROTEIN PHOSPHATASE4) in *Arabidopsis* provided further evidence that phosphorylation positively regulates and dephosphorylation negatively regulate DELLA repression of GA signaling^{44,45}.

Regarding glycosylation (O-GlcNAcylation) of DELLA proteins, the first clue came from the identification of two putative O-linked N-acetylglucosamine (O-GlcNAc) transferase (OGT) in *Arabidopsis*, SPINDLY (SPY) and its paralog, SECRET AGENT (SEC). SPY has been described as a GA signaling repressor, whereas the loss-of-function *spy* mutants partially rescue the dwarf phenotype of the GA-deficient *gal* mutant⁴⁶. Nevertheless, the levels of O-GlcNAcylated DELLA are not reduced by the loss-of-function *spy* mutant, whereas DELLA O-GlcNAcylation is abolished in a null *sec* mutant³⁸. This findings corroborated with previous studies demonstrating that, only SEC, but not SPY, has been demonstrated to display OGT enzyme activity⁴⁷. Although SEC and SPY have been reported to interact with DELLAs, further analysis demonstrated that DELLA is O-GlcNAcylated only by SEC protein, causing an inhibition of DELLA function by the block of the binding of DELLA to four interactors (BZR1, JAZ1, PIF3 and PIF4)³⁸. Therefore, SEC acts a positive regulator of GA responses. Considering the fact that the levels of OGT's donor substrate UDP-GlcNAc is positively correlated to nutrient status, the O-GlcNAcylation of DELLAs, therefore, coordinate the nutrient status with its growth and development in plants.

The mystery of the role played by SPY on DELLA was recently revealed⁴⁰. DELLA was demonstrated to be mono O-fucosylated by SPY, an O-fucosyltransferase in *Arabidopsis*. O-fucosylation by SPY may induce DELLA to adopt an open conformation, promoting the binding of DELLA with key interactors such as BZR1, PIF3 and PIF4. Nevertheless, SEC and SPY proteins were reported to compete each other in the PTM on DELLAs. As described above, O-GlcNAcylation by SEC blocked those interactions, likely due to a close conformation and less active adopt by DELLA⁴⁰.

Recent evidence in *Arabidopsis* has reported another process of GA-independent signaling through an increase in DELLA repression due to SUMO (Small Ubiquitin-like Modifier) modification of DELLA³⁹. SUMO is a short peptide (12 kDa) and like ubiquitination, its covalent conjugation on target proteins is facilitated by sequential activity of three enzymes (E1, E2 and E3). SUMOylation is a reversible and highly dynamic process, which is regulated by SUMO-conjugating and SUMO-deconjugating enzymes⁴⁸. SUMOylation of DELLA was found within the DELLA domain at a conserved lysine residue. Interestingly, GID1 receptor was shown to bind to SUMOylated

DELLA in the absence of GA via a SUMO-interacting motif (SIM). This GID1-SUMOylated DELLA interaction reduces the amount of GID1 available for GA-dependent interaction with non-SUMOylated DELLA, leading to decreased DELLA degradation via ubiquitination/proteasome^{39,49}.

3 Chapter 2 - DELLA coordinates Growth and Energy Status in Sugarcane Plants

Authors: Rafael G. Tavares^{1,2}, Prakash Lakshmanan², Edgar Peiter³, Anthony O'Connell², Camila Caldana^{4,5}, Renato Vicentini⁶, Jose S. Soares¹, Marcelo Menossi^{1*}

Affiliations

¹Functional Genome Laboratory, Department of Genetics, Evolution and Bioagents, Institute of Biology, State University of Campinas, Campinas, Brazil.

²Sugar Research Australia (SRA), Indooroopilly, Brisbane, Australia.

³Plant Nutrition Laboratory, Institute of Agricultural and Nutritional Sciences, Faculty of Natural Sciences III, Martin Luther University Halle-Wittenberg, Halle (Saale), Germany.

⁴Brazilian Bioethanol Science and Technology Laboratory, Brazilian Center for Research in Energy and Materials (CTBE), Campinas, Brazil.

⁵Max Planck Partner Group at CTBE.

⁶System Biology Laboratory, Department of Genetics, Evolution and Bioagents, Institute of Biology, State University of Campinas, Campinas, Brazil.

*The section order and the references presented here differ from the publisher's version (the final article).

3.1 Abstract

Sugarcane contributes to more than seventy percent of sugar production worldwide. Sugar accumulates in sugarcane culm and hence stalk biomass and sugar content are the major yield determining factors. Despite extensive breeding, yield plateaued for decades in most countries. We hypothesize that identifying and manipulating the genetic elements controlling source-sink regulation and hence plant growth may allow to break the yield barrier in this crop. Here we show that ScGAI, a homolog of the Arabidopsis growth repressor DELLA, is the key molecular switch of a sugar-hormone cross-regulation network that determines growth in sugarcane. ScGAI levels are inversely correlated with metabolic status and carbon availability in transgenic *ScGAI*-misexpressing sugarcane plants. In particular, silencing of *ScGAI* triggered faster growth and development in transgenic sugarcane plants without reducing sugar level. An improvement of plant growth without a penalty in carbohydrate accumulation will certainly have a positive impact on the production of food and biofuel.

3.2 Introduction

Plant growth and development are ultimately dependent on carbon allocation, which is controlled by source-sink regulation. It is now evident that soluble sugars, such as hexoses and sucrose, not only function as metabolic resources but they also act as signal molecules involved in the regulation of carbon supply and demand, thereby, modulating plant development. To add further complexity in this phenomenon, several recent studies have demonstrated the cross-talk occurring between sugar signaling, phytohormones, light, and biotic and abiotic stress-related stimuli in the source-sink context⁵⁰.

Sugarcane (*Saccharum* ssp. hybrids) accumulates sucrose to high concentrations in the culm. This distinctive feature combined with the modular development of culm characterized by inter-connected source-sink compartments, i.e. phytomers [nodes, axillary buds and internodes (sink) with a leaf (source) attached to nodes] of different maturity, provides excellent experimental system to study source-sink regulation in the context of carbon allocation, plant growth and carbohydrate accumulation⁵¹. Commercially, sugar yield is a combined outcome of cane yield and sugar content. In the past few decades, much of the yield gain in sugarcane variety improvement has been achieved from improved cane yield rather than increased sucrose content⁵². Indeed, there is now clear evidence of yield plateau in most of the sugarcane growing countries despite significant breeding and management efforts. This led us to hypothesize that breaking the sugarcane yield barriers require a deeper understanding of major regulators of growth, development and source-sink regulation. Despite the extensive physiological studies on sugar accumulation and source-sink regulation in sugarcane in the last few decades^{5,7,53,54}, the mechanistic and molecular understanding of carbon supply-demand balance in this crop remains poorly understood.

Gibberellins (GAs) are plant growth hormones involved in diverse aspects of plant growth and development. Once the bioactive GA is present in the cell, its receptor GA-INSENSITIVE DWARF1 (GID1) recognizes and binds to it, undergoing a conformational change that allows the GA-GID1 complex to bind to the N-terminal of DELLA proteins, triggering the recruitment of the components of the ubiquitin machinery¹⁰. Thus, GA responses are triggered by the rapid degradation of DELLA proteins, which function as repressors in the GA signaling pathway, and serve as a central hub for the integration of growth, other hormones and environmental cues^{55,56}. Additionally, considerable progress has recently been made in dissecting the cross-talk between GA and sugar signaling, demonstrating that sucrose stabilizes the DELLA protein in *Arabidopsis*⁵⁷. We therefore

directed our attention to study the DELLA protein in sugarcane as a potential master regulator of growth and development. As a central integrator of many different signals, we also theorized a major role for DELLA in the source-sink regulation in sugarcane.

Here, we report the identification and the role of the ScGAI protein, the growth repressor DELLA in sugarcane. Interestingly, ScGAI was found SUMOylated in a spatio-temporal manner suggesting a role in the control of leaf growth. However, this post-translational regulatory mechanism does not seem to occur in the stem, where ScGAI represses internode elongation in a GA-dependent manner. *ScGAI*-overexpressing transgenic sugarcane exhibited a stunted growth, shorter internodes and impaired energy metabolism. In contrast, *ScGAI*-silenced plants were taller, with rapid internode elongation, increased internode number, and greater carbon allocation to the stem. The present study clearly shows that ScGAI acts as an integrative hub for growth and energy metabolism, modulating carbon supply and demand to optimize sugarcane growth. Our results thus reveals new molecular insights into the source-sink relationship in sugarcane. Based on these findings, ScGAI is a promising candidate for new initiatives on renewable energy that target both sucrose content and lignocellulosic components of biomass in sugarcane.

3.3 Methods

Plant Material. All sugarcane plants were grown in the glasshouse individually in pots (diameter, 20 cm) containing a 3:1 (v/v) soil and perlite (Chillagoe Perlite, Mareeba, Qld, Australia). The plants were fertilized monthly with Osmocote granules (Scotts Australia Pty Ltd, Baulkham Hills, NSW, Australia) and watered for 30 seconds every 2 hours between 06:00 h and 18.00 h daily.

Molecular cloning and bioinformatics analyses. Through the Sugarcane EST Database (SUCEST) (<http://sucest-fun.org/wsapp/>), the cDNA clones of *ScPIF4*, *ScPIF5* and *ScEIL1* were obtained and their coding sequences amplified using specific primers (see table 5). The coding sequences from *ScGAI*, *ScPIF3* and *ScEIN3* were amplified through specific primers (see table 5) using genomic DNA from the sugarcane commercial variety SP80-3280. Protein sequences from sorghum SbD8 (Sb01g010660), maize ZmD8 (Q9ST48) and ZmD9 (Q06F07), pea CRY (B2BA71) and LA (B2BA72), tomato LeGAI (Q7Y1B6), grape VvGAI (Q8S4W7), barley SLN1 (Q8W127), wheat Rht-1 (Q9ST59), rice SLR1 (Q7G7J6) and Arabidopsis AtRGL1 (Q9C8Y3), AtRGL2 (Q8GXW1),

AtRGL3 (Q9LF53), AtGAI (Q9LQT8) and AtRGA (Q9SLH3) were aligned using ClustalX program⁵⁸ and the phylogenetic tree was constructed using the Neighbor-joining method⁵⁹ available on MEGA6⁶⁰ with bootstrap analysis of 1000 replicates. Estimates of evolutionary divergence among DELLA sequences were conducted using Poisson correction model⁶¹. Evolutionary analyses were conducted in MEGA6. Predicted tertiary structure of DELLA domain from sugarcane were performed in SWISS MODEL program⁶². The x-ray crystal structure of *Arabidopsis* AtGAI-AtGID1A/GA3 complex (PDB entry 2zsh.1.b) were used as a model.

Yeast two hybrid (YTH) assays. The coding sequences of the *ScGAI* and *gaiAdella* (201-625) were digested from pGEMTEasy vectors and cloned into pGBKT7 vectors, while the coding sequences of the *ScPIF3*, *ScPIF4*, *ScPIF5*, *ScEIN3*, *Scein3*(233-552) and *ScEIL1* were also digested from pGEMTEasy and cloned into pGADT7vectors. The yeast strain Y2HGOLD was transformed following the Matchmaker Gold Yeast Two-Hybrid System user's manual protocol (Clontech, TAKARA BIO INC., Japan).

Biomolecular Fluorescence Complementation (BIFC). Leaves from 3 to 4 week-old Col-0 *Arabidopsis* were used for protoplast isolation and subsequent DNA transfection. For generation of N-terminal YFP-tagged constructions, the coding region of the *ScGAI*, *ScPIF3*, *ScPIF4*, *ScEIN3* and *ScEIL1* were amplified using specific primers (table 5) and subcloned into pGEMTEasy, and subsequent cloned into pUC_SPYNE vector. The same procedure was used for C-terminal YFP-tagged constructs using the pUC_SPYCE vector. As a negative control, the N-terminal truncated ScGAI was cloned in the vectors above. The plasmids were co-transfected into freshly prepared *Arabidopsis* leaf mesophyll protoplasts⁶³. The images were obtained from the camera AxioCam MRM Observer Z1 Zeiss AX10 microscope (Zeiss, Germany).

Subcellular localization. For subcellular localization, the *ScGAI*, *ScPIF3*, *ScPIF4*, *ScEIN3*, *ScEIL1* and *gaiANterminal* coding regions were cloned in frame with VENUS protein into pART7 vector⁶⁴. *Arabidopsis* protoplasts were isolated and used for transient expression. The construction pART7:VENUS was used as a positive control for transient expression. Each constructions were co-transformed with the vector pART7:AtPARP3:mCherry, a positive nuclear control⁶⁵. The images were obtained from the camera AxioCam MRM Observer Z1 Zeiss AX10 microscope (Zeiss, Germany).

Agro-infiltration in tobacco leaves. The ScGAI:VENUS fusion protein was transiently expressed in tobacco leaves of *Nicotiana benthamiana*⁶⁶. Agrobacterium strain GV3101 was transformed with the binary vector pGREENII:ScGAI:VENUS and after 72 hours foliar discs (1 cm²) were excised and analyzed in the Zeiss AX10 microscope (Zeiss, Germany).

Transgenic Arabidopsis plants. For transformation of Arabidopsis ecotype Ler-0, the binary vector pGREENII0179 harboring the resistance *hyg* gene in the T-DNA region was used for overexpressing the *ScGAI:VENUS* coding region. The pGREENII:ScGAI:VENUS and pGREENII vectors were transformed into agrobacterium GV3101 strain by electroporation. The helper plasmid pSOUP was co-transformed with each vector, since it provides the replicase gene (*RepA*) for the replication of pGREEN vector. Floral dip protocol was carried out as previously described⁶⁷. Arabidopsis T1 seeds obtained after transformation were plated onto MS medium supplemented with 20 mg/L of hygromycin for selection.

Recombinant protein expression in *Escherichia coli* strain. Full-length *ScGAI* was cloned into pET21a(+) vector (Novagen, Madison, USA) using specific primers (table 5). The His-tagged ScGAI protein was expressed in *E.coli* BL21 (DE3) strain after 4 hour induction with 1mM IPTG at 37°C. Bacterial cells were harvested and the protein extraction performed⁶⁸. The samples were stored at -80°C. Both the total cell extract (soluble and insoluble fractions) were analyzed by SDS-PAGE and western blotting.

Western blotting. Total protein was extracted according to the phenol protocol as previously described⁶⁹. All protein samples were quantified by Bradford reagent (BioRad, USA). Equal amounts of total protein were separated in NuPAGE Novex 4%-12% gradient Bis-Tris gel. Proteins were transferred onto PVDF membranes and probed with polyclonal antibody raised (1:1000 dilution) against the N-terminal of sugarcane DELLA (Anti-ScGAI). Secondary HRP-conjugated anti-rabbit IgG was used at a dilution of 1:1000. Immunoblotted bands were visualized by the SuperSignal West Pico Chemiluminescent substrate (PIERCE). PVDF membranes were stained by Commassie Blue (CB).

Immunoprecipitation (IP) assay. Total crude proteins were extracted from sugarcane leaf +1. Each 300 µg of protein extracts were incubated with 3 µg of anti-SUMO1 polyclonal antibody (abcam; ab5316) bound to anti-Rabbit IgG-coated magnetic beads (Dynabeads M-280 Sheep anti-Rabbit IgG; Invitrogen) for 1 h at room temperature. Subsequent washing steps were performed with PBS solution and the target antigen was eluted with NuPAGE LDS sample buffer. Immunoprecipitated SUMO-ScGAI proteins were detected by immunoblot analysis using anti-ScGAI (GenScript). As negative control, SUMO1-coupled dynabeads were incubated onto protein extraction buffer.

Transgenic sugarcane plants. Young unfurled 3-4 innermost leaves covering the shoot apex from a sugarcane commercial variety (*Saccharum officinarum* L. var. Q208A) were collected under sterile condition and used as target tissue for transformation. The rolled leaves were sliced into 1-1.5 mm thick transverse sections and cultured on callus induction medium (MS medium supplemented with 1mg/L 2,4-D – synthetic auxin – and pH adjusted to 5.7 using KOH before autoclaving). After two weeks, the explants were placed on an osmotic medium (MS medium supplemented with 3.6% sorbitol and mannitol and pH adjusted to 5.7 using KOH before autoclaving) for 3 hours and the transgenes were introduced by biolistics (BioRad PDS-1000/He). For this procedure, gold particles were coated with a molar 1:1 mixture of plasmids pUbi:FLAG:ScGAI or pUbi:hpGAIi and pUKN (geneticin gene selection). Spermidine and calcium chloride (CaCl₂) were used to precipitate DNA onto the gold particles. After the particle bombardment, explants were placed onto callus induction medium for two weeks and then were cut into small pieces and placed onto selection medium containing 50mg/L geneticin. These plates were maintained for three weeks in the dark and replaced onto new fresh selection medium for three more weeks to regenerate plants. All regenerated plants were maintained on geneticin selection medium.

PCR Genotyping. Genomic DNA from leaves were extracted as previously described⁷⁰. PCR genotyping was performed using different set of primers (see table 5) following the protocol from GoTaq Green Master Mix (Promega, USA).

Total RNA extraction. Tissue samples were separately collected and immediately frozen in nitrogen liquid. Samples were ground in mini-bead beater Precellys 24 (Bertin Technologies) and high-quality

total RNAs were isolated and purified according to the protocol from Spectrum Plant total RNA kit (Sigma-Aldrich).

cDNA synthesis and qPCR assay. For cDNA synthesis, total RNA was treated with RQ1 RNase-Free DNase (Promega, USA) at 37°C for 30 minutes to remove genomic DNA contamination. After that, full-length cDNAs were synthesized according to the protocol from Improm-II reverse transcriptase enzyme (Promega, USA). PCR was performed to detect genomic DNA contamination before qPCR. Reagents were mixed and each reaction contained 5 µL of SensiMix SYBR Low-ROX (Bioline, Australia), 0.2 µL (200 nM) of gene-specific forward and reverse primer and 1.6 µL water. An epMotion M5073 liquid handler (Eppendorf) was used to aliquot the reagents mix and 3 µL of 5 ng/µL cDNA into MicroAmp® Fast Optical 384-Well Reaction Plates (Life technologies, Australia). The thermal profile was 95°C for 10 min, 40 cycles of 95°C for 15 s and 60°C for 50 s, followed by a dissociation step of 95°C for 2 min, 60°C for 15 s. No template controls (NTC) were used to check for contamination and primer dimers. All qPCR data generated was analysed using the DataAssist™ Software (Life technologies, Australia). For each cDNA sample, an average gene amplification level was calculated from triplicate PCR reactions (technical replicates). This average expression for each gene was normalised against the average expression level of a reference gene (ADF, Actin depolymerizing factor), to account for template variations between samples. Then each expression level was compared to a reference sample according to $2^{-\Delta\Delta Cq}$ method ⁷¹.

Gibberellin (GA₃) and paclobutrazol (PAC) treatments. Sugarcane seedlings from tissue culture were transplanted into separate sterilized containers with 100 ml of 1x Murashige and Skoog (MS) medium, adjusted to pH 5.8 with or without 50 µM GA₃ (Phytotechnology laboratories, USA) or 5 µM PAC (Phytotechnology laboratories, USA). GA₃ and PAC stock solutions were filter-sterilized before adding to MS medium. Plants were incubated in growth room at 24°C with a 16/8 h light/dark cycle for 23 days. The solutions were sterilized by filtration.

Histological analysis. Transverse cross-sections of leaves and stem were observed in bright-field microscopy Olympus BX50 (Leica, Germany). Hand-cut sections were stained in 0.05% Toluidine blue for 30 seconds or stained for lignin with phloroglucinol in 1M HCL for 0.5 minutes. Photographs were taken with Olympus DP70 (Olympus America Inc., USA) Camera.

Sugarcane leaf starch assays. Leaf disks (1 cm diameter) were collected from 4-month-old wild-type and transgenic sugarcane and depigmented with ethanol to remove chlorophylls. After rinsing with distilled water, the samples were stained with 1% Lugol's IKI solution at RT for 5 minutes and rinsed again with distilled water. Images were captured with a Sony DSC-HX200V digital camera. Enzymatic starch assay was performed as previously described⁷². Student's two-tailed t-test was performed to compare two groups.

Photosynthesis. Photosynthetic parameters were measured using intact sugarcane leaf +1 of 5 month-old plants with LI-COR Biosciences model LI-6400 (USA). The chamber light (PAR) level was set to 2000 $\mu\text{mol photons m}^{-2}\text{s}^{-1}$ and reference CO_2 to 400 $\mu\text{mol mol}^{-1}$.

Hormone analysis. Internode samples were ground, lyophilized and sent to Proteomics & Metabolomics Facility at the Center for Biotechnology/ University of Nebraska - Lincoln for gibberellin hormone analysis. Data analysis for GA_1 , GA_3 and GA_4 were performed using liquid chromatography combined with mass spectrometry LC-MS/MS.

Illumina sequencing. Total RNA from leaf, apical shoot and 5th and 9th internodes tissues from 6-month-old sugarcane plants were extracted according to the protocol from Spectrum Plant total RNA kit (Sigma-Aldrich). Samples were treated with RQ1 RNase-Free DNase (Promega, USA) according to manufacturer's protocol. For each tissues, we used three independent lines, each containing the pooled RNA from four biological replicates. One microgram of each RNA sample was used to produce libraries which were sequenced using Illumina HiSeq 2500 by Fasteris Life Science Co. (Geneva, Switzerland). The reads were mapped on *Sorghum bicolor* reference genome available in the [Illumina iGenomes \(http://support.illumina.com/sequencing/sequencing_software/igenome.html\)](http://support.illumina.com/sequencing/sequencing_software/igenome.html). The list of DEGs were identified using an FDR q-value cutoff of 1e-5.

Metabolite profile analysis. Five mg of grounded and lyophilized tissues from leaf, apical shoot and 5th and 9th internodes from four biological replicates plants (6 month-old) were extracted using

MTBE: methanol:water 3:1:1 (v/v/v). The 100 µl of the organic phase was dried and derivatized. Then 1 µl of the derivatized samples were analyzed using a Combi-PAL autosampler (Agilent Technologies GmbH, Waldbronn, Germany) coupled to an Agilent 7890 gas chromatograph connected to a Leco Pegasus 2 time-of-flight mass spectrometer (LECO, St. Joseph, MI, USA). Chromatograms were exported from Leco ChromaTOF software (version 3.25) to R software. Peak detection, retention time alignment, and library matching were performed using Target Search R-package⁷³. Metabolites were quantified by the peak intensity of a selective mass. Metabolites intensities were normalized by dividing the fresh-weight, followed by the sum of total ion count and global outlier replacement. Principal component analysis was performed using *pcaMethods* bioconductor package⁷⁴. The significance of metabolites was tested by comparing all genotypes in a given tissue by Tukey-test.

3.4 Results

3.4.1 *ScGAI* encodes a DELLA protein.

Using the SUCEST project database (<http://www.sucest-fun.org/>), we have identified and cloned the *ScGAI* gene in sugarcane. The *ScGAI* gene presents an open reading frame (ORF) of 1878 bp and encodes a protein with 625 amino acid residues. The *ScGAI*-deduced amino-acid sequence contains all conserved regions of DELLA proteins, including the N-terminal DELLA regulatory domain that contains the DELLA, TVHYNP, and poly S/T/V motifs and a C-terminal GRAS domain which comprises the leucine heptad repeats (LHI and LHII) that flank the VHIID motif, and the PFYRE and SAW motifs (Fig. 1a). However, curiously, *ScGAI* exhibited an L-to-M³⁹ point mutation (DEMLA) within the DELLA motif, which is also conserved in the SbD8 protein from sorghum. Likewise, the *Arabidopsis* DELLA protein AtRGL3 also shows an L-to-F³⁶ point mutation in this region, which does not prevent its interaction with AtGID1s receptors²⁹. Although the hydrophobic DELLA and TVHYNP motifs are important for interacting with GA receptors and effecting GA-sensitive DELLA degradation¹², a recent study confirmed that the DELL amino acid residues are not required for this interaction¹³. The predicted tertiary structure of the DELLA domain from *ScGAI* showed highly molecular spatial similarity to the solved domain structure of the AtGAI protein from *Arabidopsis* (Fig. 1b). Nevertheless, it is worth to note the presence of a Glycine-rich region (G⁶⁷xGGxGG⁷³) encompassing amino acids within the loop 2-3 in *ScGAI* protein. The sequence GxGG seems to be specific for monocot DELLA proteins (Fig. 1b). Glycine-rich loops or P-loops

are known to function as ATP-binding pocket⁷⁵, but further experiments are needed to elucidate their function in monocot DELLA proteins. Phylogenetic analysis revealed that ScGAI is highly homologous to SbD8 and ZmD8 proteins in sorghum and maize, respectively. The evolutionary divergence of DELLA proteins in monocot plants is clearly lower in comparison with that in proteins from dicotyledonous plants (Fig. 1c). This result reflects the fact that only one copy of *DELLA* gene is found in the majority of monocot species.

DELLA proteins are widely known as nuclear transcriptional regulators. Therefore, we investigated the subcellular localization of ScGAI by transient expression of VENUS-tagged ScGAI in *Arabidopsis* mesophyll protoplasts and tobacco leaf epidermal cells. ScGAI was predominantly localized in the nucleus (Fig. 1d-e), corroborating the presence of a putative SV40-like sequence (K¹⁸²RMK¹⁸⁵) before the poly S/T/V region and one well-defined bipartite NLS sequence (R²⁸¹KVAAYFGEALARR²⁹⁴) localized in the LH domain.

structure has a RMSD (root-mean-square deviation) value of 0.091. (c) Phylogenetic relationship and evolutionary divergence of DELLA family in Arabidopsis, tomato, pea, grape, barley, wheat, rice, maize, sorghum and sugarcane. The red branch and the dashed square in the evolutionary divergence correlation matrix table underline the conserved DELLA family in monocotyledonous plants. (d) and (e) Subcellular localization of ScGAI expressed in Arabidopsis mesophyll protoplast and tobacco leaf epidermal cells, respectively. The construct *AtPARP3:mCHERRY* (mCHERRY) was used as nuclear control. DIC means differential interference contrast. YFP means yellow fluorescent protein. Bars = 20 μ m.

Then, we asked whether ScGAI is indeed a functional protein involved in GA signaling. As shown in Fig. 2d, overexpression of *ScGAI* in *Arabidopsis* repressed GA responses, such as rosette diameter and stamen development, phenotypes also observed in the dominant GA-insensitive *Arabidopsis gai-1* mutant, that lacks a segment of 17 amino acids within the DELLA domain ⁷⁶. Collectively, these results demonstrated that ScGAI acts as bona-fide DELLA protein.

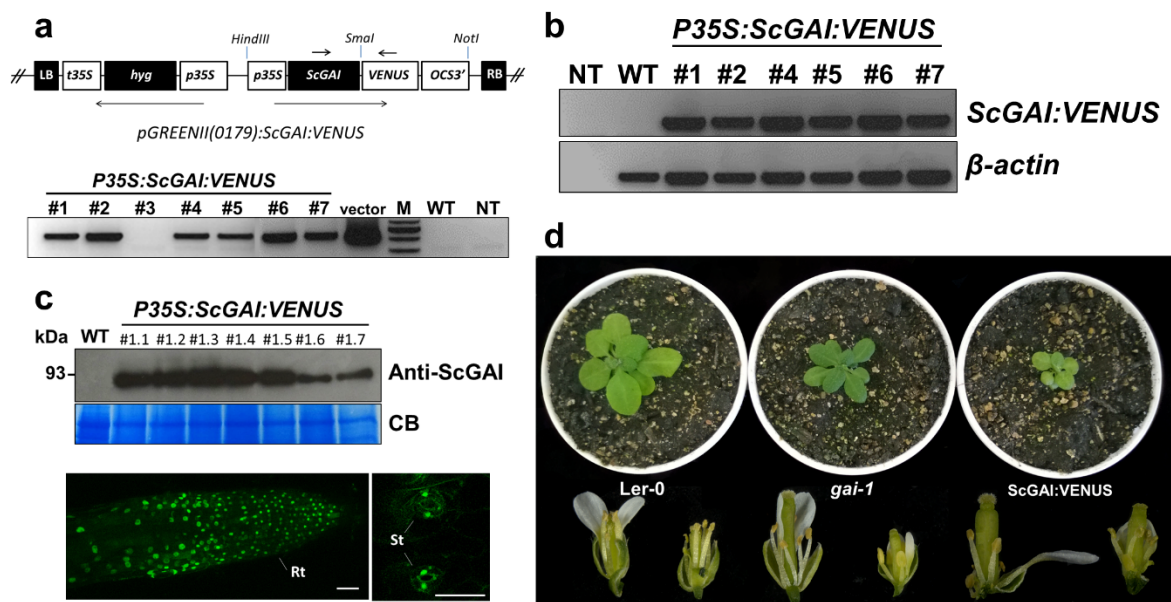


Fig. 2. ScGAI:VENUS fusion protein represses the GA-responses in transgenic *Arabidopsis*.

(a) Above, schematic representation of the *pGREENII(179):ScGAI:VENUS* fusion construct. LB and RB: left and right borders on the T-DNA, respectively; P35S: 35S promoter; T35S: 35S terminator; OCS3': *octopine synthase* terminator; Hyg: hygromycin resistance gene. Below, *ScGAI* transgene integration in transgenic plants using specific primers as indicated with an arrow in the diagram. (b) RT-PCR analysis of *35S:ScGAI:VENUS* expression in transgenic plants. The β -actin gene was used as a loading control. WT: wild type; NT: non-template. (c) Above, immunoblot analysis of *ScGAI:VENUS* fusion protein from T2 generation. WT: wild type; CB: Commassie blue-stained membrane as loading control. Below, nuclear fluorescent signal of *ScGAI:VENUS* fusion protein in root tip (Rt) and stomata (St) visualized by confocal laser microscopy. Bars = 50 μ m. (d) Two-week-old *ScGAI:VENUS* transgenic *Arabidopsis* showing a dwarf phenotype in comparison with wild-type (Ler-0) and gibberellin-insensitive (*gai-1*) mutant, and floral buds with short stamen filaments in *gai-1* and *ScGAI:VENUS* plants.

3.4.2 ScGAI was most expressed in the shoot apex whereas GA₃ content was highest in the mature part of the culm.

In sugarcane, *ScGAI* showed the highest expression level in the shoot apical meristem (SAM) (Fig. 3a) corroborating with the expression pattern of *DELLA* genes in the SAM of *Arabidopsis*, tomato and rice⁷⁷⁻⁷⁹. Moreover, western-blot analysis showed that the *ScGAI* protein is not only highly abundant in the SAM, but that it is also present in elongating internodes of the sugarcane stem (Fig. 3b). Previous studies have demonstrated that high cytokinin (CK) and low GA

levels are required for normal SAM function in plants^{80,81}. Also, we demonstrated that bioactive GAs are low at the apical shoot and increase along the stem (Supplementary Fig. S1). However, it is worth to note that among the bioactive GA₁, GA₄ and GA₃, only GA₃ was detected in higher concentration in the mature internodes. GA₃ is formed from GA₂₀ using the intermediate GA₅, which is present in several monocotyledons⁸². It is therefore possible that sucrose upregulates *ScGA20ox* (GA20 oxidase; GA synthesis) expression level and consequently the GA production in the mature internodes⁸³ (Supplementary Fig. S1). Another possible reason for this high level of GA in the basal internodes may be its role as an important regulator of lignification⁸⁴, a process more pronounced with stem maturity in sugarcane. Further studies are needed to elucidate the synthesis, transport and action of GAs in sugarcane.

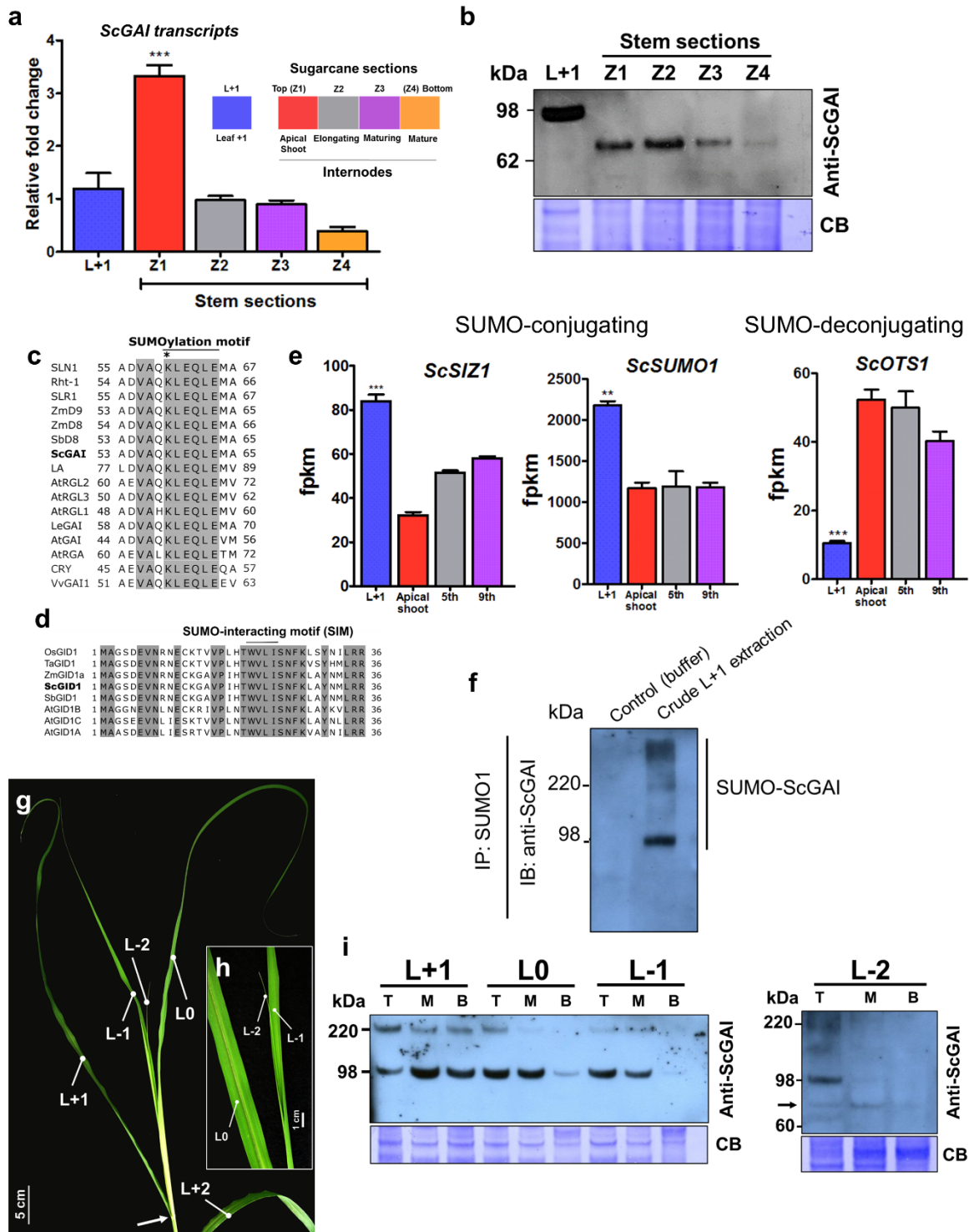


Fig. 3. ScGAI is SUMOylated in sugarcane leaves.

(a) Expression profile of native *ScGAI* in different tissues of 10-months-old sugarcane; Bar plots show means \pm SEM ($n=3$, $P < 0.05$; one way ANOVA followed by Bonferroni multiple comparisons post-test). (b) Immunoblotting of *ScGAI* protein in sugarcane tissues. (c) Sequence alignment of the noncanonical SUMOylation motif in DELLA proteins. Asterisk represents the conserved

SUMOylation site lysine residue. **(d)** Sequence alignment of GID1 from rice, wheat, maize, sorghum, *Arabidopsis* and sugarcane displaying the SUMO-interacting motif (SIM). Light gray depicts the conserved amino acids among the sequences. **(e)** Expression profile analysis of *ScSIZ1*, *ScSUMO1* and *ScOTS1* transcripts in leaf +1, 5th and 9th internodes. FPKM means fragment per kilobase of exon per million fragments mapped. Bar shows means \pm SEM (n=3, P< 0.05; One way ANOVA followed by Bonferroni multiple comparisons post-test). **(f)** Immunoprecipitation using anti-SUMO1 antibodies in crude extract of leaf +1. **(g)** The leaf numbering system proposed by Kuijper⁸⁵. The first fully-expanded leaf with visible dewlap (indicated by an arrow) and photosynthetically active was considered as leaf +1. **(h)** Close-up view of the juvenile leaf -2. **(i)** Immunoblotting of the ScGAI protein in different sections of juvenile (L0, L-1 and L-2) and fully-expanded (L+1) leaves of Q208 (one-month-old). The arrow indicates the non-SUMOylated ScGAI protein. Equal amount of protein samples (10 μ g) was loaded. CB, Commassie blue-stained membrane as loading control. T: tip; M: middle; B: base; MB: midrib base.

3.4.3 ScGAI is a regulatory component of spatio-temporal leaf growth in sugarcane, and its action is modulated by SUMOylation.

ScGAI was present in leaf +1, the youngest fully expanded leaf, with an approximate molecular weight (MW) of 98 kDa (Fig. 3b), which is higher than the predicted MW of 66 kDa found in the stem tissues and also in His-tagged ScGAI expressed in *Escherichia coli* (Supplementary Fig. S2). The DELLA protein has recently been reported to have a larger size than its theoretical MW probably due to post-translational modification by small ubiquitin-like modifier (SUMO) protein. SUMOylation modulates DELLA protein abundance despite unchanged *DELLA* transcript levels³⁹. SUMO interacts with DELLA proteins through a covalent binding in the N-terminal DELLA domain. SUMOylated DELLA interacts with the GA receptor GID1 through the SUMO-interacting motif (SIM) in a GA-independent manner³⁹. This SUMO-SIM interaction sequesters GID1, blocking its access to the DELLA domain, and consequently, preventing the GA-triggered DELLA degradation. Interestingly, ScGAI contains a conserved SUMOylation motif within the DELLA domain, and the GA receptor ScGID1 also harbours the SIM motif⁴⁹ (Fig. 3c-d). Moreover, expression profile analysis of the E3 SUMO ligase *ScSIZ1* and *ScSUMO1* genes involved in the covalent SUMO-conjugation process showed significantly higher level of expression in leaf +1 in comparison with internodes in sugarcane. On the other hand, the expression level of the SUMO protease OVERLY TOLERANT TO SALT1 *ScOTS1* gene, which mediates the deconjugation of SUMO, was drastically reduced in the leaf +1 (Fig. 3e). To confirm the sumoylation of ScGAI, we immunoprecipitated protein lysates using anti-SUMO1 antibodies, confirming that, the high MW band is indeed the SUMOylated ScGAI (Fig. 3f). In order to obtain more insights into the SUMOylation of ScGAI in

leaves, we analyzed different sections (tip, middle and base) of juvenile (0, -1 and -2) and fully-expanded (+1) leaves. ScGAI was SUMOylated in the mature tissues of the juvenile and fully-expanded leaves, but surprisingly, the SUMOylated ScGAI was gradually reduced in the middle and base sections of young developing leaves, where cell elongation and division occur⁸⁶ (Fig. 3i). In addition, we also observed the 66 kDa band (non-SUMOylated ScGAI) in the middle and base sections of the youngest leaf -2. Taken together, the results indicate that SUMOylation is a regulatory component for the ScGAI protein to control the leaf growth in a spatio-temporal manner in sugarcane.

3.4.4 *ScGAI*-misexpression alters sugarcane morphology.

To elucidate the role of ScGAI in sugarcane, we genetically manipulated *ScGAI* gene expression by overexpression (ScGAI OE) and hairpin-mediated silencing (HpScGAI) (Supplementary Fig. S3). ScGAI OE lines displayed a high *ScGAI* transgene expression level, while HpScGAI lines showed a reduced expression level of the *ScGAI* gene (Supplementary Fig. S4). As shown in Fig. 4a-b, the *ScGAI*-misexpressing lines displayed a range of alterations.

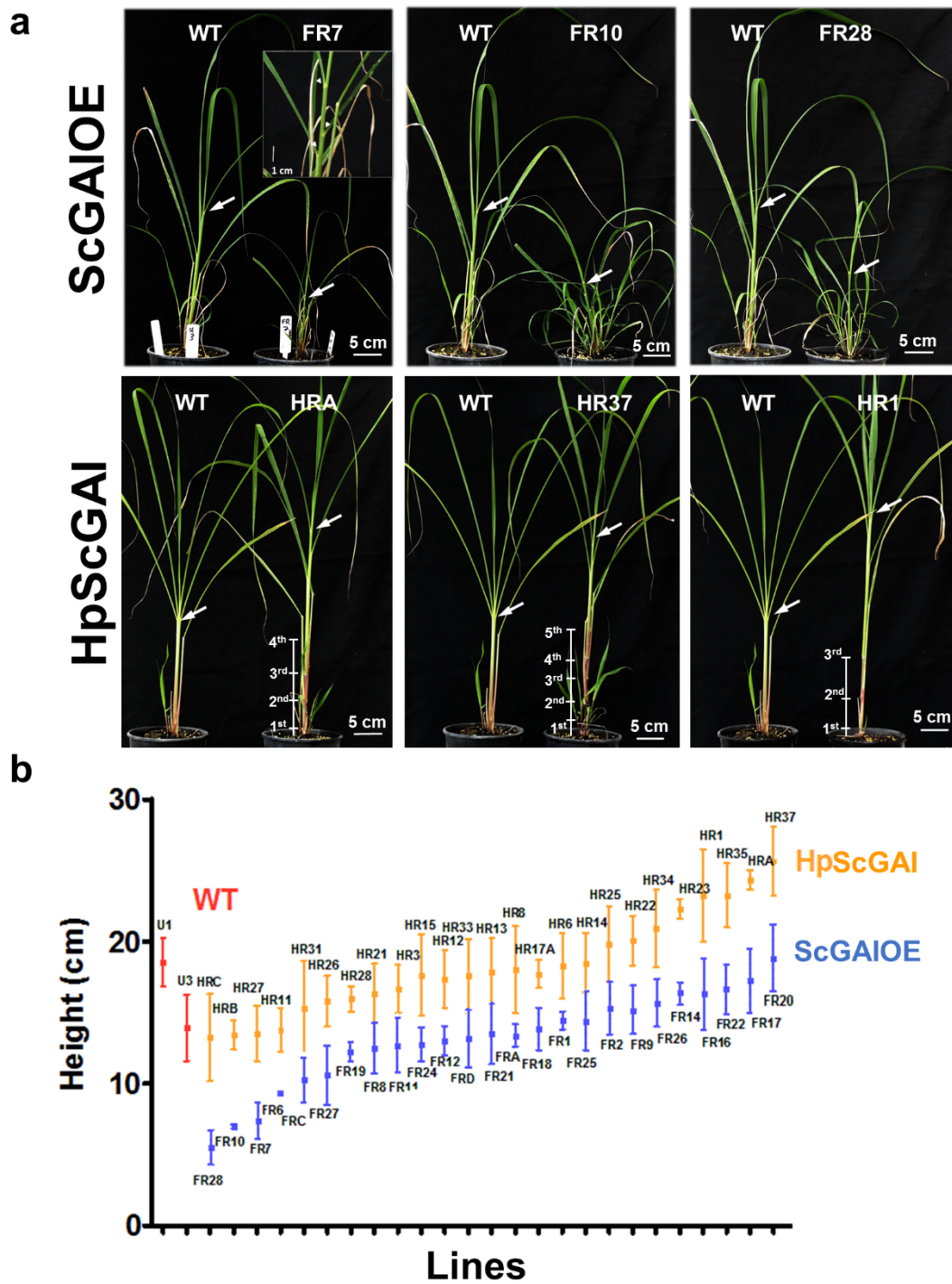


Fig. 4. *ScGAI*-misexpressing sugarcane lines.

(a) The extreme phenotype of *ScGAIOE* and *HpScGAI* lines showing the stunted and taller stems, respectively, with earlier onset of elongated internodes (in *HpScGAI*) in comparison to wild-type (WT) plants. Arrows indicate the first visible dewlap. (b) Height of sugarcane plants. Bar shows means \pm SEM ($n=3$). The lines U1 and U3 in red color represent WT plants.

The most extreme phenotypes could be clearly distinguished from wild-type (WT) plants, showing a shorter stature with high tillering capacity in ScGAI OE, and a taller stature with early onset of visible nodes and internodes in HpScGAI plants (Fig. 5b-c). In addition, silenced plants also showed an unaltered stem diameter throughout development (Supplementary Fig. S5). On the other hand, we could not observe a great difference in the length of fully-expanded leaf +1 among the juvenile plants (Fig 5d). As discussed above, SUMOylation seems to coordinate sugarcane leaf development through appropriate spatio-temporal ScGAI stabilization. As shown in Fig.5a, SUMOylated ScGAI protein levels were unaltered in leaf tissues among the *ScGAI*-misexpressing lines.

To assess whether changes in the morphology were accompanied by changes in the cellular anatomy, we made cross-sections of the leaves and stem of transgenic and WT plants (Supplementary Fig. S6). We did not observe any anatomical differences in the leaves. However, as expected, we could see a juvenile stem with a set of young rolled leaves in WT and ScGAI OE plants, and conversely, a ground tissue composed of storage parenchyma cells and vascular bundles in the HpScGAI stem, reinforcing the developmental acceleration in those plants. In agreement with this fast development rate, lignification of the basal internodes in these silenced plants was evident from reddish-brown coloration after phloroglucinol-HCl staining (Supplementary Fig. S6). In summary, our results demonstrated that misexpression of ScGAI affects stem growth, tiller numbers, and internode elongation in sugarcane.

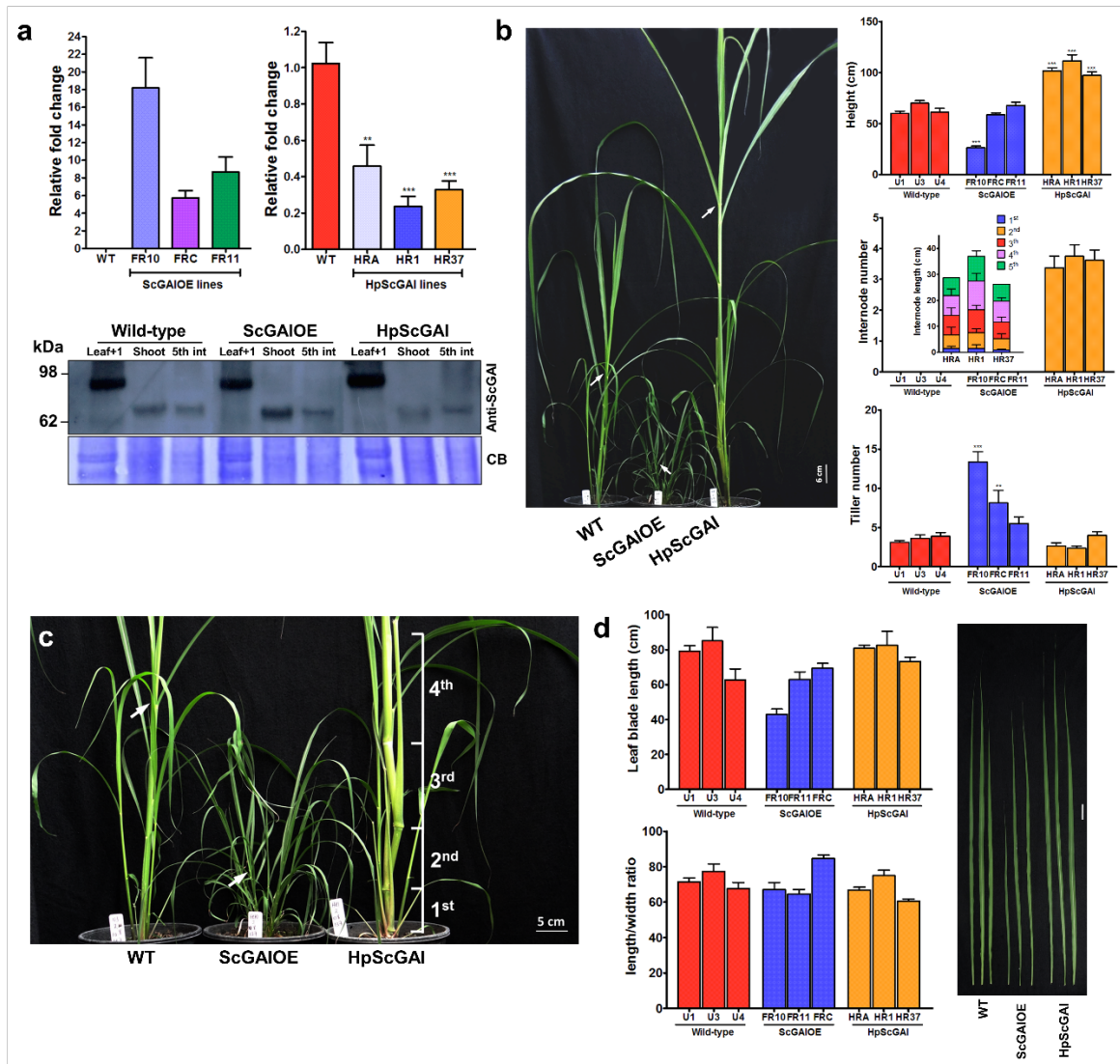


Fig. 5. ScGAI regulates tillering, stem growth, and represses internode elongation in sugarcane plants.

(a) Above, *FLAG:ScGAI* and endogenous *ScGAI* expression levels in transgenic lines; Below, immunoblot using a sugarcane anti-DELLA (Anti-ScGAI) antibody. Each lane was loaded with 20 μ g of total protein from leaf+1, apical shoot (shoot) and 5th internode (5th int) tissues of wild-type, FR10 and HR1 lines of 6-month-old; CB, Coomassie blue. (b) 3-month-old plants. Height, internode number and elongation and tiller number; Bar shows means \pm SEM ($n=8$, $P < 0.05$; One way ANOVA followed by Bonferroni multiple comparisons post-test). (c) Zoomed-in detailed view of 3-month-old plants; Internode numbers counted from soil to top; arrows indicate the first visible dewlap. (d) Leaf +1 blade length and length/width ratio in 2-month-old plants. Sugarcane leaves +1 of 2-month-old plants. Scale bar = 5 cm.

3.4.5 *ScGAI*-misexpressing lines are hypersensitive to GA and paclobutrazol (PAC) treatments.

To get further insight into the role of the GA/ScGAI regulation in sugarcane, we treated transgenic seedlings with exogenous GA₃ or PAC, an inhibitor of GA biosynthesis (Supplementary Fig. S7). Upon PAC treatment, WT plants produced a very short and thick stem. In this respect, HpScGAI plants were slightly less sensitive to PAC, evidencing the lack of the DELLA repressor. On the other hand, ScGAI^{OE} seedlings showed a stronger response to PAC. Strikingly, all PAC-treated seedlings presented an increased root growth, though to a lesser degree in ScGAI^{OE}. As expected, GA₃ treatment rescued the short phenotype of ScGAI^{OE} plants, and HpScGAI plants were hypersensitive to GA₃, showing a slender phenotype, with two-fold longer plants than GA₃-treated WT (Supplementary Fig. S7). These results further demonstrated that the GA-induced degradation of DELLA modulates growth and internode elongation of sugarcane, and that it decreases the root-to-shoot ratio in this plant.

3.4.6 *ScGAI* misexpression alters gene expression profiles.

The phenotypes of *ScGAI*-misexpressing lines suggest that ScGAI protein acts as a regulator of the sugarcane development. In order to get a better understanding of this regulation, we used RNA sequencing (RNA-seq) to identify differentially expressed genes (DEGs) in leaves and internodes of ScGAI^{OE} and HpScGAI plants. Overall, 345 DEGs showed a statistically significant difference between the lines FR10 (ScGAI^{OE}; dwarf line) and HR1 (HpScGAI; tallest line) (Supplementary Fig. S8 and Supplementary Tables S1-S4). In both plants, the highest number of DEGs was found in the stem, mainly in the 9th internode. Among the DEGs related to growth, three *ERF* (*Ethylene-responsive element binding factor*) genes were expressed at high levels in HpScGAI tissues. Two ERF subfamily groups (VII and VIII-B-1a) are known to promote internode elongation in rice and *Arabidopsis*^{87,88}. For instance, the *ScERF9* transcript is the closest relative to the *AtERF11* gene (Supplementary Fig. S9), that was recently found to be involved in GA signaling and internode elongation in *Arabidopsis*⁸⁸. Besides, *Brz-insensitive-long hypocotyls 4* (*BIL4*), a positive regulator of plant cell elongation via brassinosteroid signaling,⁸⁹ had higher expression in HpScGAI plants, indicating the cross-talk with other growth-related hormones. Regarding sugar signaling and energy status, the overexpression of *ScGAI* in ScGAI^{OE} activated several genes related to sucrose transporter and energy-saving responses, such as the Snf1-related kinase 1 (SnRK1) regulatory subunit *KINβ1*,

two key regulators of the starvation response such as the *basic region-leucine zipper transcription factor 63 (bZIP63)* and *dark-inducible 6 (DIN6)*, as well as the trehalose-6-phosphate synthase genes *TPS9* and *TPS11* which are involved in trehalose biosynthesis. All these genes form a network regulating metabolism under stress conditions in order to preserve energy⁹⁰ (Table 1). Therefore, the transcriptomic data corroborate the proposition that ScGAI regulates a transcriptional network governing growth, energy status, and stress responses in sugarcane.

Table 1. Sugar signaling and transporter-related genes upregulated in the ScGAI0E plants.

| Tissues | Annotation | ScGAI0E (FPKM) | HpScGAI (FPKM) | Fold change (Log2) | q-values |
|---------------------------------|---|----------------|----------------|--------------------|-----------|
| Leaf+1 | STP13 - Sugar transporter family protein | 43.3993 | 7.30469 | -2.57078 | 0.032348 |
| | Glucose transmembrane transporter - Polyol transporter 5-like | 18.154 | 1.98172 | -3.19546 | 0.032348 |
| Apical Shoot | SUC3 - Sucrose transporter | 40.2308 | 10.813 | -1.89553 | 0.0264797 |
| | ASN1 - Asparagine synthetase – (DIN6) | 108.814 | 32.1247 | -1.76011 | 0.0264797 |
| | TPS9 - Trehalose-6-phosphatase synthase 9 | 15.7126 | 3.433 | -2.19438 | 0.0264797 |
| 5th internode | TPS11 – Trehalose-6-phosphatase synthase 11 | 76.4698 | 20.5569 | -1.89527 | 0.022577 |
| | TPS9 - Trehalose-6-phosphatase synthase 9 | 42.6613 | 3.28255 | -3.70004 | 0.022577 |
| | BZIP63- Basic leucine zipper 63 | 54.0344 | 9.3616 | -2.52905 | 0.022577 |
| | KINβ1 - SNF1-related protein kinase regulatory subunit beta-1 | 226.435 | 38.5695 | -2.55356 | 0.022577 |
| 9th internode | SWEET7 - Bidirectional sugar transporter | 212.628 | 50.4851 | -2.0744 | 0.037292 |
| | TPS9 - Trehalose-6-phosphatase synthase 9 | 31.7242 | 5.11352 | -2.63319 | 0.045876 |

3.4.7 Metabolite profiling.

In order to investigate the carbon homeostasis in the transgenic plants, we analyzed the metabolome profile in leaves and internodes. This study revealed significant changes in the levels of sugars and amino acids in ScGAI0E leaves, while there were only minor changes in HpScGAI compared to WT leaves (Fig. 6). In agreement with this, the rate of photosynthesis was significantly reduced in the dwarf line (Supplementary Fig. S10), evidencing the low sucrose level in ScGAI0E leaves. However, surprisingly, malate also accumulated to high levels, as observed in PAC-treated *Arabidopsis*⁹¹, suggesting an alternative carbon sink for photosynthates other than sugars in response to the low sink demand in ScGAI0E sugarcane (Fig. 6). Thus, we then asked whether the diurnal rhythm of starch accumulation was also altered in these plants. At dusk, leaves of ScGAI0E plants contained much less starch than HpScGAI and WT plants (Supplementary Fig. S11). Further

enzymatic assay confirmed that starch accumulation was dramatically reduced in ScGAI OE, corroborating with our findings based on RNA-seq data analyses, which suggests that ScGAI OE plants are source-limited. At the sink level, we observed a high accumulation of amino acids in 5th and 9th immature internodes, which can be interpreted as the result of a nitrogen surplus due to limited growth and photosynthesis (Fig. 6). On the other hand, the investment of carbon into storage molecules and prenylpropanoid synthesis was markedly more evident in HpScGAI lines: metabolites such as sucrose, trehalose, galactinol, *myo*-inositol, and 4-caffeoylquinic acid showed higher levels in both internodes (Fig 6). *Myo*-inositol has been described as a central carbon-metabolite used to form the structural basis of signaling lipids, cell wall precursors, and raffinose family oligosaccharides (RFOs) ⁹². Recently, galactinol and raffinose have been proposed as C sink and storage in plants ⁹³. Therefore, our results from metabolome and transcriptome analysis clearly support the hypothesis that changes in growth and primary metabolism are interlinked by ScGAI in sugarcane.

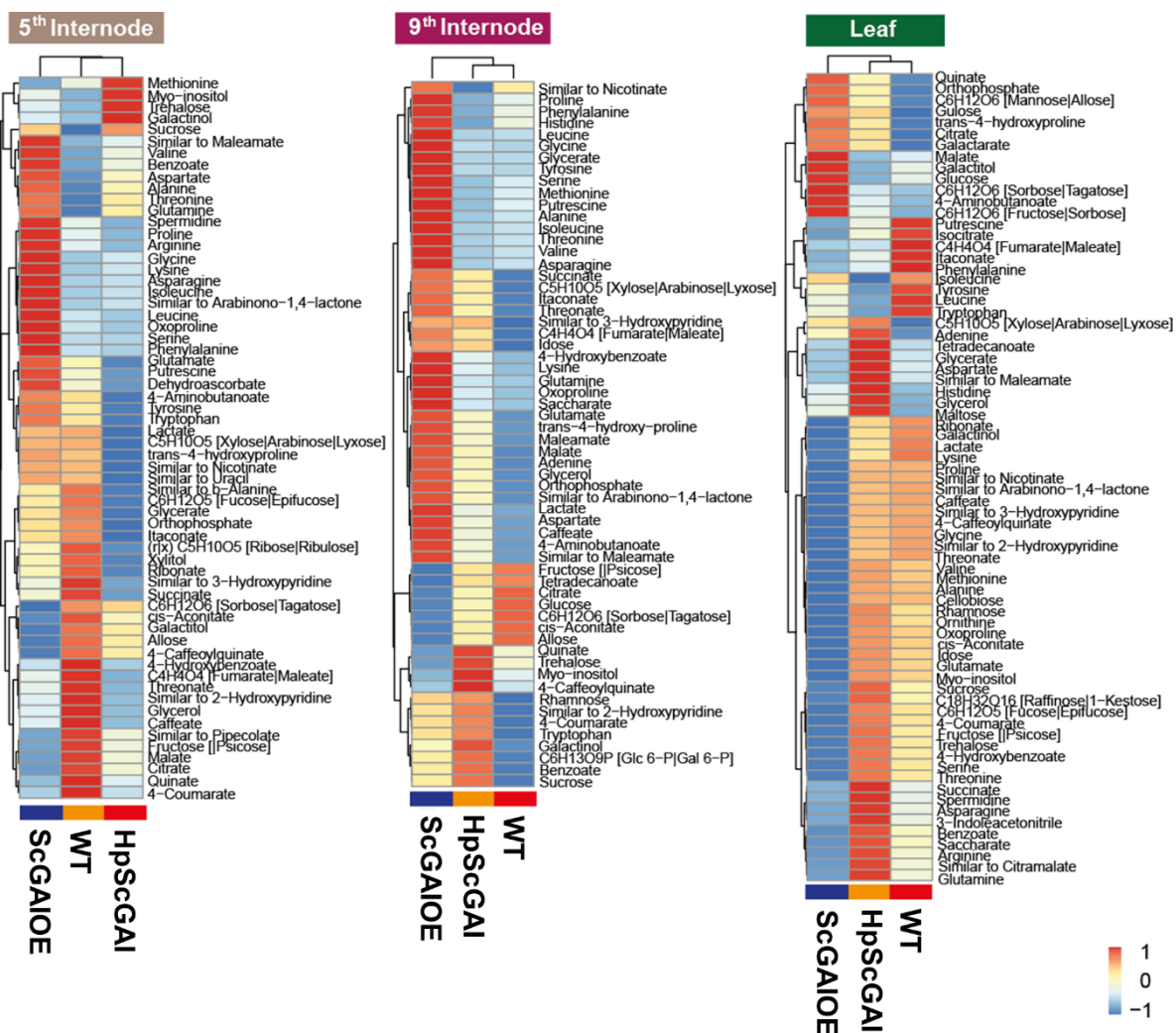


Fig. 6. Carbon balance are severely altered in transgenic plants.

Metabolite-based clustering of leaves and 5th and 9th internodes in ScGAIOE (FR10 line) and HpScGAI (HR1 line) compared to WT. The intensities are color-coded. Red color represents high and blue color low intensities.

3.4.8 ScGAI interacts with ScPIF3/PIF4 and ScEIN3/ScEIL1 proteins.

Our next question was how the ScGAI protein acts in the control of sugarcane growth. It is known that DELLA restrains growth through its interactions with PHYTOCHROME-INTERACTING FACTORS (PIF) proteins²¹. Recently, DELLA and PIF proteins have been proposed as candidates for connecting sucrose status to hormones and environmental signals in plants⁹⁴. We asked whether ScGAI protein interactions are also a conserved mechanism in sugarcane. We identified and cloned three sugarcane PIF protein-encoding genes (*ScPIF3*, *ScPIF4*, *ScPIF5*; Supplementary Fig. S12) and checked their interaction with ScGAI (Fig. 7). Similar to *Arabidopsis*,

we observed that ScGAI physically interacts with ScPIF3 and ScPIF4, but not with ScPIF5 (Fig. 7c-e), demonstrating that the DELLA-interacting proteins seem conserved between monocot and dicot plants. To further explore this interaction network and get more insight into the mechanism of early internode onset in HpScGAI plants, we identified and cloned two key transcription factors of ethylene signaling, *ScEIN3* and *ScEIL1* (Supplementary Fig. S13), homologs of proteins known to modulate the expression of ERF proteins in *Arabidopsis*⁹⁵. Interestingly, ScGAI interacted with both ScEIN3 and ScEIL1 (Fig. 7d-f). Taken together, the results suggest that ScGAI acts by inhibiting other transcription factors through both interaction/sequestration and degradation, as observed for *Arabidopsis*²⁰, indicating that these interactions underpin the mechanistic basis for integrating growth, internode elongation, and the balance between carbon supply and demand in sugarcane plants.

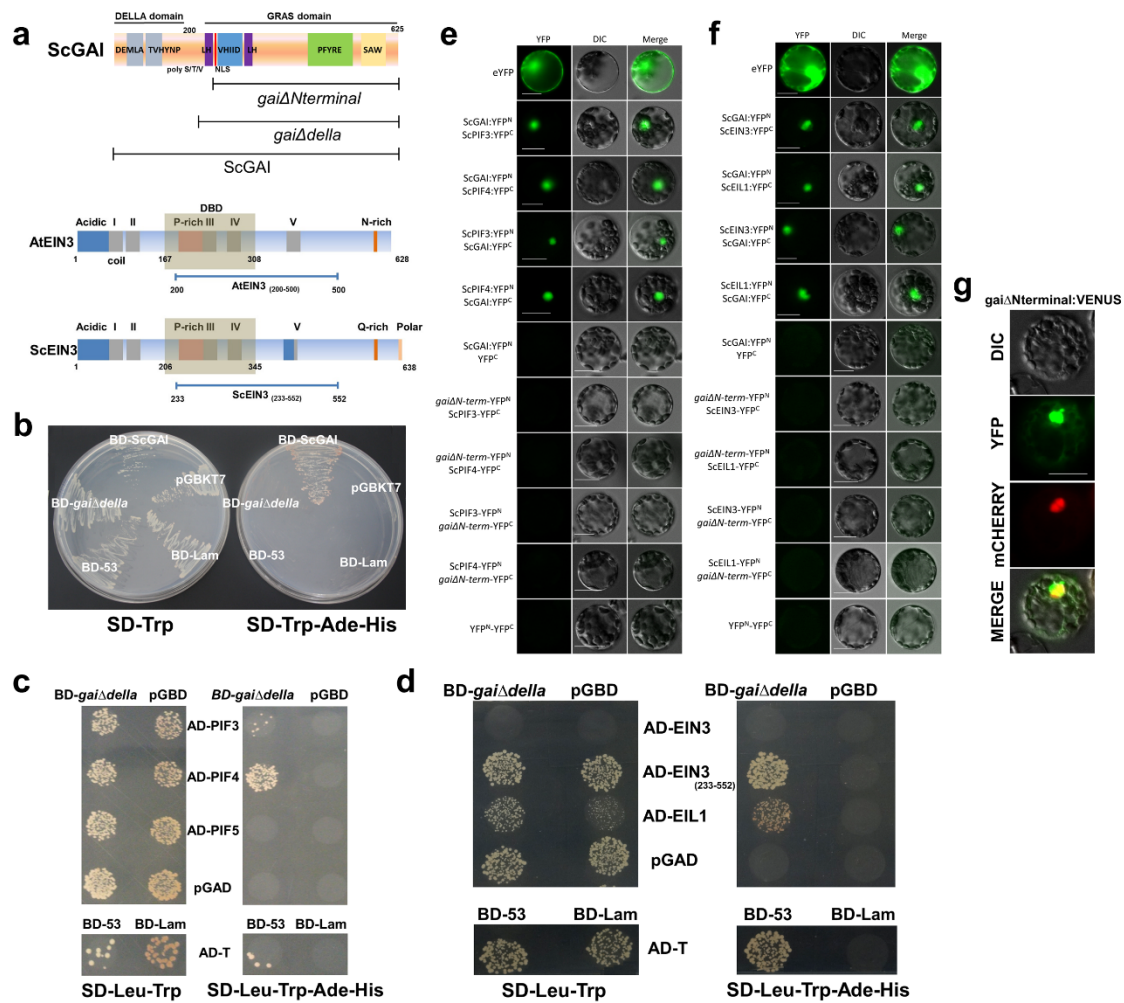


Fig. 7. ScGAI interacts with ScPIF3/4 and ScEIN3/EIL1 in sugarcane.

(a) Structure of the sugarcane DELLA ScGAI and its truncated versions used in the screening. Protein schematic comparison between AtEIN3 and ScEIN3 sequences and the protein truncation ScEIN3(233-522) used in the yeast two hybrid assay. (b) Auto-activation activity of the different bait constructs in yeast cells. Full-length DELLA was capable of activating the transcription of reporter genes in the absence of prey proteins and also be toxic upon expression in yeast cells. (c and d) Co-transformations with different combinations were performed. On SD-Leu-Trp medium, diploid yeast cells were confirmed. On SD-Leu-Trp-Ade-His medium, only positive yeast cells for protein-protein interaction grew. BD, binding domain; AD, activation domain; pGBD and pGAD, empty vectors; Positive controls: 53-BD encodes murine p53 and T-AD encodes the SV40 large T-antigen. Negative Control, Lam-BD encodes lamin. (e and f) BIFC assay was performed in Arabidopsis protoplasts. YFP^N and YFP^C N-terminal and C-terminal yellow fluorescent protein, respectively. (g) Subcellular localization of the truncated protein namely *gaiΔNterminal*:VENUS used as negative control in the BIFC assay. AtPARP3:mCHERRY was used as nuclear control. Bars = 20 μm.

3.5 Discussion

3.5.1 The GA signaling in sugarcane

Here we shed light on the role of the GA signaling in the sugarcane development through the molecular characterization of the ScGAI protein. Sugarcane seems to have a putative single-copy of the *ScGAI* gene, as described in other monocot such as rice and barley. Nevertheless, it is noteworthy that the modern cultivated sugarcane are interspecific hybrids composed by 80-90% of chromosomes derived from *Saccharum officinarum* ($2n=8x=80$) and 10-20% derived from *Saccharum spontaneum* ($2n=5x-16x=40-128$)⁹⁶. In the hexaploid wheat, which contains three A, B and D genomes, a single-copy of the *DELLA* gene (*Rht-1*; for Reduced height-1) is present per genome⁹⁷. Thereby, further studies on genetic and comparative mapping are needed to elucidate the number of *ScGAI* haplotypes in the hybrid genome of the sugarcane.

Nevertheless, given the importance of the ScGAI in the sugarcane development and in the integration of several pathways, its expression must be precisely regulated to provide the GA homeostasis. For instance, we demonstrated the highest *ScGAI* expression level in the SAM, which reinforces the low GA levels required for the proper meristem development⁸¹. On the other hand, the lowest *ScGAI* expression level could be observed in the basal internodes, where GA₃ showed the highest level in the sugarcane tissues. Such results provides some new clues for elucidating the action and transport of GA in sugarcane.

ScGAI regulates leaf and stem elongation in sugarcane

Leaf growth may be divided into temporal and spatial organization. In sugarcane, considering the developmental timing, the leaf+1 is considered fully-expanded and most photosynthetically active. This leaf may be easily identified through the most recently visible dewlap between leaf blade and leaf sheath in sugarcane (Fig. 3g). The upper whorl of leaves are still elongating and growing, being the spindle leaf (i.e., leaf -2) the youngest one with its tip just visible (Fig. 3h). Spatially, in monocot leaves, the linear organization is comprised by dividing cells at the base, followed by expanding cells and finally mature cells at the tip. Recently, the role of bioactive GAs in the spatial control of leaf growth has been clarified⁹⁸. A local and very narrow peak of GA is present at the transition (i.e., at the base) between the division and expansion zones of maize leaves. In our study, surprisingly, we found evidence supporting that SUMOylation plays a role in leaf

growth through stabilization of the ScGAI protein. This strongly supports the idea that GA targets SUMOylated ScGAI for destruction in the immature tissues of younger leaves in the upper whorl, whereas DELLAs have been described to restrain both cell division and expansion rate in *Arabidopsis* leaf growth⁹⁹. Therefore, we propose that SUMO-mediated ScGAI stabilization represses growth of the mature leaf tissue, and in contrast, increased non-SUMOylated ScGAI results in a decreased repression in elongating and dividing leaf tissue (Fig. 8).

SUMOylation also plays a central role in environmental responses such as drought and salt stress. In rice and *Arabidopsis* plants, OTS SUMO proteases are rapidly degraded upon salt stress, leading to an increase in the SUMO conjugation of target proteins^{100,101}. Previous work has shown that drought stress slows leaf elongation in sugarcane, which reduces photosynthetic area and total plant photosynthesis⁵¹. In addition, recently, GA biosynthesis was demonstrated to be downregulated in sugarcane leaf under drought stress⁸. Therefore, the fact that SUMO binds to ScGAI, leads us to speculate that, as in *Arabidopsis* and rice, OTS protease degradation may contribute to hyperSUMOylation and stabilization of ScGAI in the elongating and dividing sections of younger sugarcane leaves upon abiotic stresses, acting then as a rapid growth retardation mechanism. Our study is the first step in elucidating the function of ScGAI in the leaf growth. Future work should be directed toward the determination of whether ScGAI-dependent growth control is a GA-independent mechanism in the elongating and dividing sections of younger leaves upon drought stress.

In stem growth, the SUMOylation process does not seem to be involved in the regulation of the ScGAI protein. ScGAI showed a molecular weight of the 66 kDa in the upper internodes (Fig. 3b). Besides, the highest levels of the *ScOTS1* expression along the stem (Fig. 3e), suggest an attenuation and repression of SUMO conjugation of target proteins. Nevertheless, we do not discard the possibility that SUMO-conjugated ScGAI may restrain growth in the stem, as a rapid mechanism, under abiotic stresses. Further studies will be needed to address this question.

In sugarcane, growth inhibitors or ripeners based on hormones such as Moddus, an inhibitor of GA biosynthesis, or Ethephon an ethylene-releasing compound, are commonly used on the field in order to restrain stem growth and in turn to enhance sucrose content closer to harvest. In a recent work, we demonstrated that Ethephon-treated sugarcane showed a stunted stem and an upregulated *ScGAI* expression level in the upper internodes¹⁰². Corroborating with this observation, the present results using *ScGAI*-misexpressing sugarcane confirmed that ScGAI regulates stem growth and represses internode elongation (Fig. 5). We observed that while stem elongation was

inhibited, tillering was promoted by GA signaling repression in sugarcane (Fig. 5b). Conversely, the silencing of *ScGAI* gene resulted in a constitutively active GA response and an earlier onset of internode elongation. Therefore, our above-mentioned results provide compelling evidence that ScGAI regulates leaf and stem growth in sugarcane.

ScGAI is a central hub for integration of growth and energy metabolism in sugarcane

We modified the source-sink relationship through the modulation of *ScGAI* expression in sugarcane. Our results demonstrate that ScGAI coordinates the interaction between energy metabolism and GA-mediated control of growth in sugarcane. ScGAI upregulated several marker genes for energy deprivation in dwarf plants (table 1). Among them, SnRK1 is widely known as the central integrator of low energy signaling in plants⁹⁰. Corroborating with our observation, recently, the SnRK1/DELLA interaction has emerged from interactome studies in *Arabidopsis*, which demonstrated that the DOMAIN OF UNKNOWN FUNCTION (DUF) 581-2 proteins may mediate the cross-talk of both proteins¹⁰³. Such results could explain how plants communicate to modulate growth with appropriate channeling of energy resources and nutrients in plants.

Starch and sucrose were reduced in ScGAI OE leaves. Conversely, glucose and malate were found at high levels in leaves, indicating that these alterations are likely due to the sink limitation in ScGAI OE. Sugars have been shown to act as signaling molecules to regulate sugarcane photosynthesis⁷. In line with these results, photosynthetic rates were reduced in those plants, corroborating with previous studies showing that sink demand regulates photosynthesis through a feedback mechanism mediated by hexose accumulation in the leaves^{5,54}. However, on the other hand, it is interesting to note that the photosynthetic rate in HpScGAI plants did not show a significant difference in comparison with WT plants. This indicates that other limiting factors besides increased sink strength may be regulating photosynthesis in sugarcane. Further detailed carbon acquisition studies will be needed to understand the photosynthetic plasticity in sugarcane.

In the stem, immature internodes partition carbon into protein and fiber, while mature ones partition mainly into sucrose for storage⁵¹. In our study, ScGAI OE plants showed a higher level of amino acids and metabolites associated with the tricarboxylic acid (TCA) cycle in the internodes. These results are comparable to studies on *Arabidopsis* plants, where an increase in the levels of amino acids was also observed under PAC treatment⁹¹. On the other hand, silenced plants presented a higher level of trehalose, myo-inositol, galactinol and sucrose in those internodes. Corroborating with our observation, a previous study of the sugarcane metabolome during stem development

demonstrated that metabolites such as trehalose and raffinose showed a positive correlation with sucrose accumulation along the stem ¹⁰⁴.

From all the results presented here, it is clear that the ScGAI/GA regulon integrates growth and carbon availability in sugarcane. To add another piece to the puzzle of growth-sugar-hormone cross-talk in sugarcane, we also showed that ScGAI interacted directly with the ScPIF3 and ScPIF4 proteins (Fig. 7). GA and PIFs are essential to promote growth under carbon availability at night in plants ¹⁰⁵, which substantiates the fact that sugarcane stem elongation occurs primarily at night ¹⁰⁶. Furthermore, in *Arabidopsis*, sucrose was shown to upregulate the transcript levels of PIF1, 3, 4, 5 in the darkness only in the presence of GA ⁸³. Based on observations, we may infer that ScGAI interacts with ScPIFs, leading to their sequestration and destabilization, and consequently impairing their DNA-binding capacity in targeting growth-related genes during the night. On the other hand, via EIN3 ethylene promotes stem elongation in light-grown plants by increasing PIF3 expression ¹⁰⁷. Similar to *Arabidopsis* ¹⁰⁸, the interaction with ScGAI likely destabilizes ScEIN3/ScEIL1 proteins suggesting that ScGAI is likely a regulation point between gibberellin and ethylene cross-talk to modulate growth in sugarcane. All these observations support the phenotypes observed in *ScGAI*-misexpressing plants. Collectively, we have shown that ScGAI by acting as an integrator of sugar-hormone cross-talk plays a central regulatory role in sugarcane growth, development and sugar metabolism (Fig 8).

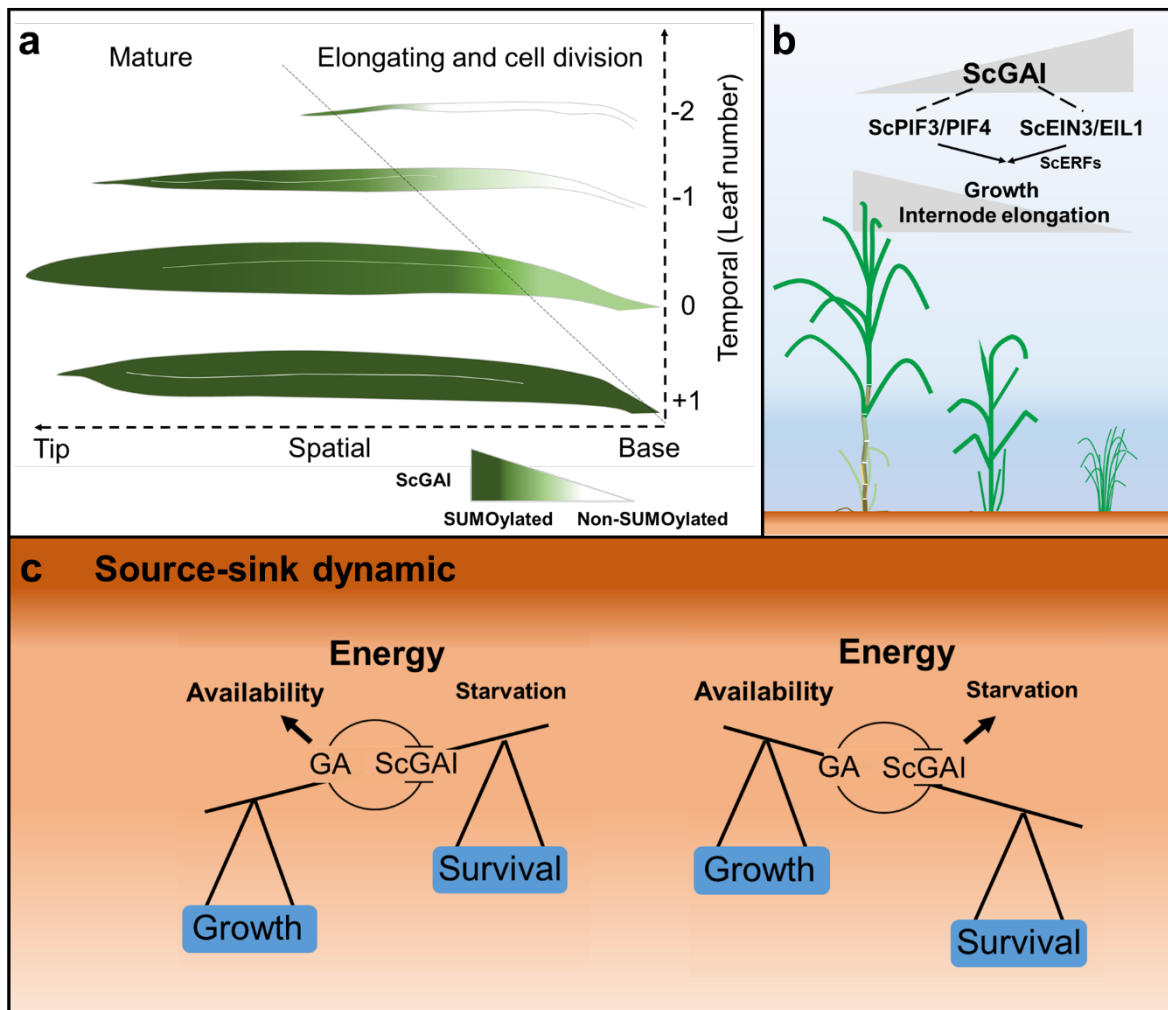


Fig. 8. ScGAI coordinates growth and energy status in sugarcane plants.

(a) Schematic illustration of the sugarcane leaf growth. Spatially, the growth occurs unidirectionally from the base to the tip, and it decreases with time, being the leaf +1 the youngest fully-expanded and photosynthetically active. ScGAI is SUMOylated in a spatio-temporal manner. (b) In stem, the modulation of the ScGAI expression level allows sugarcane to control growth, internode elongation and tillering. Dashed lines indicate the protein-protein interactions. (c) GA/ScGAI regulon promotes carbon supply-demand balance in sugarcane. Fluctuation of energy status is a part of plants' adaptive response in order to reach energy homeostasis to plant growth and survival. For this, plants coordinate hormone-dependent growth responses to manage growth under varying nutrient supply and environmental stresses. In sugarcane, GA and ScGAI (DELLA) integrate energy status and growth in the source-sink.

4 Concluding remarks

In this study, we demonstrated that ScGAI is involved in the control of leaf and internode elongation in sugarcane. Thereby, the *ScGAI* gene expression regulation is an important factor for the sink strength and, therefore, in the involvement of the source-sink communication. This conclusion may be observed in the *ScGAI*-misexpressing sugarcane, in which the overexpression of *ScGAI* (decreasing sink) caused an energy deficit and the upregulation of various starvation-related genes in those plants. On the other hand, silenced plants (increasing sink capacity and assimilate demand) showed a balance source supply at a whole-plant level. Therefore, we provided important insights into the source-sink and hormone cross-talk in sugarcane.

5 Supplementary Materials

DELLA Coordinates Growth and Energy Status in Sugarcane Plants

Rafael G. Tavares, Prakash Lakshmanan, Edgar Peiter, Anthony O'Connell, Camila Caldana, Renato Vicentini, Jose S. Soares, Marcelo Menossi*

correspondence to: menossi@lgf.ib.unicamp.br

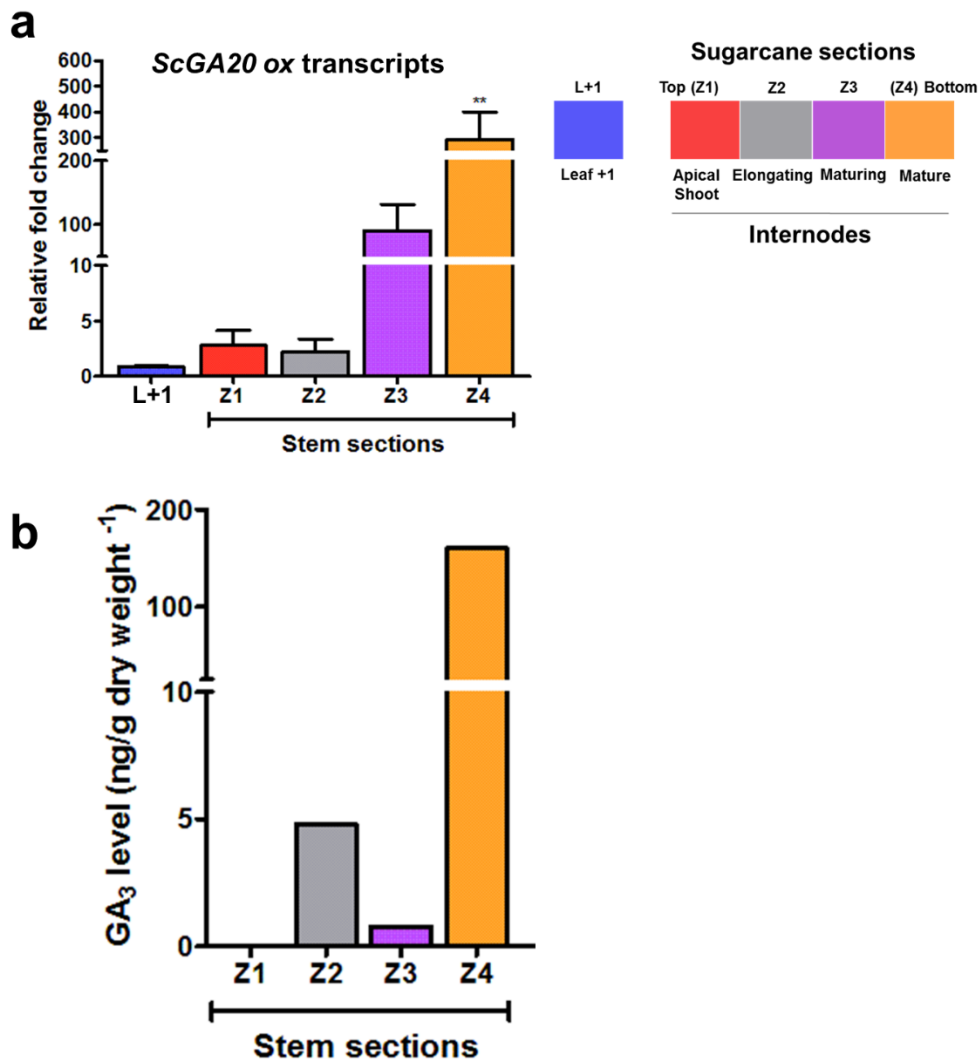


Fig. S1. GA hormone is highly synthesized in the basal internodes in sugarcane.

(a) Expression profile of the native *ScGA20 oxidase* gene in different tissues of 10-months-old sugarcane; Bar plots show means \pm SEM ($n=5$, $P < 0.05$; one way ANOVA followed by Bonferroni multiple comparisons post-test). (b) GA₃ hormone level in sugarcane tissues. Neither GA₁ nor GA₄ were detected in the analyzed samples. Each samples correspond to a pool from five biological replicates.

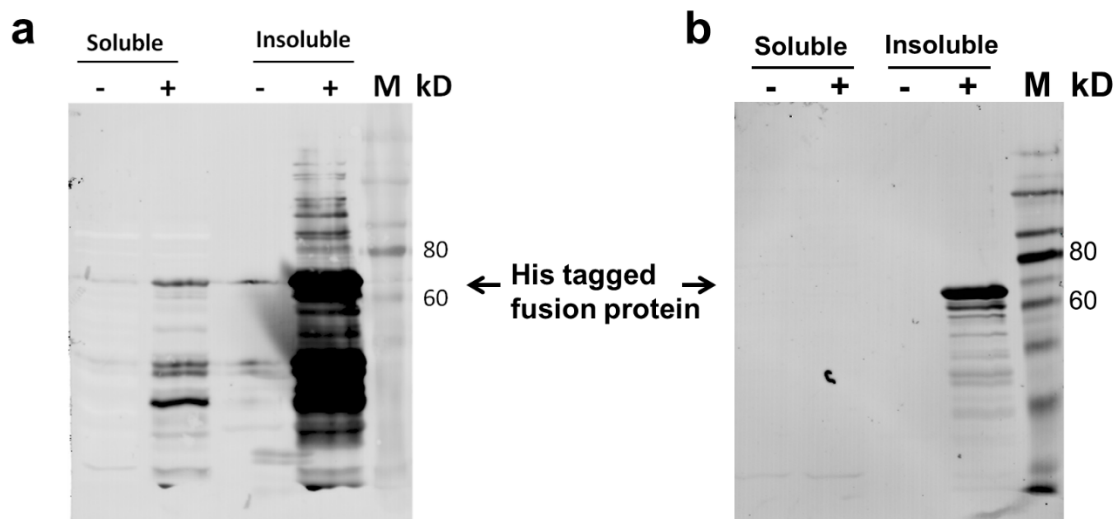


Fig. S2. Expression of His-tagged ScGAI protein conferring its molecular weight of 66 kDa in *Escherichia coli*.

Expression of recombinant ScGAI protein was induced in *E. coli*. Total protein was extracted and assessed by immunoblotting using the **(a)** anti-ScGAI (1:1000 dilution) and **(b)** the anti-His (1:1000 dilution) antibodies; lane 1 and 3, non-induced extracts, and lane 2 and 4, induced extracts. Lane 5, Molecular weight marker; Recombinant proteins are indicated with arrows.

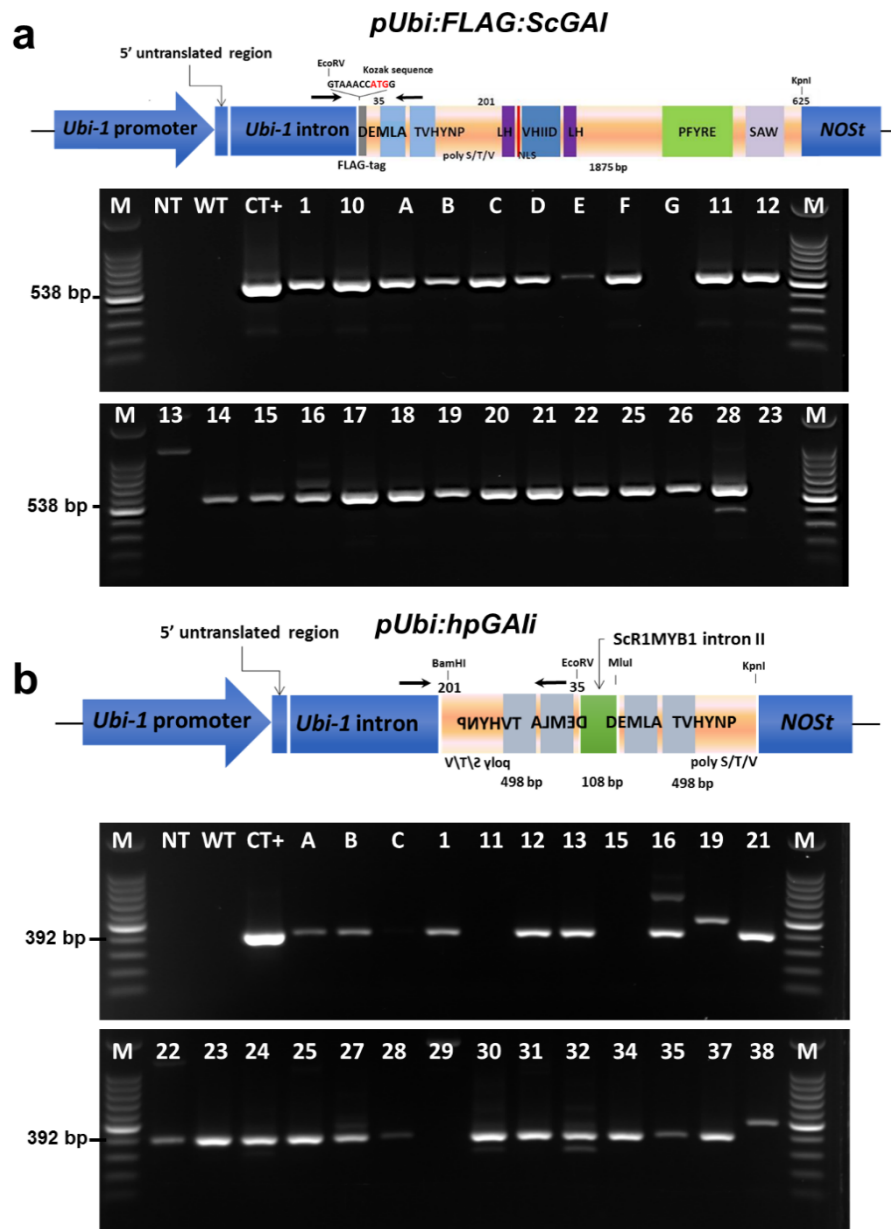


Fig. S3. Transgene constructs and PCR genotyping for identification of putative transgenic lines.

(a) Overexpression cassette *pUbi:FLAG:ScGAI* and the positive transgenic lines identified with the expected PCR band. (b) Hairpin-mediated silencing cassette *pUbi:hpGAI* and the positive lines confirmed by the expected PCR band. M: 100 bp ladder (Promega); NT: non-template; WT: untransformed wild-type plant; CT+: positive control (vectors); Numbers and letters correspond to the putative transformed lines; The set of primers used is shown as arrows in each construct diagram.

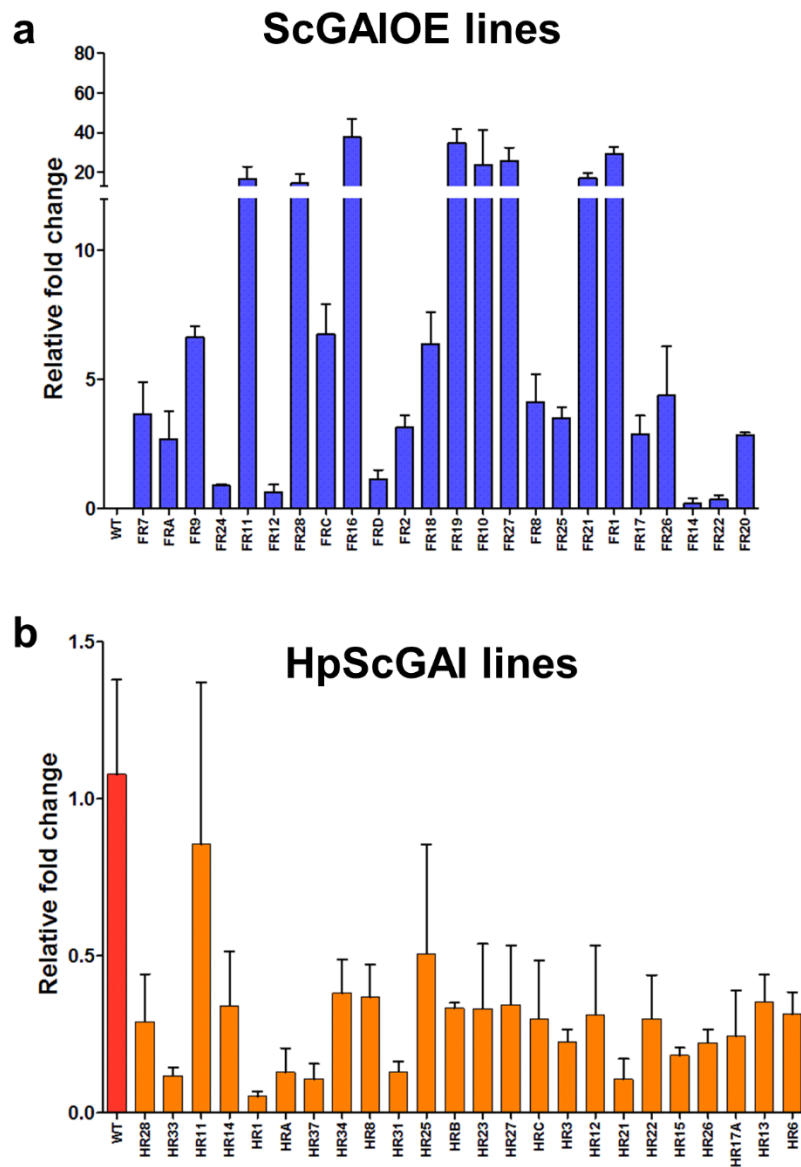


Fig. S4. *ScGAI* gene expression in the ScGAIOE and HpScGAI transgenic sugarcane lines. (a) Expression level of the *FLAG:ScGAI* transgene. (b) Expression level of endogenous *ScGAI* in wild-type (WT) and hairpin-mediated DELLA silencing lines. Data represent the mean \pm SEM; n =3 independent biological replicates.

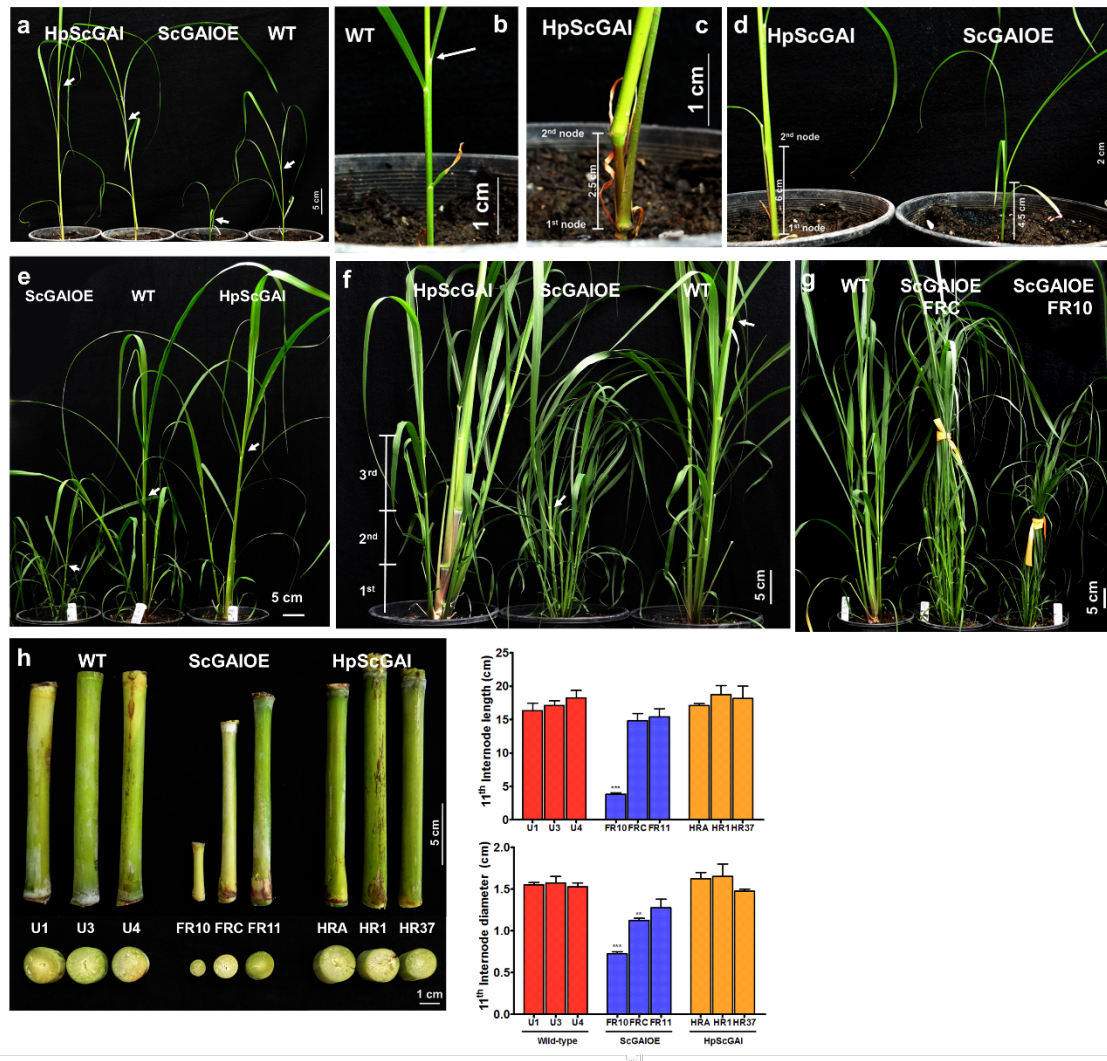


Fig. S5. Gross phenotype of ScGAIOE and HpScGAI transgenic sugarcane plants. One-month-old in (a) and close-up in (b, c and d) showing the earliest formation of internodes in HpGAI lines; (e) Two-month-old (f) and (g) Three-month-old showing the high tiller numbers. Arrows indicate the first visible dewlap; (h) 11th internode length and diameter measurement of six-month-old plants. Bar plots show means \pm SEM (n=4, P< 0.05; One way ANOVA followed by Bonferroni multiple comparisons post-test). U1, U3 and U4: untransformed plants; FR10, FRC and FR11: ScGAIOE plants; HRA, HR1 and HR37: HpScGAI plants.

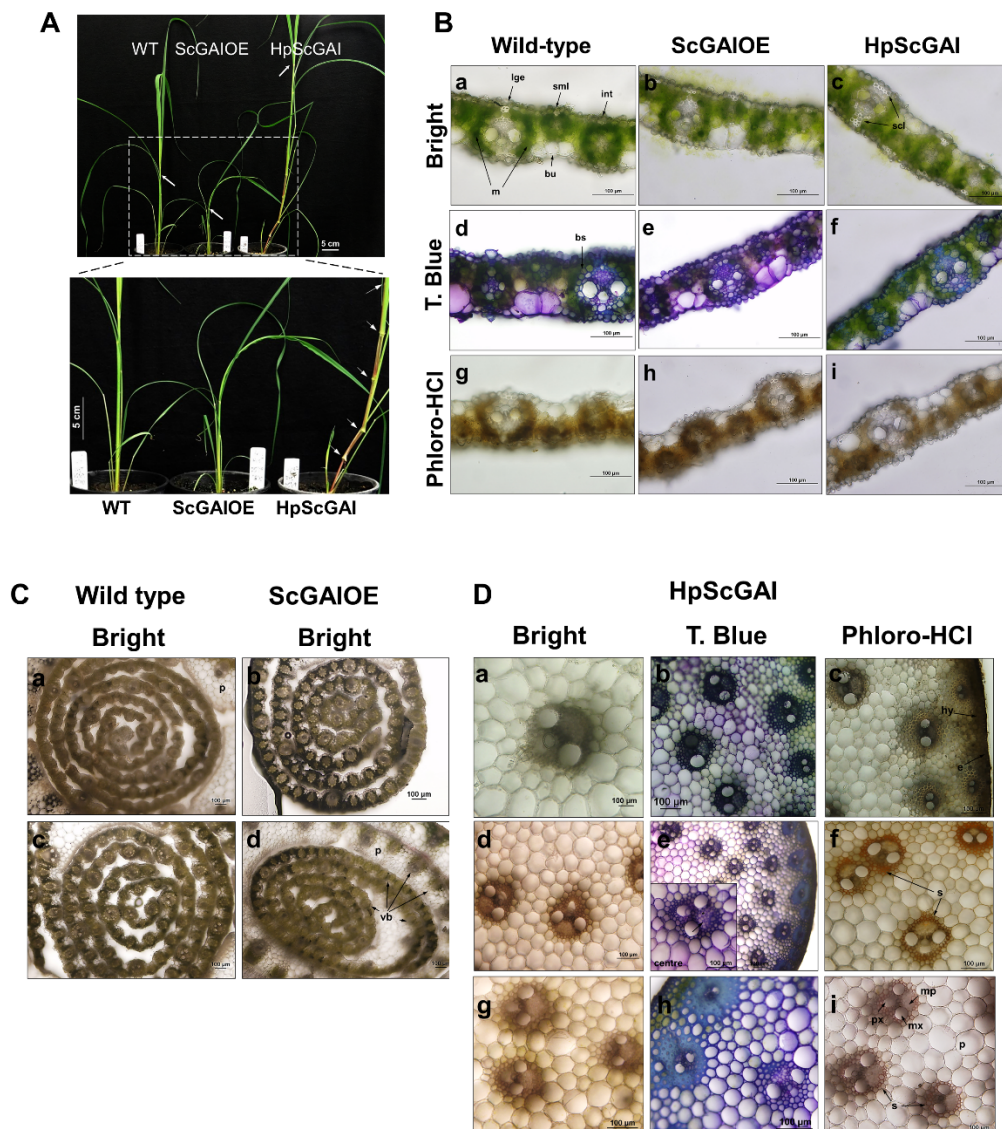


Fig. S6. Leaf and stem histology of wild type (WT), ScGAIOE and HpScGAI transgenic sugarcane plants.

(A) Two-month-old plants. Close-up view displaying the stunted growth in SCGAI and the presence of internodes in HpGAI plants. Arrows indicate the first visible dewlap. (B) Cross section of leaves in bright-field light (a, b and c), and stained with toluidine blue (T. blue; d, e and f) or phloroglucinol-HCl (Phloro-HCl; g, h and i). Large (lge), small (sml) and intermediate (int) vascular bundle, scl – sclerenchyma, bu – buliform cells, bs – bundle sheath, m- mesophyll cell. (C) Cross-section of the leaf roll from WT in bright-field in a and c, and from ScGAIOE (FR10 line) in bright-field in b and d. (D) Cross-section of the stem from HpScGAI plants (HR1 line) in bright-field light in a, d and g, toluidine blue (T. blue) stained in b, e and h, and phloroglucinol-HCl (Phloro-HCl) stained in c, f and i. When we stained the HpGAI stem with phloroglucinol-HCl, the reddish-brown color in lignified tissues increased in internodes more mature close to the soil. Parenchyma cells (p), vascular bundles (vb), metaxylem (mx), protoxylem (px), metaphloem (mp), sclerenchyma (s), epidermis (e), hypodermis (hy).

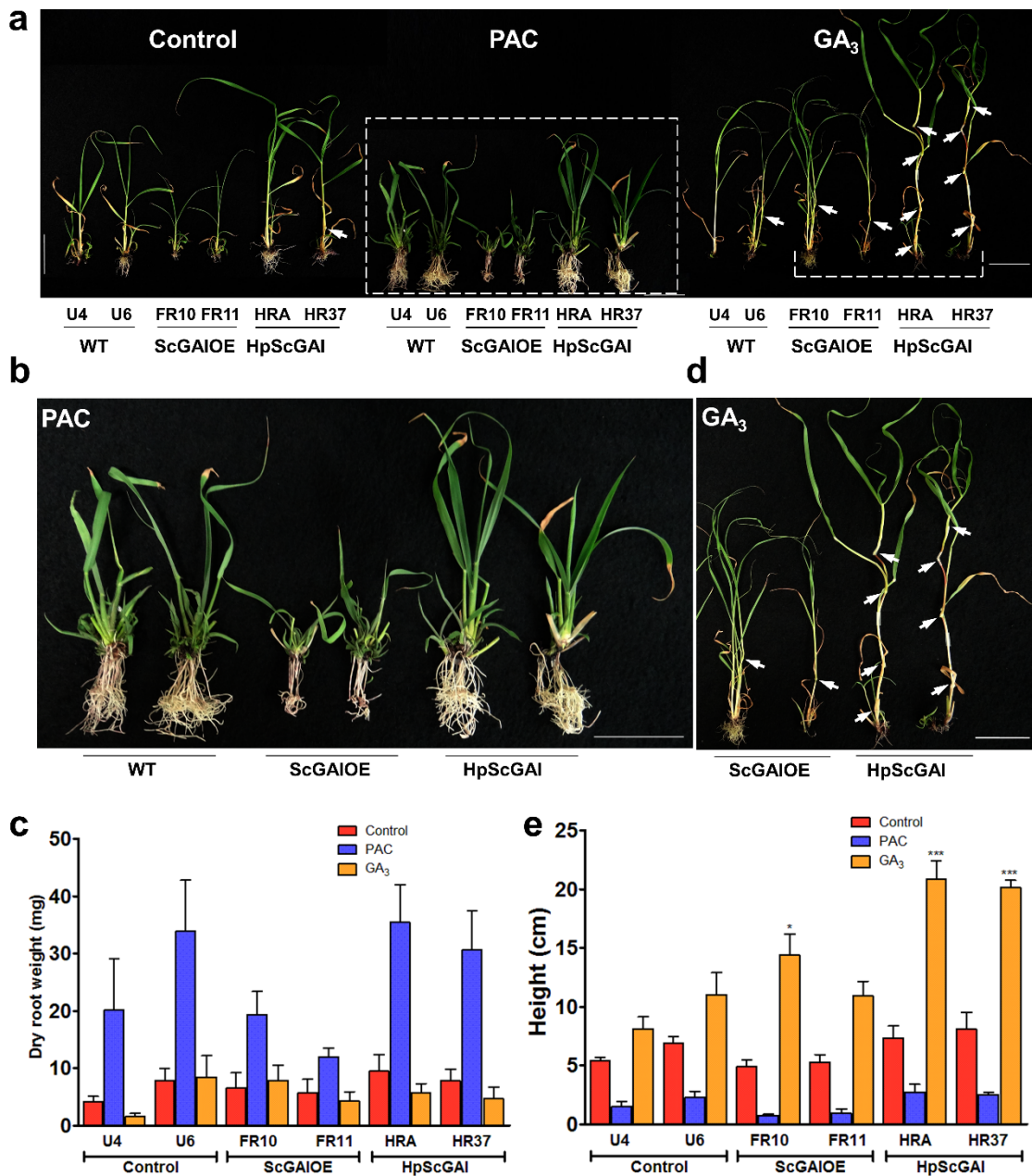


Fig. S7. Transgenic sugarcane plants showed stronger responses to gibberellin (GA_3) and paclobutrazol (PAC) than wild type (WT) plants.

(a) Morphology of sugarcane plants after 23 days of treatment with GA_3 (50 μ M) and PAC (5 μ M). Arrows indicate the nodes. Scale bars = 5 cm. (b) Close-up view of PAC-treated seedlings. Scale bars = 5 cm. (c) Dry root weight of WT, ScGAIOE and HpScGAI plants. (d) Close-up view of GA_3 -treated transgenic plants. Arrows indicate the nodes; Scale bars = 5 cm. (e) Height of WT, ScGAIOE and HpScGAI transgenic lines. Error bars indicate the SEM of the mean. (n=4). One way ANOVA was used and Dunnett's multiple comparison applied (p value < 0.05).

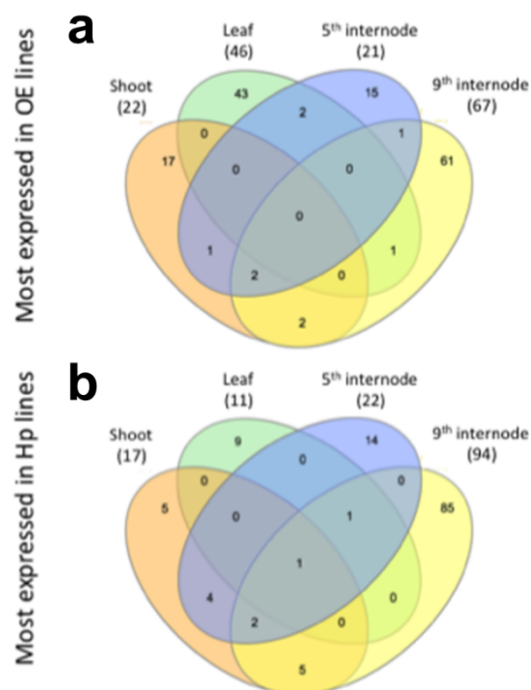


Fig. S8. Transcriptional responses of ScGAIOE and HpScGAI plants.

Venn diagram showing the differentially expression genes (DEGs) (number in parentheses) **(a)** in ScGAIOE and **(b)** in HpScGAI tissues.

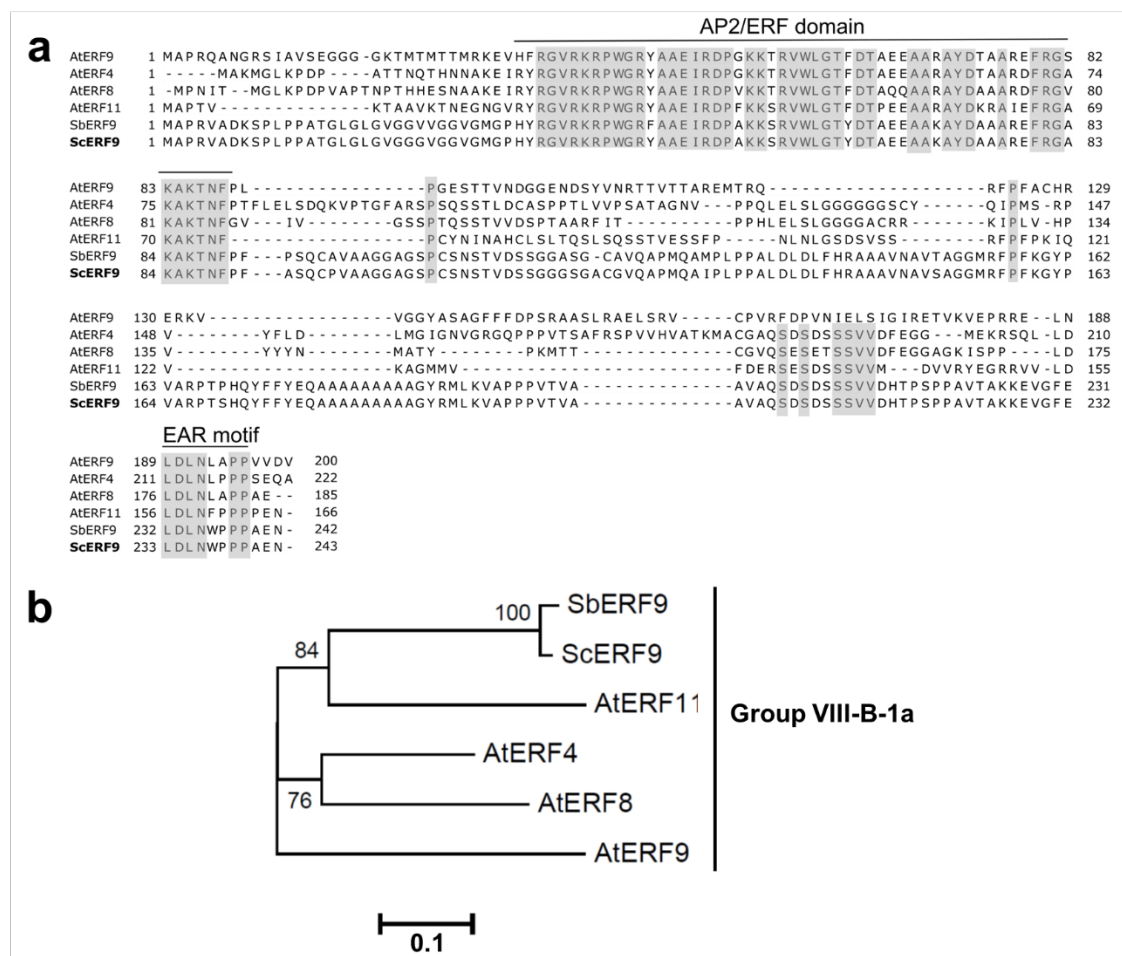


Fig. S9. ScERF9 belongs to ERF (ETHYLENE RESPONSE FACTOR) subfamily VIII-B-1a of AP2/ERF transcript factors.

(a) Protein alignment of sorghum and sugarcane ERF9 with four *Arabidopsis* ERF proteins of the group VIII-B1-a. Similar sequences are colored in gray shadow boxes highlighting the AP2/ERF and EAR conserved domains. (b) Phylogenetic analysis shows that ScERF9 clustered together with SbERF9 and AtERF11 proteins. The bootstrap percentages indicate the reliability of the cluster.

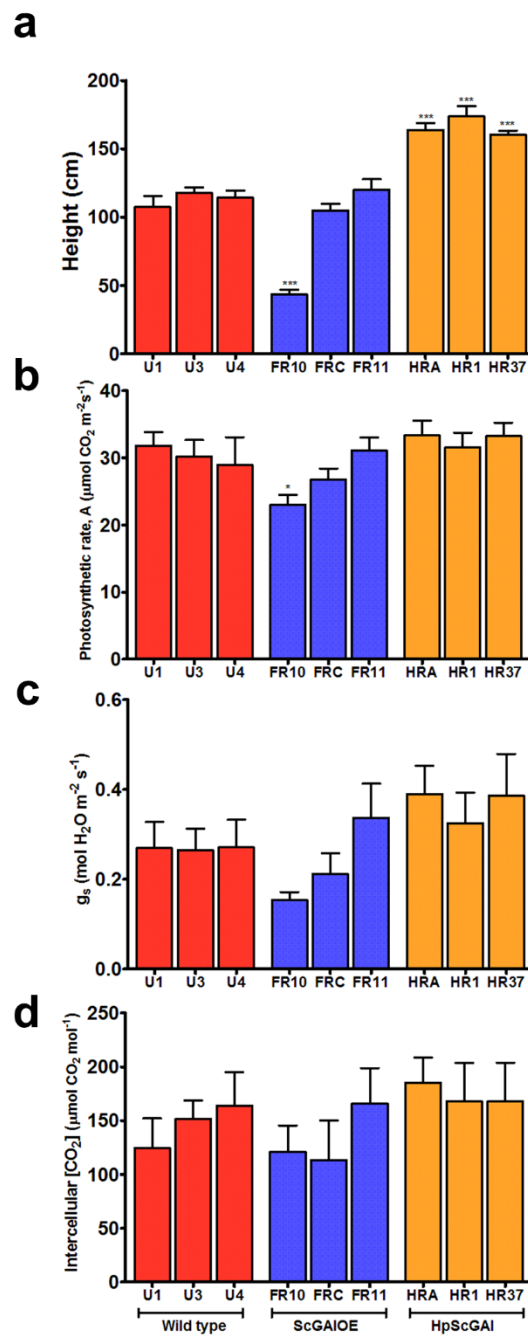


Fig. S10. Photosynthesis in the ScGAIOE and HpScGAI transgenic sugarcane.

(a) Height, (b) Photosynthesis rate (A), (c) Stomatal conductance (g_s) and (d) Intercellular $[\text{CO}_2]$, (c_i). Parameters were measured in 5-months-old plants. Bar plots show means \pm SEM ($n=7$, $P < 0.05$; One way ANOVA followed by Bonferroni multiple comparisons post-test).

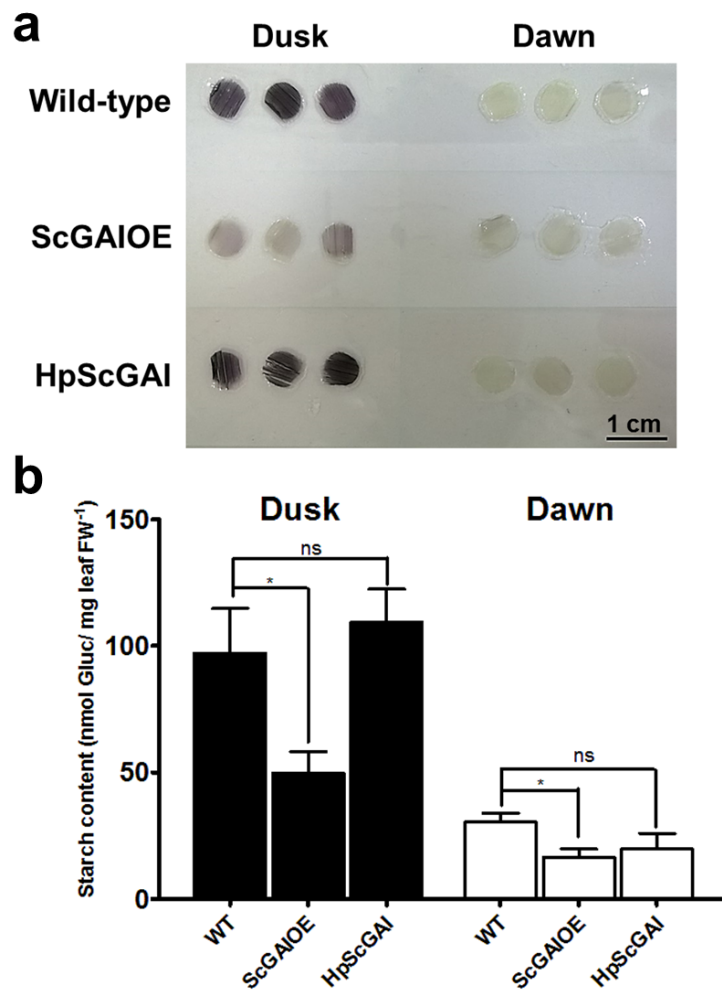


Fig. S11. ScGAIOE shows impaired starch accumulation during the day.

Starch turnover was evaluated in diurnal cycle by **(a)** Lugol's iodine solution in leaf+1 discs ($n=3$, independent biological replicates), and confirmed by **(b)** enzymatic starch assay ($n=5$, independent biological replicates; $P<0.05$ via paired Student's two-tailed t-test; ns = not significant).

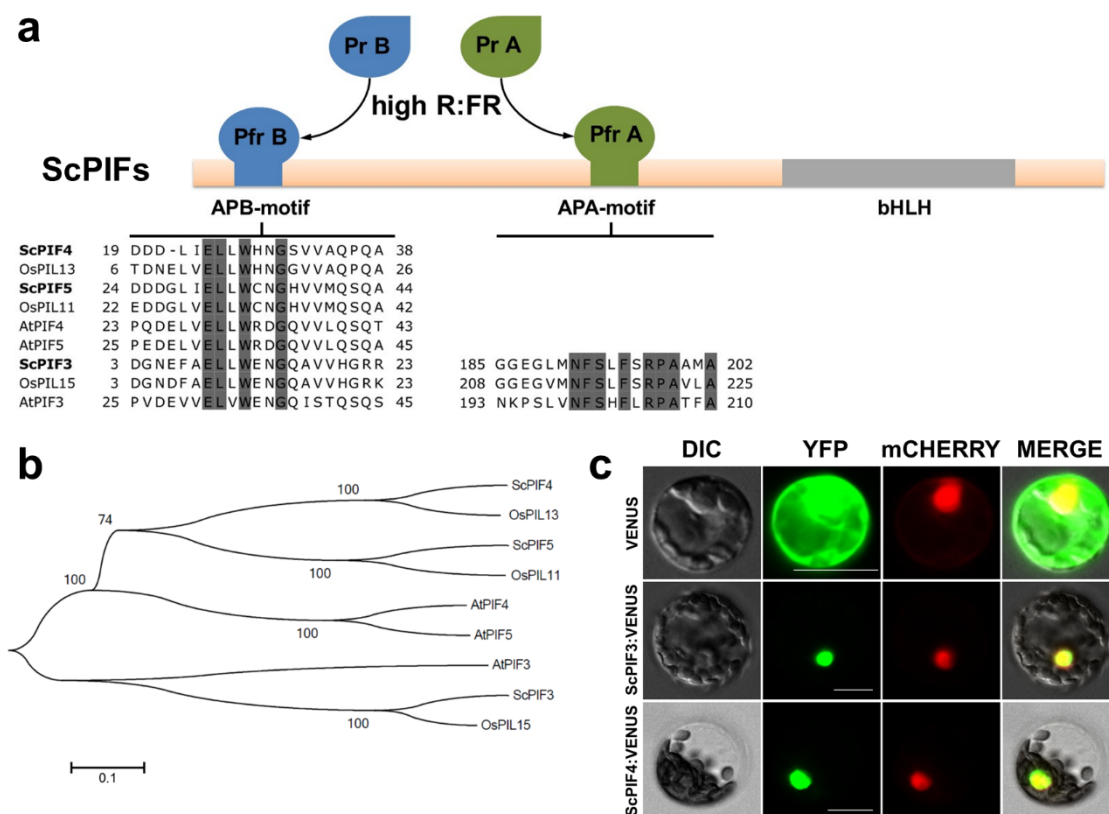


Fig. S12. Phytochrome-Interacting Factors (PIFs) 3 and 4 are nuclear basic helix-loop-helix (bHLH) proteins in sugarcane.

(a) Schematic representation of PIF proteins showing their conserved domains along the sequence; APB and APA-motifs mediate the binding to phyB Pfr and phyA Pfr, respectively. (b) Phylogenetic tree of PIF proteins. (c) Subcellular localization of ScPIF:VENUS fusion proteins in Arabidopsis mesophyll protoplast. The construct *AtPARP3:mCHERRY* (mCHERRY) was used as nuclear control. DIC: Differential Interference Contrast; YFP: Yellow Fluorescent protein. Bars = 20 μ M

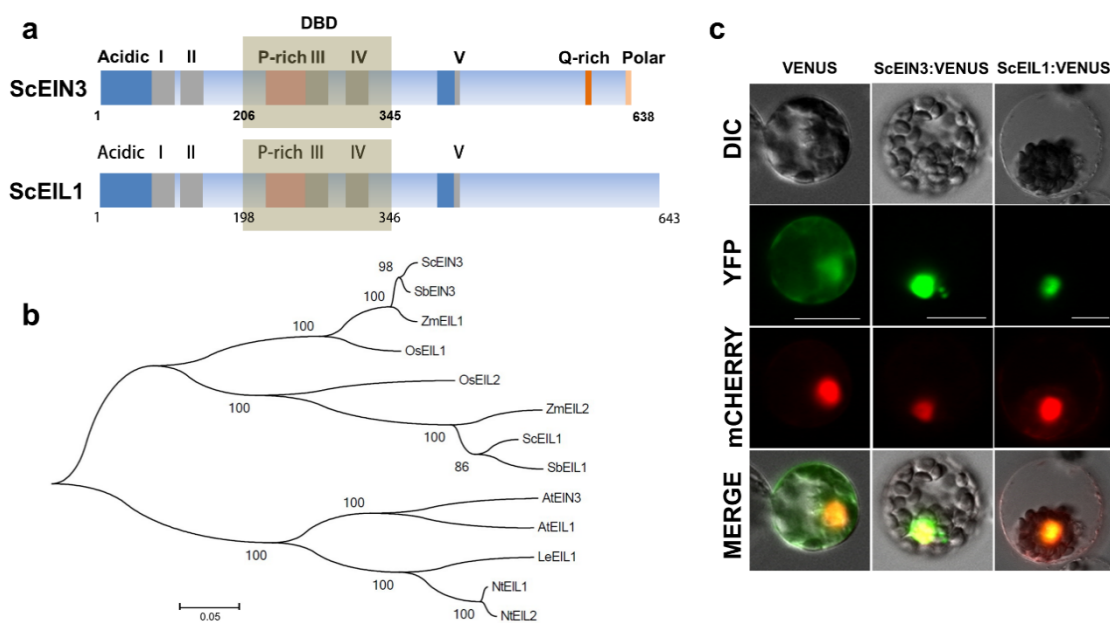


Fig. S13. ScEIN3 and ScEIL1, the master transcription factors of ethylene signaling.

(a) Schematic representation of ScEIN3/EIL1 proteins showing their conserved domains along the sequences. (b) Phylogenetic tree of ScEIN3/EIL1 proteins. (c) Subcellular localization of ScEIN3/EIL1 proteins in Arabidopsis mesophyll protoplast. The construct *AtPARP3:mCHERRY* (mCHERRY) was used as nuclear control. DIC means Differential Interference Contrast. YFP means Yellow Fluorescent protein. Bars = 20 μ M

Table S1. Composite list of DEGs in leaves between ScGAIOE and HpScGAI.

| GeneID | Annotation | ScGAIOE | HpScGAI | Fold change (Log2) | q-values |
|-------------|---|----------|---------|--------------------|----------|
| Sb01g007360 | Gibberellic acid - stimulated Arabidopsis (GASA8) gene | 3.63978 | 0 | inf | 0.018663 |
| Sb01g029310 | Expansin B2 – (EXPB2) | 1.82334 | 0 | inf | 0.018663 |
| Sb01g036580 | Euonymus lectin S3 - EULS3 | 125.358 | 12.1324 | -3.36912 | 0.018663 |
| Sb01g042690 | Sugar transporter family protein – (STP13) | 43.3993 | 7.30469 | -2.57078 | 0.032348 |
| Sb01g043720 | Glycosyl hydrolase family 10 protein | 0.990486 | 0 | inf | 0.018663 |
| Sb01g044580 | Alcohol dehydrogenase GroES-like | 68.0263 | 11.0143 | -2.62672 | 0.04479 |
| Sb01g007590 | UDP-glucuronosyl/UDP-glucosyltransferase | 0 | 3.645 | inf | 0.032348 |
| Sb01g010660 | DELLA | 39.7408 | 4.80204 | -3.0489 | 0.018663 |
| Sb01g020150 | KAT2 – 3- Ketoacyl-Coa thiolase 2 | 252.081 | 23.083 | -3.44899 | 0.018663 |
| Sb01g033820 | Transducin/WD40 repeat-like superfamily protein | 57.6083 | 7.64138 | -2.91437 | 0.018663 |
| Sb01g042270 | Cytochrome P450 74A – (CYP74A) | 360.304 | 52.1615 | -2.78816 | 0.032348 |
| - | NI | 3.43827 | 0 | inf | 0.018663 |
| Sb10g029300 | Thylakoid lumenal 16.5 kDa protein | 23.6458 | 123.636 | 2.38644 | 0.04479 |
| Sb10g028360 | GDSL-like Lipase/Acylhydrolase | 15.4885 | 82.5155 | 2.41347 | 0.04479 |
| Sb02g037570 | Glucose transmembrane transporter - Polyol transporter 5-like | 18.154 | 1.98172 | -3.19546 | 0.032348 |
| Sb02g037650 | Scarecrow-like 5 | 216.577 | 18.8808 | -3.51989 | 0.018663 |
| Sb02g003010 | Early-responsive to dehydration – (ERD4) | 182.848 | 5.04105 | -5.18078 | 0.018663 |
| Sb02g007870 | Metal transporter Nramp6 – (NRAMP1) | 1.79574 | 0 | inf | 0.018663 |
| Sb02g010810 | Aquaporin-like – (PIP2B) | 0 | 2.58132 | inf | 0.018663 |
| Sb02g026360 | Galactosyltransferase | 33.9953 | 2.60119 | -3.70809 | 0.018663 |
| Sb02g031550 | Copper amine oxidase | 0 | 2.81452 | inf | 0.018663 |
| Sb02g036750 | Polygalacturonase inhibitor 1 – (PGIP2) | 2.29455 | 0 | inf | 0.018663 |
| - | NI | 0 | 51.842 | inf | 0.018663 |
| Sb03g000850 | Putative bark storage protein | 104.951 | 17.2066 | -2.60868 | 0.018663 |
| Sb03g029790 | CTP synthase – (emb2742) | 40.2019 | 5.45801 | -2.88082 | 0.018663 |
| Sb03g007380 | Mannose-6-phosphate isomerase – (PM11) | 9.95695 | 56.4115 | 2.50221 | 0.018663 |
| Sb03g023990 | Early-responsive to dehydration – (ERD) | 76.1976 | 11.114 | -2.77737 | 0.018663 |
| Sb03g030330 | MYB family transcription factor – (RL6) | 0 | 46.0747 | inf | 0.018663 |
| Sb03g040490 | C2H2 zinc finger protein – (WIP4) | 0.803423 | 0 | inf | 0.018663 |
| Sb03g042450 | Lipoxygenase – (LOX1) | 318.627 | 28.708 | -3.47234 | 0.018663 |
| Sb03g044980 | Glutathione S-transferase – (GSTF13) | 109.402 | 21.297 | -2.36092 | 0.018663 |
| Sb03g046090 | BHLH039 | 3.72414 | 0 | inf | 0.018663 |
| Sb04g000620 | Vacuolar invertase 2 – (VAC-INV 2) | 83.5824 | 14.485 | -2.52864 | 0.032348 |

“NI” means no identified; “inf” indicates no ratio.

Table S1. Continuation.

| GeneID | Annotation | ScGAI OE | HpScGAI | Fold change (Log2) | q-values |
|-------------|--|----------|---------|--------------------|----------|
| Sb04g000830 | HPL1 (Hydroperoxide Lyase 1) (CYP74B2) | 36.3315 | 3.85201 | -3.23754 | 0.018663 |
| Sb04g021410 | Early-responsive to dehydration – (ERD1) | 92.2606 | 14.9928 | -2.62145 | 0.018663 |
| Sb04g024090 | NPF8.3. NRT1/ PTR family 8.3 - Peptide transporter (PTR2) | 118.224 | 13.927 | -3.08557 | 0.018663 |
| Sb04g024440 | Glycerophosphoryl diester phosphodiesterase – (GPD2) | 27.8855 | 3.19227 | -3.12686 | 0.018663 |
| Sb04g033350 | Cytochrome b5-like Heme/Steroid binding domain - CB5-E | 8.58836 | 0 | inf | 0.018663 |
| Sb04g025550 | APK1 - Serine-threonine/tyrosine-protein kinase | 246.684 | 28.4504 | -3.11615 | 0.018663 |
| Sb04g026690 | Uncharacterized protein | 4.67203 | 0 | inf | 0.018663 |
| Sb04g031040 | Jumonji transcription factor/ zinc finger (C5HC2 type) | 23.0275 | 1.20107 | -4.26097 | 0.018663 |
| - | NI | 0 | 20.0573 | inf | 0.018663 |
| - | NI | 48.5983 | 319.451 | 2.71662 | 0.018663 |
| Sb05g003860 | LTP1 – Lipid transfer protein 1 | 4.46598 | 0 | inf | 0.018663 |
| - | NI | 0 | 4.64044 | inf | 0.018663 |
| - | NI | 0 | 3.87019 | inf | 0.018663 |
| Sb06g021790 | Wall-associated receptor kinase-like 20 precursor-(CRCK3) | 74.8249 | 14.0611 | -2.41181 | 0.04479 |
| Sb06g028200 | Protease inhibitor/seed storage/LTP family | 243.106 | 34.7061 | -2.80832 | 0.018663 |
| Sb06g000660 | Heat shock protein – (HSP90.1) | 9.17577 | 60.5537 | 2.72231 | 0.018663 |
| Sb06g003280 | HIPP27 - Heavy metal associated isoprenylated plant protein 27 | 112.18 | 8.56149 | -3.71181 | 0.018663 |
| Sb06g022460 | Beta-glucosidase 45 – (BGLU45) | 15.1642 | 77.432 | 2.35226 | 0.032348 |
| Sb06g027770 | ACA8 (auto-inhibited CA ²⁺ -ATPASE, isoform 8) | 19.1969 | 2.89684 | -2.72832 | 0.04479 |
| Sb06g032460 | PAO4. Polyamine Oxidase 4 | 64.6633 | 10.8507 | -2.57516 | 0.018663 |
| Sb07g004700 | Chalcone synthase – (CHS) transparent testa 4. TT4 | 0 | 2.47114 | inf | 0.018663 |
| Sb07g005130 | Terpene synthase – (TPS21) | 183.727 | 21.3089 | -3.10804 | 0.018663 |
| Sb07g021950 | Receptor-like protein kinase precursor – (PEPR1) | 46.2865 | 3.24164 | -3.83579 | 0.018663 |
| Sb07g024030 | Oxidoreductase. 2OG-Fe(II) oxygenase family protein | 1.12088 | 0 | inf | 0.018663 |
| Sb08g023140 | AAA-ATPASE 1 | 36.0458 | 3.73987 | -3.26877 | 0.032348 |
| Sb08g023150 | AAA-ATPASE 1 | 46.4186 | 5.42508 | -3.09699 | 0.018663 |
| - | NI | 0 | 15.3463 | inf | 0.018663 |
| Sb09g001020 | PR (pathogenesis-related) -PR-6 proteinase inhibitor family | 2615.37 | 278.046 | -3.23362 | 0.018663 |
| Sb09g001050 | PR (pathogenesis-related) -PR-6 proteinase inhibitor family | 1802.67 | 189.723 | -3.24817 | 0.018663 |
| Sb09g003060 | Proteolipid membrane potential modulator – (RCI2A) | 499.02 | 47.4797 | -3.39371 | 0.018663 |
| Sb09g005800 | Histidine-containing phosphotransfer protein 4 – (AHP4) | 0 | 5.34066 | inf | 0.018663 |
| - | NI | 0 | 80.8544 | inf | 0.032348 |

“NI” means no identified; “inf” indicates no ratio.

Table S2. Composite list of DEGs in Apical shoot between ScGAIOE and HpScGAI.

| GeneID | Annotation | ScGAIOE | HpScGAI | Fold change (Log2) | q-values |
|-------------|--|---------|---------|--------------------|-----------|
| Sb01g016810 | DYL1 (Dormancy-associated protein-like 1) | 109.977 | 33.15 | -1.73013 | 0.0264797 |
| Sb01g028256 | Tetratricopeptide repeat 10. TPR10 | 0 | 3.05063 | inf | 0.0264797 |
| Sb01g029610 | LTPL144 - Protease inhibitor/seed storage/LTP family protein precursor | 4.14948 | 0 | #NOME? | 0.0477927 |
| Sb01g036310 | HAD superfamily phosphatase | 135.969 | 26.6852 | -2.34917 | 0.0264797 |
| Sb01g045720 | sucrose transporter. SUC3 | 40.2308 | 10.813 | -1.89553 | 0.0264797 |
| Sb01g008350 | transmembrane BAX inhibitor motif-containing protein BIL4 | 43.0404 | 194.978 | 2.17955 | 0.0264797 |
| Sb01g014460 | VRN1 –Reduced vernalization response 1 | 2.80241 | 0 | #NOME? | 0.0264797 |
| - | NI | 0 | 18.0663 | inf | 0.0477927 |
| - | NI | 0 | 4.02684 | inf | 0.0477927 |
| Sb10g003890 | GDSL-like lipase/acylhydrolase | 143.286 | 42.2648 | -1.76137 | 0.0264797 |
| Sb10g012970 | Peptidyl-prolyl cis-trans isomerase FKBP65 – ROF2 | 50.2692 | 1091.04 | 4.43988 | 0.0264797 |
| Sb10g019360 | AQP1 –Delta tonoplast integral protein | 89.4797 | 6.54048 | -3.77409 | 0.0264797 |
| Sb10g026090 | Chloride transporter A – CLC-A | 16.1588 | 3.30871 | -2.28798 | 0.0264797 |
| Sb02g027900 | Photosystem I subunit G - PSAG | 250.123 | 91.8949 | -1.44458 | 0.0264797 |
| Sb02g032040 | Chlorophyll A-B binding protein LHB1B2.LHCB1.5 | 134.08 | 47.9085 | -1.48474 | 0.0264797 |
| Sb02g035600 | Beta-amylase 1 – RAM1 | 66.8796 | 223.019 | 1.73753 | 0.0264797 |
| Sb02g043260 | Euonymus lectin S3 - EULS3 | 148.289 | 43.8698 | -1.75711 | 0.0264797 |
| Sb03g005280 | FLA11 - Fasciclin-like arabinogalactan proteins | 242.591 | 86.7392 | -1.48377 | 0.0264797 |
| Sb03g006880 | HSP18.2 – Heat shock | 134.315 | 397.858 | 1.56663 | 0.0264797 |
| Sb03g041190 | NPF5.10 – Peptide transporter (PTR2) | 50.1346 | 15.1805 | -1.72359 | 0.0264797 |
| Sb03g006870 | HSP18.2 – Heat shock | 227.072 | 789.49 | 1.79777 | 0.0264797 |
| Sb03g042330 | MLP423- Pathogenesis-related Bet v I family protein | 3.32405 | 0 | #NOME? | 0.0264797 |
| Sb04g008670 | MYB-like HTH transcriptional regulator | 1.44684 | 0 | #NOME? | 0.0264797 |
| Sb04g009670 | BAG6 (BCL-2-associated athanogene 6) | 6.80622 | 27.3091 | 2.00446 | 0.0264797 |
| Sb04g009690 | BAG5 (BCL-2-associated athanogene 5) | 129.521 | 406.876 | 1.65141 | 0.0264797 |
| Sb04g001130 | CAT1 - Catalase isozyme A | 57.9455 | 14.5686 | -1.99184 | 0.0477927 |
| Sb04g026430 | RNA-binding (RRM/RBD/RNP motifs) family protein | 57.6438 | 183.417 | 1.66989 | 0.0264797 |
| Sb04g027330 | HSP20-like - Heat shock | 96.6096 | 669.184 | 2.79217 | 0.0264797 |
| Sb05g000440 | ASN1 - Asparagine synthetase – (DIN6) | 108.814 | 32.1247 | -1.76011 | 0.0264797 |
| Sb05g004100 | ASR1 - Abscisic stress-ripening 1 | 288.25 | 60.0521 | -2.26303 | 0.0264797 |
| Sb06g024780 | LTPL120 - Protease inhibitor/seed storage/LTP family protein | 0 | 8.15305 | inf | 0.0264797 |
| Sb06g024790 | LTPL120 - Protease inhibitor/seed storage/LTP family protein | 10.1617 | 485.377 | 5.57789 | 0.0264797 |
| Sb06g032310 | Leucine-rich repeat (LRR) family protein | 84.8772 | 27.8199 | -1.60926 | 0.0264797 |

“NI” means no identified; “inf” indicates no ratio.

Table S2. Continuation.

| GeneID | Annotation | ScGAI OE | HpScGAI | Fold change (Log2) | q-values |
|-------------|---|----------|---------|--------------------|-----------|
| Sb06g033030 | PORA - Protochlorophyllide reductase A | 329.404 | 100.367 | -1.71457 | 0.0264797 |
| Sb06g000660 | HSP83 - Heat shock protein | 24.7329 | 521.226 | 4.39741 | 0.0264797 |
| Sb07g020270 | TPS9 - Trehalose-6-phosphatase synthase 9 | 15.7126 | 3.433 | -2.19438 | 0.0264797 |
| Sb09g023060 | PDC1 – Pyruvate decarboxylase 1 | 7.68714 | 39.1058 | 2.34686 | 0.0264797 |
| Sb09g019930 | PPDK - Pyruvate orthophosphate dikinase | 6.44379 | 25.8605 | 2.00477 | 0.0264797 |
| Sb09g022260 | Putative uncharacterized protein | 58.5064 | 8.82706 | -2.72859 | 0.0264797 |
| Sb09g025900 | HSP101 - Heat shock protein | 87.2806 | 457.537 | 2.39016 | 0.0264797 |
| Sb09g029500 | Pectin lyase-like superfamily protein | 26.2983 | 111.757 | 2.08733 | 0.0264797 |

“NI” means no identified; “inf” indicates no ratio.

Table S3. Composite list of DEGs in internode 5th between ScGAIOE and HpScGAI.

| GeneID | Annotation | ScGAIOE | HpScGAI | Fold change (Log2) | q-values |
|-------------|--|---------|---------|--------------------|----------|
| Sb01g009080 | GRF1-interacting factor 1 | 0 | 1.76847 | inf | 0.035812 |
| Sb01g020430 | Glycine-rich protein DOT1 | 110.538 | 449.668 | 2.02431 | 0.022577 |
| Sb01g036020 | CBL-interacting serine/threonine-protein kinase 10 – CIPK10 | 67.7524 | 15.3461 | -2.1424 | 0.022577 |
| Sb01g043630 | Dwarf 14 - D14 | 131.511 | 28.1199 | -2.22552 | 0.022577 |
| Sb01g047020 | Calmodulin-binding receptor-like cytoplasmic kinase 2 –CRCK2 | 29.0656 | 5.49055 | -2.40429 | 0.035812 |
| Sb01g047160 | RZFP34/CHYR1 | 113.677 | 27.805 | -2.03152 | 0.035812 |
| - | NI | 0 | 4.80613 | inf | 0.022577 |
| - | NI | 517.286 | 2730.2 | 2.39997 | 0.022577 |
| Sb10g012970 | Peptidyl-prolyl cis-trans isomerase FKBP65 – ROF2 | 42.3328 | 999.134 | 4.56083 | 0.022577 |
| Sb10g023670 | EIN3-binding F-box protein 1 – EBF1 | 132.585 | 30.6841 | -2.11135 | 0.022577 |
| Sb10g026090 | Chloride channel protein CLC-a | 37.4577 | 3.88015 | -3.27108 | 0.022577 |
| Sb02g033240 | xyloglucan endotransglucosylase/hydrolase protein 32 – XTH32 | 30.1725 | 107.884 | 1.83818 | 0.035812 |
| Sb02g003010 | Early-responsive to dehydration 4 - ERD4 | 90.6823 | 20.9488 | -2.11396 | 0.022577 |
| Sb02g031550 | Copper amine oxidase family protein | 0 | 4.77988 | inf | 0.022577 |
| - | NI | 0 | 53.1402 | inf | 0.022577 |
| Sb03g042860 | AKS2- ABA-responsive kinase substrate 2 | 73.8751 | 13.9807 | -2.40166 | 0.022577 |
| Sb03g002020 | NA ⁺ /CA ²⁺ Exchanger | 268.712 | 75.106 | -1.83906 | 0.035812 |
| Sb03g039530 | Laccase-17 – LAC17 | 31.3293 | 3.59022 | -3.12537 | 0.022577 |
| Sb04g009670 | BAG family molecular chaperone regulator 6 – BAG6 | 8.12306 | 31.1694 | 1.94004 | 0.035812 |
| Sb04g017450 | Inositol-tetrakisphosphate 1-kinase 1 – ITPK1 | 0 | 1.75114 | inf | 0.035812 |
| Sb04g024090 | Protein NRT1/ PTR FAMILY 6.4 –NPF6.4 | 45.4655 | 4.44484 | -3.35457 | 0.022577 |
| Sb04g035560 | TPS11 – Trehalose-6-phosphatase synthase 11 | 76.4698 | 20.5569 | -1.89527 | 0.022577 |
| Sb04g021590 | Copper transport protein- CCH | 23.4383 | 170.208 | 2.86036 | 0.022577 |
| Sb04g027330 | heat shock protein- HSP23.5 | 52.6493 | 545.481 | 3.37304 | 0.022577 |
| - | NI | 0 | 21.772 | inf | 0.022577 |
| - | NI | 0 | 32.9927 | inf | 0.022577 |
| Sb05g007030 | heat shock protein –HSP22 | 0 | 5.28697 | inf | 0.022577 |
| Sb05g008440 | carboxylesterase 17 –CXE17 | 3.2307 | 0 | #NOME? | 0.022577 |
| - | NI | 0 | 5.99304 | inf | 0.022577 |
| - | NI | 0 | 5.65168 | inf | 0.022577 |
| - | NI | 0 | 4.18415 | inf | 0.035812 |
| Sb06g001410 | Pectate lyase 15 | 17.9248 | 83.0608 | 2.21221 | 0.022577 |
| Sb06g002500 | Hypothetical protein | 117.531 | 1082.81 | 3.20367 | 0.022577 |

“NI” means no identified; “inf” indicates no ratio.

Table S3. Continuation

| GeneID | Annotation | ScGAIOE | HpScGAI | Fold change (Log2) | q-values |
|-------------|--|---------|---------|--------------------|----------|
| Sb06g021870 | Leucine-rich repeat (LRR) family protein | 11.792 | 52.4498 | 2.15313 | 0.022577 |
| Sb06g024770 | Bifunctional inhibitor/lipid-transfer protein/seed storage 2S albumin superfamily protein –LTPL121 | 0 | 175.476 | inf | 0.022577 |
| Sb06g024780 | Bifunctional inhibitor/lipid-transfer protein/seed storage 2S albumin superfamily protein –LTPL120 | 0 | 16.2181 | inf | 0.022577 |
| Sb06g025890 | Ethylene-responsive transcription factor ERF025 (DREB A-4) | 7.01096 | 0 | inf | 0.022577 |
| Sb06g028200 | Bifunctional inhibitor/lipid-transfer protein/seed storage 2S albumin superfamily protein | 90.7623 | 463.277 | 2.35171 | 0.022577 |
| Sb06g000660 | Heat shock protein 90-1 – HSP90.1 | 32.6025 | 393.163 | 3.59207 | 0.022577 |
| - | NI | 35.2548 | 274.777 | 2.96237 | 0.022577 |
| - | NI | 450.491 | 3722.99 | 3.04689 | 0.022577 |
| - | NI | 224.836 | 1937.85 | 3.10751 | 0.022577 |
| - | NI | 215.998 | 1309.36 | 2.59977 | 0.035812 |
| - | NI | 144.461 | 1120.93 | 2.95594 | 0.022577 |
| - | NI | 0 | 107.561 | inf | 0.022577 |
| Sb07g020270 | TPS9 - Trehalose-6-phosphatase synthase 9 | 42.6613 | 3.28255 | -3.70004 | 0.022577 |
| Sb08g000980 | Peroxidase 52- PRX52 | 127.791 | 11.9137 | -3.42309 | 0.035812 |
| Sb08g002740 | CBL-interacting serine/threonine-protein kinase 2 – CIPK2 | 95.0556 | 26.1821 | -1.86019 | 0.035812 |
| Sb08g020600 | BZIP63- Basic leucine zipper 63 | 54.0344 | 9.3616 | -2.52905 | 0.022577 |
| Sb08g021580 | APG1 – Albino or pale green mutant 1 | 47.5267 | 6.52539 | -2.8646 | 0.022577 |
| Sb09g023060 | Pyruvate decarboxylase 1 –PDC1 | 1.95158 | 28.5127 | 3.86889 | 0.035812 |
| Sb09g029610 | ADPGLC-PPASE large subunit - APL2 | 44.3375 | 158.499 | 1.83788 | 0.022577 |
| Sb09g018080 | Transducin/WD-40 repeat-containing protein | 10.8563 | 40.7806 | 1.90935 | 0.022577 |
| Sb09g022260 | Unknown protein | 428 | 43.4989 | -3.29856 | 0.022577 |
| Sb09g024060 | KINβ1 - SNF1-related protein kinase regulatory subunit beta-1 | 226.435 | 38.5695 | -2.55356 | 0.022577 |
| Sb09g024230 | CYS6 - Cysteine proteinase inhibitor 6 | 63.9594 | 240.365 | 1.91 | 0.022577 |
| Sb09g029500 | PG2 - Polygalacturonase | 7.38358 | 47.9777 | 2.69997 | 0.022577 |
| - | NI | 0 | 76.565 | inf | 0.022577 |

“NI” means no identified; “inf” indicates no ratio.

Table S4. Composite list of DEGs in internode 9th between ScGAIOE and HpScGAI.

| GeneID | Annotation | ScGAIOE | HpScGAI | Fold change (Log2) | q-values |
|-------------|--|----------|---------|--------------------|----------|
| Sb01g000580 | GA20ox2 - Gibberellin 20 oxidase 2 | 1.48898 | 0 | inf | 0.009611 |
| Sb01g004295 | SMT1 – Sterol methyltransferase 1 | 61.391 | 0 | inf | 0.023238 |
| Sb01g007170 | ZAT6 - Zinc finger protein | 4.21876 | 75.7109 | 4.16561 | 0.023238 |
| Sb01g007340 | PP2C clade D5 – ADP5 | 30.8246 | 241.756 | 2.9714 | 0.009611 |
| Sb01g013190 | SPX (SYG1/Pho81/XPR1) domain-containing protein / zinc finger (C3HC4-type RING finger) protein-related | 5.91843 | 0 | inf | 0.009611 |
| Sb01g014350 | Cytochrome P450. family 87. subfamily A. polypeptide 2 – CYP87A2 | 12.3886 | 57.9573 | 2.22598 | 0.033482 |
| Sb01g020430 | Unknown protein | 129.822 | 16.4984 | -2.97613 | 0.009611 |
| Sb01g020570 | PHT1.4 -Inorganic phosphate transporter 1-4 | 16.15 | 82.9606 | 2.36089 | 0.023238 |
| Sb01g021130 | GDSL esterase/lipase EXL3 | 3.00806 | 0 | inf | 0.009611 |
| Sb01g027285 | PSBC - Photosystem II reaction center protein C | 0 | 15.7927 | inf | 0.033482 |
| Sb01g027810 | Early-responsive to dehydration – (ERD4) | 38.451 | 8.18857 | -2.23134 | 0.033482 |
| Sb01g029330 | EXPβ2 - Expansin-β2 | 3.53089 | 0 | inf | 0.017156 |
| Sb01g032610 | Terpene synthase –TPS21 | 15.0758 | 114.789 | 2.92867 | 0.009611 |
| Sb01g035970 | Putative uncharacterized protein | 2.17049 | 0 | inf | 0.037292 |
| Sb01g043030 | BGLU40 - Beta-glucosidase 40 | 1.65775 | 0 | inf | 0.017156 |
| Sb01g001160 | CYP71B23 - Cytochrome P450 | 1.13987 | 0 | inf | 0.023238 |
| Sb01g003270 | C2H2-type zinc finger family protein | 0 | 8.10497 | inf | 0.009611 |
| Sb01g003280 | C2H2-type zinc finger family protein | 0 | 8.15342 | inf | 0.009611 |
| Sb01g003710 | ATAF2 – NAC domain protein | 12.1639 | 161.214 | 3.7283 | 0.009611 |
| Sb01g004320 | Cupredoxin superfamily protein | 3.59622 | 0 | inf | 0.009611 |
| Sb01g004740 | AAA-ATPASE 1 | 25.9359 | 194.583 | 2.90736 | 0.009611 |
| Sb01g005900 | Syntaxin-121 | 11.6421 | 84.0838 | 2.85247 | 0.009611 |
| Sb01g007220 | Putative uncharacterized protein | 0 | 83.1714 | inf | 0.009611 |
| Sb01g008350 | BIL4 - BRZ-Insensitive-long hypocotyls 4 | 29.4707 | 285.007 | 3.27364 | 0.009611 |
| Sb01g010050 | Uncharacterized protein | 33.4779 | 220.235 | 2.71776 | 0.009611 |
| Sb01g013270 | YAB1 - Axial regulator YABBY 1 | 5.88927 | 0 | inf | 0.045876 |
| Sb01g014120 | SHY2/IAA3 - Auxin-responsive protein | 1.9053 | 0 | inf | 0.037292 |
| Sb01g015070 | Terpenoid cyclases | 0.980916 | 0 | inf | 0.037292 |
| Sb01g018360 | ABCG11 - ABC transporter G family member 11 | 1.18957 | 0 | inf | 0.017156 |
| Sb01g036020 | CBL-interacting serine/threonine-protein kinase 10 – CIPK10 | 53.221 | 10.0121 | -2.41025 | 0.029034 |
| Sb01g037090 | GOLS1 - Galactinol synthase 1 | 14.5121 | 85.3798 | 2.55664 | 0.009611 |
| Sb01g037850 | COBL7 - COBRA-like protein 7 | 5.25721 | 50.5362 | 3.26495 | 0.009611 |
| Sb01g038410 | AP2C1 - PP2C clade B | 18.8677 | 500.749 | 4.7301 | 0.009611 |

“inf” indicates no ratio.

Table S4. Continuation.

| GeneID | Annotation | ScGAIOE | HpScGAI | Fold change (Log2) | q-values |
|-------------|--|---------|---------|--------------------|----------|
| Sb01g039530 | HSP70 - Heat shock protein | 74.932 | 394.979 | 2.39812 | 0.009611 |
| Sb01g041310 | Glycosyl hydrolase family 10 | 1.31809 | 0 | inf | 0.009611 |
| Sb01g043460 | Uncharacterized protein | 57.5594 | 228.242 | 1.98744 | 0.029034 |
| - | NI | 29.0104 | 161.221 | 2.4744 | 0.009611 |
| Sb10g000980 | CSLD3 - Cellulose synthase-like protein D3 | 13.2009 | 76.3735 | 2.53243 | 0.009611 |
| Sb10g001620 | CBF3 - Dehydration-responsive element-binding protein 1A | 0 | 1.86575 | inf | 0.041518 |
| Sb10g003340 | GDSL esterase/lipase | 1.00144 | 0 | inf | 0.045876 |
| Sb10g003890 | GDSL esterase/lipase | 265.057 | 47.8687 | -2.46915 | 0.009611 |
| Sb10g012970 | Peptidyl-prolyl cis-trans isomerase FKBP65 – ROF2 | 23.5841 | 706.669 | 4.90515 | 0.009611 |
| Sb10g023970 | Uncharacterized protein | 86.9415 | 10.8877 | -2.99735 | 0.009611 |
| Sb10g025210 | LTP129 - Protease inhibitor/seed storage/LTP family protein | 1.70765 | 0 | inf | 0.009611 |
| Sb10g027000 | Patellin-4 | 1.42238 | 0 | inf | 0.009611 |
| Sb10g000660 | Pectate lyase-like superfamily protein | 83.7454 | 16.5356 | -2.34043 | 0.009611 |
| Sb10g002070 | ADC2 - Arginine decarboxylase 2 | 8.75275 | 46.4398 | 2.40755 | 0.029034 |
| Sb10g004240 | UDGT71C5 - UDP-glycosyltransferase 71C5 | 1.09525 | 0 | inf | 0.037292 |
| Sb10g006630 | Putative uncharacterized | 6.03264 | 73.3782 | 3.60449 | 0.009611 |
| Sb10g008130 | FTSH6 - ATP-dependent zinc metalloprotease | 5.40909 | 33.3836 | 2.62568 | 0.029034 |
| Sb10g012220 | BGLU17 - Beta-glucosidase 17 | 50.3167 | 4.58139 | -3.45718 | 0.017156 |
| - | NI | 35.7038 | 0 | inf | 0.009611 |
| Sb02g009340 | Putative lipid-transfer protein DIR1 | 0 | 32.7424 | inf | 0.023238 |
| Sb02g022290 | WRKY53 | 3.48877 | 80.0604 | 4.5203 | 0.009611 |
| Sb02g028240 | SAP5 – Stress associated protein 5 | 23.4327 | 126.628 | 2.434 | 0.009611 |
| Sb02g033240 | xyloglucan endotransglucosylase/hydrolase protein 32 – XTH32 | 5.67153 | 0 | inf | 0.009611 |
| Sb02g035460 | O-Glycosyl hydrolases family 17 protein | 2.16182 | 0 | inf | 0.009611 |
| Sb02g001740 | Uncharacterized protein | 1.2766 | 0 | inf | 0.017156 |
| Sb02g004390 | ELIP1 - Early light-induced protein 1. chloroplastic | 0 | 6.35111 | inf | 0.009611 |
| Sb02g004670 | SHY2/IAA3 - Auxin-responsive protein | 20.1516 | 248.64 | 3.62509 | 0.009611 |
| Sb02g005780 | GALT6 – O-galactosyltransferase | 3.79149 | 29.0339 | 2.9369 | 0.033482 |
| Sb02g009600 | CRSP – CO2-response secreted protease | 49.9568 | 3.84074 | -3.70122 | 0.009611 |
| Sb02g023660 | Glycosyl hydrolase family 81 protein | 5.3742 | 38.8393 | 2.85339 | 0.009611 |
| Sb02g023910 | SAP12 – Stress associated protein 12 | 0 | 7.34847 | inf | 0.009611 |
| Sb02g031550 | Copper amine oxidase family protein | 0 | 6.2105 | inf | 0.009611 |
| Sb02g035930 | B-120 -G-type lectin S-receptor-like serine/threonine-protein kinase | 0 | 1.01966 | inf | 0.009611 |

“NI” means no identified; “inf” indicates no ratio.

Table S4. Continuation.

| GeneID | Annotation | ScGAIOE | HpScGAI | Fold change (Log2) | q-values |
|-------------|---|----------|---------|--------------------|----------|
| Sb02g036605 | Unknown protein | 0 | 7.34847 | inf | 0.009611 |
| Sb02g037350 | OSM34 - Osmotin-like protein | 1.52028 | 0 | inf | 0.033482 |
| Sb02g042280 | GDSL esterase/lipase | 2.92582 | 0 | inf | 0.009611 |
| Sb02g043060 | Putative uncharacterized protein | 2.41391 | 116.664 | 5.59484 | 0.009611 |
| - | NI | 0 | 68.2309 | inf | 0.023238 |
| Sb03g003000 | Unknown protein | 7.38097 | 43.0973 | 2.54571 | 0.037292 |
| Sb03g003530 | HSP17.6II - Heat shock | 18.5509 | 136.753 | 2.88201 | 0.009611 |
| Sb03g006880 | HSP18.2 - Heat shock | 149.763 | 1297.54 | 3.11503 | 0.009611 |
| Sb03g013210 | Peroxidase superfamily protein | 1.44158 | 0 | inf | 0.037292 |
| Sb03g026050 | Unknown protein | 2.10569 | 56.9051 | 4.75619 | 0.017156 |
| Sb03g029790 | EMB2742 – Embryo defective 2742 | 19.6885 | 1.34664 | -3.86992 | 0.023238 |
| Sb03g030340 | MAN7 - Mannan endo-1.4-beta-mannosidase 7 | 1.94234 | 0 | inf | 0.009611 |
| Sb03g037080 | ERF9 - Ethylene-responsive transcription factor 9 | 23.8588 | 173.638 | 2.86349 | 0.009611 |
| Sb03g038290 | EXPA8 – Expansin A8 | 9.11544 | 0 | inf | 0.009611 |
| Sb03g038880 | 2-oxoglutarate (2OG) and Fe(II)-dependent oxygenase superfamily protein | 1.81198 | 0 | inf | 0.009611 |
| Sb03g041100 | CP22 Photosystem II subunit S | 16.5613 | 131.253 | 2.98646 | 0.009611 |
| Sb03g003310 | Unknown protein | 3.70572 | 186.675 | 5.65463 | 0.009611 |
| Sb03g006870 | HSP18.2 - Heat shock | 254.858 | 1830.2 | 2.84424 | 0.009611 |
| Sb03g020184 | GRP1 – Glycine-rich RNA binding protein 1 | 5.2335 | 44.5266 | 3.08882 | 0.017156 |
| Sb03g025730 | Calmodulin-binding family protein | 1.92449 | 62.3619 | 5.01812 | 0.029034 |
| Sb03g029520 | AKT1 – K ⁺ transporter | 1.90883 | 18.1015 | 3.24535 | 0.023238 |
| Sb03g032140 | MAPKKK17 - Mitogen-activated protein kinase kinase kinase 17 | 0 | 3.77935 | inf | 0.009611 |
| Sb03g034090 | OXS3 – Oxidative stress 3 | 57.4861 | 298.396 | 2.37594 | 0.009611 |
| Sb03g039330 | Pathogenesis-related thaumatin superfamily protein | 1.73687 | 0 | inf | 0.041518 |
| Sb03g040300 | HSPRO1 - Nematode resistance protein-like | 4.23374 | 88.2553 | 4.38168 | 0.017156 |
| Sb03g040950 | ASFT- Aliphatic suberin feruloyl-transferase | 2.04455 | 0 | inf | 0.009611 |
| Sb03g043430 | Unknown protein | 321.263 | 1793.6 | 2.48103 | 0.009611 |
| Sb03g045000 | Calcium-dependent lipid-binding (CaLB domain) family protein | 3.19283 | 57.1091 | 4.16081 | 0.041518 |
| - | NI | 0 | 50.8151 | inf | 0.041518 |
| - | NI | 0 | 16.6245 | inf | 0.009611 |
| Sb04g002950 | SRF1 - Strubbelig-receptor family 1 | 0.949692 | 0 | inf | 0.033482 |
| Sb04g005520 | WRKY40 | 7.67975 | 66.5328 | 3.11493 | 0.009611 |
| Sb04g008670 | Myb-like HTH transcriptional regulator-like protein | 1.26062 | 0 | inf | 0.017156 |

“NI” means no identified; “inf” indicates no ratio.

Table S4. Continuation.

| GenID | Annotation | ScGAIOE | HpScGAI | Fold change (Log2) | q-values |
|-------------|--|---------|---------|--------------------|----------|
| Sb04g009690 | UGT84B2 - UDP-glucosyl transferase 84B2 | 272.006 | 1080.61 | 1.99014 | 0.045876 |
| Sb04g026560 | PAL1 - Phenylalanine ammonia-lyase 1 | 2.70701 | 32.8481 | 3.60104 | 0.033482 |
| Sb04g028460 | GATL9 - Galacturonosyltransferase-like 9 | 7.07327 | 117.151 | 4.04985 | 0.009611 |
| Sb04g028490 | Actin-binding FH2 (formin homology 2) family protein | 5.46972 | 47.7885 | 3.12713 | 0.033482 |
| Sb04g028830 | SGNH hydrolase-type esterase superfamily protein | 5.40017 | 0 | inf | 0.009611 |
| Sb04g030080 | GALS1 – Galactan synthase 1 | 29.9729 | 162.196 | 2.43601 | 0.029034 |
| Sb04g032250 | ERD10 – Early responsive to dehydration 10 | 43.0117 | 201.862 | 2.23057 | 0.023238 |
| Sb04g032820 | EXPβ4 - Expansin-β4 | 1.83753 | 0 | inf | 0.009611 |
| Sb04g035630 | GAE1 - UDP-glucuronate 4-epimerase 1 | 6.30856 | 50.7312 | 3.00749 | 0.009611 |
| Sb04g035810 | BRS1 - BRI1 suppressor 1 | 2.83118 | 0 | inf | 0.009611 |
| Sb04g007190 | KCS11 - 3-ketoacyl-CoA synthase 11 | 4.05567 | 41.0833 | 3.34054 | 0.009611 |
| Sb04g007230 | UGT73C6 - UDP-glycosyltransferase 73C6 | 1.03048 | 0 | inf | 0.041518 |
| Sb04g008110 | Leucine-rich repeat receptor-like protein kinase | 36.2994 | 3.48495 | -3.38073 | 0.009611 |
| Sb04g015420 | SWEET7 - Bidirectional sugar transporter | 212.628 | 50.4851 | -2.0744 | 0.037292 |
| Sb04g027330 | HSP20 - Heat shock protein | 21.7175 | 429.757 | 4.30659 | 0.009611 |
| Sb04g029960 | XCP1 - Xylem cysteine proteinase 1 | 14.063 | 0 | inf | 0.009611 |
| Sb04g032830 | EXPβ4 - Expansin-β4 | 9.63691 | 0 | inf | 0.009611 |
| Sb04g033150 | DALL1 - Phospholipase A1-1beta2 | 5.62398 | 65.7296 | 3.54688 | 0.009611 |
| Sb04g036920 | PPPDE putative thiol peptidase family protein | 39.4882 | 297.702 | 2.91438 | 0.009611 |
| - | NI | 0 | 28.1379 | inf | 0.009611 |
| Sb05g002640 | Ankyrin repeat-containing protein | 3.95258 | 82.5697 | 4.38475 | 0.009611 |
| Sb05g017960 | HSD1 - 11-beta-hydroxysteroid dehydrogenase 1B | 2.19215 | 0 | inf | 0.009611 |
| Sb05g019180 | TPS21 - Terpene synthase | 0 | 4.2059 | inf | 0.009611 |
| Sb05g022580 | Subtilisin-like protease | 2.5171 | 0 | inf | 0.009611 |
| Sb05g022620 | Subtilisin-like protease | 90.7985 | 9.38795 | -3.27379 | 0.009611 |
| - | NI | 0 | 6.62481 | inf | 0.009611 |
| - | NI | 0 | 12.8641 | inf | 0.009611 |
| - | NI | 0 | 20.9474 | inf | 0.029034 |
| Sb06g001970 | APX3- Ascorbate peroxidase 3 | 0 | 8.9377 | inf | 0.009611 |
| Sb06g002500 | Unknown protein | 373.849 | 0 | inf | 0.009611 |
| Sb06g024110 | Homeodomain-like superfamily protein | 16.6101 | 175.367 | 3.40025 | 0.009611 |
| Sb06g025870 | MATE efflux family protein | 4.61271 | 41.5433 | 3.17093 | 0.029034 |
| Sb06g028090 | ERF7 - Ethylene-responsive transcription factor 7 | 6.68328 | 101.31 | 3.92208 | 0.009611 |

“NI” means no identified; “inf” indicates no ratio.

Table S4. Continuation.

| GeneID | Annotation | ScGAIOE | HpScGAI | Fold change (Log2) | q-values |
|-------------|--|----------|----------|--------------------|----------|
| Sb06g033520 | CCR4-associated factor 1B | 6.62306 | 120.969 | 4.191 | 0.009611 |
| Sb06g000660 | HSP90.1 - Heat shock | 19.1757 | 356.74 | 4.21752 | 0.009611 |
| Sb06g015940 | XTH25 - Xyloglucan endotransglucosylase/hydrolase protein 25 | 15.8663 | 106.42 | 2.74573 | 0.009611 |
| Sb06g022880 | GA2OX8 - Gibberellin 2-beta-dioxygenase 8 | 0 | 2.33684 | inf | 0.017156 |
| Sb06g025170 | CYP86A4 - Cytochrome P450 86A4 | 1.06864 | 0 | inf | 0.023238 |
| Sb06g026160 | ACS6 - 1-aminocyclopropane-1-carboxylate synthase 6 | 2.62987 | 46.1604 | 4.13359 | 0.009611 |
| Sb06g031300 | Peroxidase superfamily protein | 1.4164 | 0 | inf | 0.017156 |
| Sb06g033570 | NDR1/HIN1-LIKE 2 | 59.3943 | 275.639 | 2.21438 | 0.023238 |
| - | NI | 164.003 | 0 | inf | 0.037292 |
| - | NI | 64.7768 | 0 | inf | 0.009611 |
| - | NI | 1037.36 | 0 | inf | 0.009611 |
| - | NI | 532.815 | 0 | inf | 0.009611 |
| - | NI | 173.809 | 0 | inf | 0.009611 |
| - | NI | 325.53 | 0 | inf | 0.009611 |
| - | NI | 421.92 | 0 | inf | 0.009611 |
| - | NI | 18.1711 | 0 | inf | 0.037292 |
| Sb07g000510 | CYP71B34 - Cytochrome P450 71B34 | 1.92836 | 0 | inf | 0.017156 |
| Sb07g023030 | ERF109 - Ethylene-responsive transcription factor109 | 0 | 5.07173 | inf | 0.023238 |
| Sb07g001090 | Core-2/l-branching beta-1.6-N-acetylglucosaminyltransferase family protein | 18.7012 | 231.186 | 3.62785 | 0.009611 |
| Sb07g009580 | Eukaryotic aspartyl protease family protein | 0.835311 | 0 | inf | 0.045876 |
| Sb07g020270 | TPS9 - Trehalose-6-phosphatase synthase 9 | 31.7242 | 5.11352 | -2.63319 | 0.045876 |
| Sb07g023210 | PLP2 - Patatin-like protein 2 | 0 | 0.903477 | inf | 0.041518 |
| Sb07g023340 | UCP5 - Mitochondrial uncoupling protein 5 | 32.0565 | 198.451 | 2.6301 | 0.009611 |
| Sb08g004980 | AAP3 - Amino acid permease 3 | 6.62457 | 49.2703 | 2.89482 | 0.017156 |
| Sb08g005680 | HXXXD-type acyl-transferase family protein | 1.39852 | 0 | inf | 0.037292 |
| Sb08g015237 | CRK10 - Cysteine-rich receptor-like protein kinase 10 | 1.52622 | 0 | inf | 0.033482 |
| Sb08g004960 | AAP3 - Amino acid permease 3 | 9.06995 | 79.2295 | 3.12687 | 0.009611 |
| Sb08g021800 | LATE FLOWERING | 6.28197 | 0 | inf | 0.009611 |
| Sb08g022450 | OSM34 – Osmotin 34 | 1.56038 | 0 | inf | 0.041518 |
| - | NI | 0 | 26.0123 | inf | 0.009611 |
| - | NI | 0 | 16.652 | inf | 0.041518 |
| Sb09g002390 | TZF9 – Tandem Zinc finger protein 9 | 19.2684 | 164.072 | 3.09002 | 0.009611 |
| Sb09g003230 | Phosphoglycerate mutase family protein | 41.2426 | 197.18 | 2.25731 | 0.033482 |

“NI” means no identified; “inf” indicates no ratio.

Table S4. Continuation.

| GeneID | Annotation | ScGAIOE | HpScGAI | Fold change (Log2) | q-values |
|-------------|--|---------|---------|--------------------|----------|
| Sb09g006030 | PFK3 - Phosphofructokinase 3 | 0 | 7.30325 | inf | 0.009611 |
| Sb09g015900 | WRKY33 | 5.95004 | 64.2507 | 3.43274 | 0.009611 |
| Sb09g017190 | Glycine-rich protein family | 8.96748 | 0 | inf | 0.009611 |
| Sb09g023380 | ARM repeat superfamily protein | 1.51129 | 75.3009 | 5.63881 | 0.009611 |
| Sb09g025090 | Protein of unknown function (DUF567) | 0 | 2.78348 | inf | 0.033482 |
| Sb09g026830 | WRKY51 | 5.3416 | 49.6088 | 3.21525 | 0.009611 |
| Sb09g000270 | CYP722A1 - Cytochrome P450, family 722, subfamily A, polypeptide 1 | 33.9448 | 5.2331 | -2.69745 | 0.045876 |
| Sb09g003060 | RCI2A - Rare-cold-inducible 2a | 99.5521 | 501.7 | 2.3333 | 0.037292 |
| Sb09g005340 | Unknown protein | 0 | 16.4329 | inf | 0.009611 |
| Sb09g019930 | PPDK - Pyruvate orthophosphate dikinase 1 | 29.8375 | 129.252 | 2.11498 | 0.023238 |
| Sb09g022260 | Unknown protein | 765.238 | 75.2771 | -3.34562 | 0.009611 |
| Sb09g027360 | PMEAMT - Phosphomethylethanolamine N-methyltransferase | 98.5499 | 6.18125 | -3.99488 | 0.009611 |
| Sb09g029130 | CTP synthase | 56.7059 | 14.5123 | -1.96622 | 0.037292 |
| Sb09g029575 | RL6 - Protein RADIALIS-like 6 | 24.0965 | 0 | inf | 0.033482 |
| Sb09g029860 | LEA27 - Late embryogenesis abundant 27 | 85.0088 | 516.241 | 2.60236 | 0.009611 |
| - | NI | 0 | 62.1164 | inf | 0.029034 |

“NI” means no identified; “inf” indicates no ratio.

Table S5. Primers used in this study.

| Primer | Sequences | Used for |
|----------------|---|----------------------|
| ScUbi-1_fw | 5'-CCGGTCCTTTAAACCAACTCAGT-3' | cDNA |
| ScUbi-1_rev | 5'-CCCTCTGGTGACCTCCATTTG-3' | |
| ScGAI_fw | 5'-CATATGAAGCGCGAGTACCAAGACGC-3' | Cloning and YTH |
| ScGAI_rev | 5'-CTGCAGCCCCACCCCTCGATCAC-3' | |
| ScPIF3_fw | 5'- CATATGTCCGACGGCAACGAGT -3' | Cloning and YTH |
| ScPIF3_rev | 5'-CTCGAGGCTGACTGTTTTTATGTTTCAGCT-3' | |
| ScPIF4_fw | 5'- CATATGGACGGCAATGCGAG-3' | Cloning and YTH |
| ScPIF4_rev | 5'-GAGCTCTTACGAGATTTTCTCATTCTAAAC-3' | |
| ScPIF5_fw | 5'-CGCCCCATATGAACCAG-3' | Cloning and YTH |
| ScPIF5_rev | 5'- GGATCCATCAACCTAACACCATCATATCA-3' | |
| ScGAI_fw | 5'-TCTAGAATGAAGCGCGAGTACCAAGACGC-3' | BIFC |
| ScGAI_rev | 5'-CCCGGGCCCCACCCCTCGACGGAGC-3' | |
| ScGAI_trunc_fw | 5'-TCTAGAATGCGCAAGGTCGCCGCTACTT-3' | BIFC |
| ScPIF3_fw | 5'- TCTAGAATGTCCGACGGCAACGAGT -3' | |
| ScPIF3_rev | 5'-GTCGACTGTTTCAGCTTCATTTCTTCC-3' | BIFC |
| ScPIF4_fw | 5'- TCTAGAATGGACGGCAATGCGAG-3' | |
| ScPIF4_rev | 5'-GTCGACAACCTCCAAAAGTAGGTGG-3' | BIFC |
| oxScGAI_fw | 5'- GATATCGTAAACCATGGACTACAAGGACGACGATGACAAAATGAAGC GCGAGTACCAAGACGC-3' | ScGAI overexpressing |
| oxScGAI_rev | 5'-GGGGTACCCCCACCCCTCGATCAC-3' | |
| asScGAI_fw | 5'-CGGGATCCGGATGACGACGAGGAAGAGGAA-3' | ScGAI silencing |
| asScGAI_rev | 5'-GGCCAGATATCGAGGAGATGGACGAGATGCT-3' | |
| sScGAI_fw | 5'-CGACGCGTCGAGGAGATGGACGAGATGCT-3' | ScGAI silencing |
| sScGAI_rev | 5'-GGGGTACCCCGGATGACGACGAGGAAGAGGAA-3' | |
| IntronII_fw | 5'-GGCCAGATATCATGCGTAACTGATCTGAATT-3' | ScGAI silencing |
| IntronII_rev | 5'-CGACGCGTCACCTGCAGAGTGTGTAGATAA-3' | |
| ScEIN3_fw | 5'-AAAATCTAGAATGATGGGAGGCGGGCTGATGA-3' | Cloning and BIFC |
| ScEIN3_rev | 5'-AAAACCCGGGTAGAACCAATTGGTCCCGTCGT-3' | |
| ScEIL1_fw | 5'-AAAATCTAGATACCTCTACGCTCGGCGTGATG-3' | Cloning and BIFC |
| ScEIL1_rev | 5'-AAAACCCGGGATTCTGCCGAGGTAGAACCAATT-3' | |
| ScEIN3_fw | 5'-AAAACATATGATGGGAGGCGGGCTGATGA -3' | YTH |
| ScEIN3_rev | 5'-AAAACCTCGAGTCAGTAGAACCAATTGGTCCCGT -3' | |
| ScEIL1_fw | 5'-AAAACATATGATGGGAGGAAGAGGGGC -3' | YTH |
| ScEIL1_rev | 5'-AAAAGAATTCTCAGTAGAACCAATTGGCGTTGGAT -3' | |

Table S5. Continuation.

| Primer | Sequences | Used for |
|--------------------|--|--------------------------|
| ScEIN3_tr_fw | 5'-CATATGATGCAGCACTGTGACCCCCACAG -3' | YTH |
| ScEIN3_tr_rev | 5'-GAATTCTCACTGGGGCATGGCATTAGGCCTCTC -3' | |
| ScGAI_SAW_fw | 5'-GCTGGCACTCTTCAACG-3' | Arabidopsis screening |
| VENUS_rev | 5'- CCAGCTCGACCAGGATG-3' | |
| β actin2_fw | 5'-TTCTCTCCTTGTACGCC -3' | Arabidopsis screening |
| β actin2_rev | 5'- AACGATTCCTGGACCTGCCTCATC-3' | |
| ScPIF3_fw | 5'- GAATTCATGTCCGACGGCAACGAGT -3' | Subcellular localization |
| ScPIF3_rev | 5'-AAGCTTTGTTTCAGCTTCATTTCTTCC-3' | |
| ScPIF4_fw | 5'- AAGCTTATGGACGGCAATGCGAG-3' | Subcellular localization |
| ScPIF4_rev | 5'-AAGCTTAACTCCAAAAGTAGGTGG-3' | |
| ScGA20ox_fw | 5'-GCTTCTCCAGGTGGTCAAC-3' | qPCR |
| ScGA20ox_rev | 5'-CGTGAAGAAGGCGTCCAT-3' | |
| ScGA2ox_fw | 5'-GAGGCCGTCAGGTTCTTC-3' | qPCR |
| ScGA2ox_rev | 5'-GCGAGGAGGAGGTACTIONCG-3' | |
| Ubi1_intron_fw | 5'-TTGTCGATGCTCACCCCTGTTGTTTG-3' | Genotype screening |
| ScGAI_rev | 5'-GGGAGATCGAAGTAGCCAGC-3' | |
| ScGAI_fw | 5'- CACCGTGCACTACAATCCCT-3' | |
| qUTR_della_fw | 5'-CACCTCCGCTTCAAGGTC-3' | qPCR |
| qUTR_della_rev | 5'-CTTGGTACTCGCGCTTCAT-3' | |
| qDELLA_fw | 5'-CCAAGGACAAGATGATGGTG-3' | qPCR |
| qDELLA_rev | 5'-GACGAACGCACCTTGTACC-3' | |

6 References

1. Tammisola, J. Towards much more efficient biofuel crops - can sugarcane pave the way? *GM Crops* **1**, 181–98 (2010).
2. Wang, J., Nayak, S., Koch, K. & Ming, R. Carbon partitioning in sugarcane (*Saccharum* species). *Front. Plant Sci.* **4**, 201 (2013).
3. Braun, D. M. & Slewinski, T. L. Genetic control of carbon partitioning in grasses: roles of sucrose transporters and tie-dyed loci in phloem loading. *Plant Physiol.* **149**, 71–81 (2009).
4. Leite, G. H. ., Crusciol, C. A. . & Silva, M. . Desenvolvimento e produtividade da cana-de-açúcar após aplicação de reguladores vegetais em meio de safra. *Semina: Ciências Agrárias, Londrina*, v.32, n.1 129–138 (2011). Available at: file:///C:/Users/Rafael Garcia/Downloads/Semina, v.32, n.1, p.129-138, 2011.pdf. (Accessed: 2nd July 2014)
5. McCormick, a J., Cramer, M. D. & Watt, D. a. Sink strength regulates photosynthesis in sugarcane. *New Phytol.* **171**, 759–70 (2006).
6. McCormick, a J., Watt, D. a & Cramer, M. D. Supply and demand: sink regulation of sugar accumulation in sugarcane. *J. Exp. Bot.* **60**, 357–64 (2009).
7. McCormick, a J., Cramer, M. D. & Watt, D. a. Changes in photosynthetic rates and gene expression of leaves during a source-sink perturbation in sugarcane. *Ann. Bot.* **101**, 89–102 (2008).
8. Li, C. *et al.* Differential expression profiles and pathways of genes in sugarcane leaf at elongation stage in response to drought stress. *Sci. Rep.* **6**, 25698 (2016).
9. Cardozo, N. P. Modelagem da maturação da cana-de-açúcar em função de variáveis meteorológicas. (Universidade de São Paulo - Escola Superior de Agricultura ‘Luiz de Queiroz’ - Piracicaba, 2012).
10. Davière, J.-M. *et al.* Gibberellin signaling in plants. *Development* **140**, 1147–51 (2013).
11. Hirsch, S. & Oldroyd, G. E. D. GRAS-domain transcription factors that regulate plant development. *Plant Signal. Behav.* **4**, 698–700 (2009).
12. Murase, K., Hirano, Y., Sun, T. & Hakoshima, T. Gibberellin-induced DELLA recognition by the gibberellin receptor GID1. *Nature* **456**, 459–63 (2008).

13. Sheerin, D. J. *et al.* Inter- and intra-molecular interactions of Arabidopsis thaliana DELLA protein RGL1. *Biochem. J.* **435**, 629–39 (2011).
14. Peng, J. *et al.* The Arabidopsis GAI gene defines a signaling pathway that negatively regulates gibberellin responses. *Genes Dev.* **11**, 3194–205 (1997).
15. Hirano, K. *et al.* The suppressive function of the rice DELLA protein SLR1 is dependent on its transcriptional activation activity. *Plant J.* **71**, 443–53 (2012).
16. Yoshida, H. *et al.* DELLA protein functions as a transcriptional activator through the DNA binding of the INDETERMINATE DOMAIN family proteins. *Proc. Natl. Acad. Sci.* **111**, 7861–7866 (2014).
17. Park, J., Nguyen, K. T., Park, E., Jeon, J.-S. & Choi, G. DELLA Proteins and Their Interacting RING Finger Proteins Repress Gibberellin Responses by Binding to the Promoters of a Subset of Gibberellin-Responsive Genes in Arabidopsis. *Plant Cell* **25**, 927–943 (2013).
18. Park, J. *et al.* Gibberellin Signaling Requires Chromatin Remodeler PICKLE to Promote Vegetative Growth and Phase Transitions. *Plant Physiol.* **173**, 1463–1474 (2017).
19. Sarnowska, E. A. *et al.* DELLA-Interacting SWI3C Core Subunit of Switch/Sucrose Nonfermenting Chromatin Remodeling Complex Modulates Gibberellin Responses and Hormonal Cross Talk in Arabidopsis. *PLANT Physiol.* **163**, 305–317 (2013).
20. Li, K. *et al.* DELLA-mediated PIF degradation contributes to coordination of light and gibberellin signalling in Arabidopsis. *Nat. Commun.* **7**, 11868 (2016).
21. de Lucas, M. *et al.* A molecular framework for light and gibberellin control of cell elongation. *Nature* **451**, 480–4 (2008).
22. Li, Q.-F. *et al.* An Interaction Between BZR1 and DELLAs Mediates Direct Signaling Crosstalk Between Brassinosteroids and Gibberellins in Arabidopsis. *Sci. Signal.* **5**, ra72-ra72 (2012).
23. Yu, S. *et al.* Gibberellin regulates the Arabidopsis floral transition through miR156-targeted SQUAMOSA promoter binding-like transcription factors. *Plant Cell* **24**, 3320–32 (2012).
24. Arnaud, N. *et al.* Gibberellins control fruit patterning in Arabidopsis thaliana. *Genes Dev.* **24**,

- 2127–32 (2010).
25. Wang, H. *et al.* The DELLA-CONSTANS Transcription Factor Cascade Integrates Gibberellic Acid and Photoperiod Signaling to Regulate Flowering. *Plant Physiol.* **172**, 479–88 (2016).
 26. Hedden, P. & Sponsel, V. A Century of Gibberellin Research. *J. Plant Growth Regul.* **34**, 740–60 (2015).
 27. Yamaguchi, S. Gibberellin metabolism and its regulation. *Annu. Rev. Plant Biol.* **59**, 225–51 (2008).
 28. Yamaguchi, S. & Kamiya, Y. Gibberellin biosynthesis: its regulation by endogenous and environmental signals. *Plant Cell Physiol.* **41**, 251–7 (2000).
 29. Nakajima, M. *et al.* Identification and characterization of Arabidopsis gibberellin receptors. *Plant J.* **46**, 880–9 (2006).
 30. Hirano, K. *et al.* Characterization of the molecular mechanism underlying gibberellin perception complex formation in rice. *Plant Cell* **22**, 2680–96 (2010).
 31. Achard, P. & Genschik, P. Releasing the brakes of plant growth: how GAs shutdown DELLA proteins. *J. Exp. Bot.* **60**, 1085–92 (2009).
 32. Ariizumi, T., Murase, K., Sun, T.-P. & Steber, C. M. Proteolysis-independent downregulation of DELLA repression in Arabidopsis by the gibberellin receptor GIBBERELLIN INSENSITIVE DWARF1. *Plant Cell* **20**, 2447–59 (2008).
 33. Griffiths, J. *et al.* Genetic characterization and functional analysis of the GID1 gibberellin receptors in Arabidopsis. *Plant Cell* **18**, 3399–414 (2006).
 34. Ueguchi-Tanaka, M. *et al.* Molecular interactions of a soluble gibberellin receptor, GID1, with a rice DELLA protein, SLR1, and gibberellin. *Plant Cell* **19**, 2140–55 (2007).
 35. Yamamoto, Y. *et al.* A Rice *gid1* Suppressor Mutant Reveals That Gibberellin Is Not Always Required for Interaction between Its Receptor, GID1, and DELLA Proteins. *PLANT CELL ONLINE* **22**, 3589–3602 (2010).
 36. Nelson, S. K. & Steber, C. M. in *Annual Plant Reviews, Volume 49* 153–188 (John Wiley & Sons, Ltd, 2016). doi:10.1002/9781119210436.ch6

37. Itoh, H. *et al.* Dissection of the phosphorylation of rice DELLA protein, SLENDER RICE1. *Plant Cell Physiol.* **46**, 1392–9 (2005).
38. Zentella, R. *et al.* O-GlcNAcylation of master growth repressor DELLA by SECRET AGENT modulates multiple signaling pathways in Arabidopsis. 164–176 (2016). doi:10.1101/gad.270587.115.modulated
39. Conti, L. *et al.* Small Ubiquitin-like Modifier protein SUMO enables plants to control growth independently of the phytohormone gibberellin. *Dev. Cell* **28**, 102–10 (2014).
40. Zentella, R. *et al.* The Arabidopsis O-fucosyltransferase SPINDLY activates nuclear growth repressor DELLA. *Nat. Chem. Biol.* (2017). doi:10.1038/nchembio.2320
41. Nguyen, L. K. *et al.* When ubiquitination meets phosphorylation: a systems biology perspective of EGFR/MAPK signalling. *Cell Commun. Signal.* **11**, 52 (2013).
42. Fu, X. *et al.* Gibberellin-mediated proteasome-dependent degradation of the barley DELLA protein SLN1 repressor. *Plant Cell* **14**, 3191–200 (2002).
43. Hussain, A., Cao, D., Cheng, H., Wen, Z. & Peng, J. Identification of the conserved serine/threonine residues important for gibberellin-sensitivity of Arabidopsis RGL2 protein. *Plant J.* **44**, 88–99 (2005).
44. Dai, C. & Xue, H.-W. Rice early flowering1, a CKI, phosphorylates DELLA protein SLR1 to negatively regulate gibberellin signalling. *EMBO J.* **29**, 1916–27 (2010).
45. Qin, Q. *et al.* Arabidopsis DELLA Protein Degradation Is Controlled by a Type-One Protein Phosphatase, TOPP4. *PLoS Genet.* **10**, e1004464 (2014).
46. Jacobsen, S. E., Binkowski, K. A. & Olszewski, N. E. SPINDLY, a tetratricopeptide repeat protein involved in gibberellin signal transduction in Arabidopsis. *Proc. Natl. Acad. Sci. U. S. A.* **93**, 9292–6 (1996).
47. Hartweck, L. M., Scott, C. L. & Olszewski, N. E. Two O-linked N-acetylglucosamine transferase genes of Arabidopsis thaliana L. Heynh. have overlapping functions necessary for gamete and seed development. *Genetics* **161**, 1279–91 (2002).
48. Colby, T., Matthäi, A., Boeckelmann, A. & Stäubli, H.-P. SUMO-conjugating and SUMO-deconjugating enzymes from Arabidopsis. *Plant Physiol.* **142**, 318–32 (2006).

49. Nelis, S., Conti, L., Zhang, C. & Sadanandom, A. A functional Small Ubiquitin-like Modifier (SUMO) interacting motif (SIM) in the gibberellin hormone receptor *GID1* is conserved in cereal crops and disrupting this motif does not abolish hormone dependency of the *DELLA-GID1* interaction. *Plant Signal. Behav.* **10**, e987528 (2015).
50. Rosa, M. *et al.* Soluble sugars--metabolism, sensing and abiotic stress: a complex network in the life of plants. *Plant Signal. Behav.* **4**, 388–93 (2009).
51. Moore, P. H. & Botha, F. C. *Sugarcane - Physiology, Biochemistry & Functional Biology*. (Wiley Blackwell, 2014).
52. Jackson, P. A. Breeding for improved sugar content in sugarcane. *F. Crop. Res.* **92**, 277–290 (2005).
53. McCormick, A. J., Watt, D. A. & Cramer, M. D. Supply and demand: sink regulation of sugar accumulation in sugarcane. *J. Exp. Bot.* **60**, 357–64 (2009).
54. McCormick, A. J., Cramer, M. D. & Watt, D. A. Regulation of photosynthesis by sugars in sugarcane leaves. *J. Plant Physiol.* **165**, 1817–1829 (2008).
55. Achard, P. *et al.* Integration of Plant Responses to Environmentally Activated Phytohormonal Signals. *Science (80-.)*. **311**, 91–94 (2006).
56. Weiss, D. & Ori, N. Mechanisms of cross talk between gibberellin and other hormones. *Plant Physiol.* **144**, 1240–6 (2007).
57. Li, Y., Van den Ende, W. & Rolland, F. Sucrose Induction of Anthocyanin Biosynthesis Is Mediated by *DELLA*. *Mol. Plant* **7**, 570–572 (2014).
58. Larkin, M. A. *et al.* Clustal W and Clustal X version 2.0. *Bioinformatics* **23**, 2947–8 (2007).
59. Saitou, N. & Nei, M. The neighbor-joining method: a new method for reconstructing phylogenetic trees. *Mol. Biol. Evol.* **4**, 406–425 (1987).
60. Tamura, K., Stecher, G., Peterson, D., Filipski, A. & Kumar, S. MEGA6: Molecular Evolutionary Genetics Analysis version 6.0. *Mol. Biol. Evol.* **30**, 2725–9 (2013).
61. Zuckerkandl, E. & Pauling, L. Evolutionary divergence and convergence in proteins. *Evol. Genes Proteins* 97–166 (1965).
62. Biasini, M. *et al.* SWISS-MODEL: modelling protein tertiary and quaternary structure using

- evolutionary information. *Nucleic Acids Res.* **42**, W252-8 (2014).
63. Yoo, S.-D., Cho, Y.-H. & Sheen, J. Arabidopsis mesophyll protoplasts: a versatile cell system for transient gene expression analysis. *Nat. Protoc.* **2**, 1565–72 (2007).
 64. Gleave, A. P. Short communication A versatile binary vector system with a T-DNA organisational structure conducive to efficient integration of cloned DNA into the plant genome. *Plant Mol. Biol.* **20**, 1203–1207 (1992).
 65. Rissel, D., Losch, J. & Peiter, E. The nuclear protein Poly(ADP-ribose) polymerase 3 (AtPARP3) is required for seed storability in Arabidopsis thaliana. *Plant Biol. (Stuttg.)* (2014). doi:10.1111/plb.12167
 66. Sparkes, I. a, Runions, J., Kearns, A. & Hawes, C. Rapid, transient expression of fluorescent fusion proteins in tobacco plants and generation of stably transformed plants. *Nat. Protoc.* **1**, 2019–25 (2006).
 67. Logemann, E., Birkenbihl, R. P., Ulker, B. & Somssich, I. E. An improved method for preparing Agrobacterium cells that simplifies the Arabidopsis transformation protocol. *Plant Methods* **2**, 16 (2006).
 68. Soares, J. S. M. *et al.* Oligomerization, membrane association, and in vivo phosphorylation of sugarcane UDP-glucose pyrophosphorylase. *J. Biol. Chem.* **289**, 33364–77 (2014).
 69. Amalraj, R. S. *et al.* Sugarcane proteomics: Establishment of a protein extraction method for 2-DE in stalk tissues and initiation of sugarcane proteome reference map. *Electrophoresis* **31**, 1959–1974 (2010).
 70. Aljanabi, S. Universal and rapid salt-extraction of high quality genomic DNA for PCR-based techniques. *Nucleic Acids Res.* **25**, 4692–4693 (1997).
 71. Livak, K. J. & Schmittgen, T. D. Analysis of Relative Gene Expression Data Using Real-Time Quantitative PCR and the $2^{-\Delta\Delta CT}$ Method. *Methods* **25**, 402–408 (2001).
 72. Marquardt, A., Scalia, G., Joyce, P., Basnayake, J. & Botha, F. C. Changes in photosynthesis and carbohydrate metabolism in sugarcane during the development of Yellow Canopy Syndrome. *Funct. Plant Biol.* **43**, 523 (2016).
 73. Cuadros-Inostroza, Á. *et al.* TargetSearch - a Bioconductor package for the efficient

- preprocessing of GC-MS metabolite profiling data. *BMC Bioinformatics* **10**, 428 (2009).
74. Stacklies, W., Redestig, H., Scholz, M., Walther, D. & Selbig, J. pcaMethods--a bioconductor package providing PCA methods for incomplete data. *Bioinformatics* **23**, 1164–7 (2007).
 75. Saraste, M., Sibbald, P. R. & Wittinghofer, A. The P-loop — a common motif in ATP- and GTP-binding proteins. *Trends Biochem. Sci.* **15**, 430–434 (1990).
 76. Cheng, H. *et al.* Gibberellin regulates Arabidopsis floral development via suppression of DELLA protein function. *Development* **131**, 1055–64 (2004).
 77. Jain, M. *et al.* F-box proteins in rice. Genome-wide analysis, classification, temporal and spatial gene expression during panicle and seed development, and regulation by light and abiotic stress. *Plant Physiol.* **143**, 1467–83 (2007).
 78. Schmid, M. *et al.* A gene expression map of Arabidopsis thaliana development. *Nat. Genet.* **37**, 501–6 (2005).
 79. Jasinski, S. *et al.* PROCERA encodes a DELLA protein that mediates control of dissected leaf form in tomato. *Plant J.* **56**, 603–12 (2008).
 80. Sakamoto, T., Kamiya, N., Ueguchi-Tanaka, M., Iwahori, S. & Matsuoka, M. KNOX homeodomain protein directly suppresses the expression of a gibberellin biosynthetic gene in the tobacco shoot apical meristem. *Genes Dev.* **15**, 581–90 (2001).
 81. Jasinski, S. *et al.* KNOX action in Arabidopsis is mediated by coordinate regulation of cytokinin and gibberellin activities. *Curr. Biol.* **15**, 1560–5 (2005).
 82. Hedden, P. & Thomas, S. G. Gibberellin biosynthesis and its regulation. *Biochem. J.* **444**, (2012).
 83. Liu, Z. *et al.* Phytochrome interacting factors (PIFs) are essential regulators for sucrose-induced hypocotyl elongation in Arabidopsis. *J. Plant Physiol.* **168**, 1771–9 (2011).
 84. Townsley, B. T., Sinha, N. R. & Kang, J. KNOX1 genes regulate lignin deposition and composition in monocots and dicots. *Front. Plant Sci.* **4**, 121 (2013).
 85. Kuijper, J. De groei van bladschijf, bladscheede en stengel van het suikerriet. *Arch. Suikerind. Ned-Indie* **23**, 528–556 (1915).

86. Avramova, V. *et al.* The Maize Leaf: Another Perspective on Growth Regulation. *Trends Plant Sci.* **20**, 787–797 (2015).
87. Hattori, Y. *et al.* The ethylene response factors SNORKEL1 and SNORKEL2 allow rice to adapt to deep water. *Nature* **460**, 1026–30 (2009).
88. Zhou, X. *et al.* ERF11 Promotes Internode Elongation by Activating Gibberellin Biosynthesis and Signaling Pathways in Arabidopsis. *Plant Physiol.* (2016). doi:10.1104/pp.16.00154
89. YAMAGAMI, A. *et al.* Chemical Genetics Reveal the Novel Transmembrane Protein BIL4, Which Mediates Plant Cell Elongation in Brassinosteroid Signaling. *Biosci. Biotechnol. Biochem.* **73**, 415–421 (2009).
90. Avin-Wittenberg, T., Tzin, V., Angelovici, R., Less, H. & Galili, G. Deciphering energy-associated gene networks operating in the response of Arabidopsis plants to stress and nutritional cues. *Plant J.* **70**, 954–66 (2012).
91. Ribeiro, D. M., Araújo, W. L., Fernie, A. R., Schippers, J. H. M. & Mueller-Roeber, B. Transcriptome and metabolome effects triggered by gibberellins during rosette growth in Arabidopsis. *J. Exp. Bot.* **63**, 2769–86 (2012).
92. Valluru, R. & Van den Ende, W. Myo-inositol and beyond--emerging networks under stress. *Plant Sci.* **181**, 387–400 (2011).
93. Dobrenel, T. *et al.* Sugar metabolism and the plant target of rapamycin kinase: a sweet operaTOR? *Front. Plant Sci.* **4**, 93 (2013).
94. Ljung, K., Nemhauser, J. L. & Perata, P. New mechanistic links between sugar and hormone signalling networks. *Curr. Opin. Plant Biol.* **25**, 130–137 (2015).
95. Chang, K. N. *et al.* Temporal transcriptional response to ethylene gas drives growth hormone cross-regulation in Arabidopsis. *Elife* **2**, e00675 (2013).
96. Grivet, L. & Arruda, P. Sugarcane genomics: depicting the complex genome of an important tropical crop. *Curr. Opin. Plant Biol.* **5**, 122–7 (2002).
97. Pearce, S. *et al.* Molecular characterization of Rht-1 dwarfing genes in hexaploid wheat. *Plant Physiol.* **157**, 1820–31 (2011).

98. Nelissen, H. *et al.* A local maximum in gibberellin levels regulates maize leaf growth by spatial control of cell division. *Curr. Biol.* **22**, 1183–7 (2012).
99. Achard, P. *et al.* Gibberellin signaling controls cell proliferation rate in Arabidopsis. *Curr. Biol.* **19**, 1188–93 (2009).
100. Conti, L. *et al.* Small Ubiquitin-Like Modifier Proteases OVERLY TOLERANT TO SALT1 and -2 Regulate Salt Stress Responses in Arabidopsis. *PLANT CELL ONLINE* **20**, 2894–2908 (2008).
101. Srivastava, A. K. *et al.* SUMO Is a Critical Regulator of Salt Stress Responses in Rice. *Plant Physiol.* **170**, 2378–91 (2016).
102. Cunha, C. P. *et al.* Ethylene-induced transcriptional and hormonal responses at the onset of sugarcane ripening. *Sci. Rep.* **7**, 43364 (2017).
103. Nietzsche, M., Landgraf, R., Tohge, T. & Börnke, F. A protein–protein interaction network linking the energy-sensor kinase SnRK1 to multiple signaling pathways in Arabidopsis thaliana. *Curr. Plant Biol.* **5**, 36–44 (2016).
104. Glassop, D., Roessner, U., Bacic, A. & Bonnett, G. D. Changes in the Sugarcane Metabolome with Stem Development. Are They Related to Sucrose Accumulation? *Plant Cell Physiol.* **48**, 573–584 (2007).
105. Stewart, J. L., Maloof, J. N. & Nemhauser, J. L. PIF genes mediate the effect of sucrose on seedling growth dynamics. *PLoS One* **6**, e19894 (2011).
106. Van Dillewijn, C. *Botany of Sugarcane*. (The Chronic Botanica Company, Wlatham Mass, 1952).
107. Zhong, S. *et al.* A molecular framework of light-controlled phytohormone action in Arabidopsis. *Curr. Biol.* **22**, 1530–5 (2012).
108. Zheng, Y., Gao, Z. & Zhu, Z. DELLA–PIF Modules: Old Dogs Learn New Tricks. *Trends Plant Sci.* **21**, 813–815 (2016).

7 Anexos

Declaração

As cópias de artigos de minha autoria ou de minha co-autoria, já publicados ou submetidos para publicação em revistas científicas ou anais de congressos sujeitos a arbitragem, que constam da minha Dissertação/Tese de Mestrado/Doutorado, intitulada **DELLA, o gene da revolução verde. Caracterização e análise de sua função no acúmulo de sacarose e na regulação fonte-dreno em cana-de-açúcar**, não infringem os dispositivos da Lei n.º 9.610/98, nem o direito autoral de qualquer editora.

Campinas, 17 de maio de 2017

Assinatura : _____

Nome do(a) autor(a): **Rafael Garcia Tavares**

RG n.º 19892510-4

Assinatura : _____

Nome do(a) orientador(a): **Marcelo Menossi Teixeira**

RG n.º 42.310.263

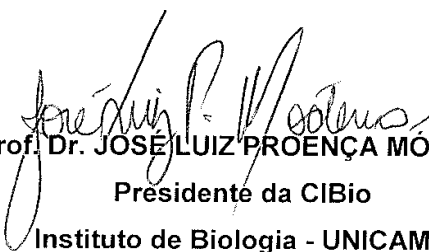


INFORMAÇÃO

INFORMAMOS que o projeto **CIBio 2007/03 - Genômica Funcional de Plantas**, cujo pesquisador responsável é o Prof. Dr. Marcelo Menossi Teixeira, sub-projeto DELLA, O GENE DA REVOLUÇÃO VERDE. CARACTERIZAÇÃO E ANÁLISE DE SUA FUNÇÃO NO ACÚMULO DE SACAROSE E NA REGULAÇÃO FONTE- DRENO EM CANA-DE-AÇÚCAR, do pós-graduando Rafael Garcia Tavares, encontra-se devidamente aprovado e regularizado junto a CIBio/IB-UNICAMP e a CTNBio, conforme legislação vigente.

Cidade Universitária "Zeferino Vaz",

22 de maio de 2017.


Prof. Dr. JOSÉ LUIZ PROENÇA MÓDENA
Presidente da CIBio
Instituto de Biologia - UNICAMP